A MODEL FOR MOLTEN FUEL MOVEMENT IN AN UNFAILED LMFBR PIN

by

JAMES ALFRED KEE
B.S., U.S. MILITARY ACADEMY
(1970)

SUBMITTED IN PARTIAL FULFILLMENT
OF THE REQUIREMENTS FOR THE
DEGREE OF NUCLEAR ENGINEER
AND THE DEGREE OF MASTER
OF SCIENCE IN NUCLEAR ENGINEERING
at the
Massachusetts Institute of
Technology
September, 1972 (i.e. Feb. 1973)

Signature of Author Signature redacted
Department of Nuclear Engineering
September, 1972

Certified by Signature redacted
Thesis Supervisor

Accepted by
Chairman Departmental Committee on Graduate
Studies

A Model for Molten Fuel Movement in an Unfailed LMFBR Pin

by

James Alfred Kee

Submitted to the Department of Nuclear Engineering on September 11, 1972 in partial fulfillment of the requirement for the degree of Nuclear Engineer and the degree of Master of Science in Nuclear Engineering.

ABSTRACT

A knowledge of the mechanisms that cause fuel movements inside an unfailed pin and eject fuel from a failed pin is a prerequisite for further studies in several LMFBR safety areas. In this work, a model for molten fuel movement in an unfailed pin subjected to an overpower transient was developed. The pressure due to the fission gases released and the volume increase of the melted fuel was considered to be the driving force. The primary assumption was that the trapped fission gas was released after the fuel had gone through heat of fusion.

The model was applied to TREAT tests C5A and C5B. A computer-hand calculation combination was employed. The calculated behavior of the pins correspond to the observed pin behavior.

Thesis Advisor: Dr. Neil E. Todreas

Title: Associate Professor of Nuclear Engineering

TABLE OF CONTENTS

LIST OF TABLES

LIST OF FIGURE

LIST OF FIGURE (cont'd)

CHAPTER 1.

INTRODUCTION

1.1 General Purpose

In this work, basic theoretical assumptions concerning fuel movement in a liquid metal fast breeder reactor (LMFBR) undergoing a power transient have been postulated and arranged in a unified model which was applied to a specific series of fuel pin transient tests. Work of this type to analytically describe and predict fuel motion is important, since the fuel movement question is basic to several important safety issues in the LMFBR.

An A.N.L. study lists the four most important questions about the LMFBR (considered most important because they "touch on areas where there is concern that an LMFBR may be unacceptable for safety reasons" (21)):

a. Vapor explosions, i.e. fuel-coolant interactions (when and how do they occur?)

b. Fuel pin failure and failure propagation (How does it fail and can failure propagate?)

c. Motion of molten fuel (How does it move?)

d. Severe power excursions (How much energy is released?)

Although fuel movement is considered explicitly in c , it can be shown that detailed knowledge about the motion of fuel is necessary for the study of a , b and d .

For example, the actual physical mechanism involved in a fuel-coolant thermal interaction is not understood, and further work is necessary. A key area for such further work is the determination of the conditions under which fuel is ejected into the coolant. This includes determining the forces that eject the fuel from the pin and the form in which that fuel is ejected (i.e., all molten fuel, a fission gas and molten fuel mixture, etc.).

The work of this thesis on a fuel movement model was originally undertaken to complement work underway at M.I.T. on the fuel-sodium thermal interaction.

1.2 Scope of Research

Fuel pin failure can be either spontaneous or induced. Spontaneous failure takes place during the normal operation of the reactor (and thus initiates the accident). Induced failure takes place during accident conditions (it is induced as a result of an accident initiated somewhere else in the reactor). If spontaneous failure of a pin was such as to cause failure propagation, either through blockage of the flow channel or the blanketing of pins by fission gas, it would be a serious problem. It has been recently shown that fission gas blanketing alone is not a problem (8). No propagation effects have been, up to now, reported to result from a spontaneous failure. Thus the damage remains local and, although hard to detect,

it is usually acceptable, from both economic and safety viewpoints. (21)

Induced failures, on the other hand, have led to violent pressure effects. In addition the accident condition inducing the failure often affects more than one pin. Thus other pins may be past or very near failure thresholds and the possibility of some degree of propagation exists. Induced failures thus seem more significant for safety analysis.

One method of studying induced pin failures is to subject pins in test capsules to severe overpower transients. The increased power causes fuel temperatures to climb. The melting point is reached in a portion of the pin and failures ensues. The use of such a test to attempt to glean knowledge about molten fuel ejection, however, has several disadvantages. First the failure itself destroys much of the evidence. Post-transient examination of the pin is usually of little benefit because the transient destroys the pin's integrity. In addition, little can be determined about the various stages leading to failure. One can theoretically model the driving force for fuel motion in such a transient and predict the failure threshold and thus the time of failure. This can be checked against an observed failure time which can be determined from pressure transducers placed in the coolant channels.

It is impossible, however, to check any more detailed analysis of the movement of the fuel (a device called a hodoscope can theoretically allow the experimenter to "see" the motion of the fuel (9), but the available data are very limited and the method has not yet been perfected).

The actual failure mechanism is complicated. It is hypothesized that once the inner segment of the fuel melts, the molten fluid forces its way toward the cladding by utilizing existing cracks in the outer fuel or forcing new cracks to form in weakened areas. The exact location of the cracks or weakened areas is almost impossible to predict. The cladding is either melted through or subjected to a yield stress originating from the pressure increase associated with the melting of the inner fuel. This increase in pressure results from the fuel volume expansion and the compression of fission gas. In this case, the clad yields at its weakest point. The location of the weakest point is probably determined by fabrication imperfections. In any case, it is not always possible to predict the exact point. The strength and behavior of the clad and the fuel itself is of course a complex function of the temperature and irradiation history, as well as the fabrication. In short, the entire failure mechanism is a complicated, somewhat random process. This makes verifi-

cation of even the most basic theoretical assumptions all but impossible through the use of an integral type overpower transient test.

It has been suggested, however, that one can verify many of the important assumptions by examining fuel motion in an unfailed pin (33). In a unfailed pin, it is possible to perform a post-transient destructive analysis and obtain detailed information about the final condition of the pin. Normally, there would not be a great amount of fuel motion in an unfailed pin. Fortunately, however, in one General Electric test, designated C5B, a pin experienced significant fuel motion without failure, presumably due to the existence of a hole (.070 inch i.d.) in the annular blanket. A companion pin, C5A, with a solid blanket, was subjected to a similar transient for comparison (10). The pin configurations are shown in Figure 1-1. In the C5B test, the cladding was intact, with only a small, almost uniform, permanent strain and minor deformation at one axial location. The fuel moved in an axial, rather than a radial, direction and therefore the cracks in the outer fuel did not play a significant part in determining the extent of motion. In this "clean", uncomplicated case of axial movement it is thus much simpler to compare the observed results with theoretical predictions. This is the specific goal of this work: to

FIGURE 1.1

Cross-section of Fuel Pins

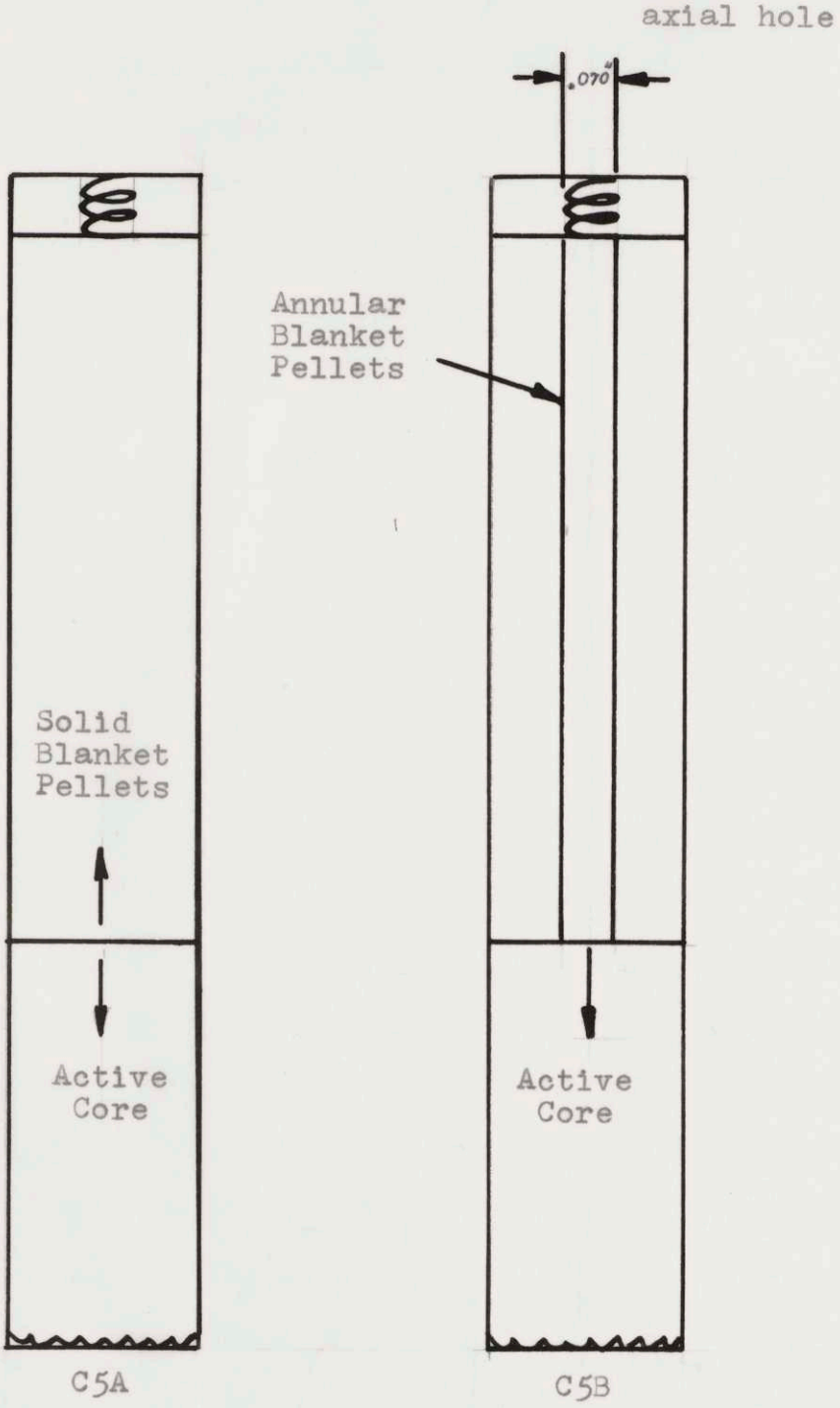

postulate and verify basic theoretical assumptions concerning fuel movement through the use of the C5A and C5B tests. The specific assumptions include the role of fission gas, friction, two-phase flow and heat transfer in fuel movement. Of primary importance is the verification of the theory that fission gas is the prime driving force behind fuel movement.

1.3 Review of Current State of Work in the Area of Fuel Movement

SAS1A, developed at Argonne National Laboratory, is a computer code designed to analyze power and flow transients in fast reactors. Designed to be a complete accident package, SAS1A was the first attempt at modelling the entire spectrum of fast-reactor mishaps, and was the first in a planned series of SAS codes, with the later versions expected to be more accurate and to encompass more effects. Although a later version, 2A, is now available, SAS1A will be examined first, for the purpose of a historical survey of advances in the field. The code consists of a complex linkage of several different modules, with each module containing all calculations pertaining to one analytical model.

The fuel deformation module and the fuel dynamics module from SAS1A parallel in scope the problem that has been taken for this thesis: modelling fuel movement.

The fuel deformation module calculates the thermo-elastic deformation of the fuel and the elastic-plastic deformation of the clad based on temperature profiles which are the product of another module. For partial melting, the module assumes that the material in a cell, a division of the pin, behaves mechanically as a liquid with density and bulk modulus between those for liquid and solid states. Fuel and cladding stresses and deformations are calculated, assuming that the fuel does not cross cell boundaries (7).

When the fuel centerline temperature exceeds a specified input value, control is shifted to the fuel dynamics model. It is assumed that at this point there is extensive melting and fuel motion is beginning. The fuel dynamics model calculates axial motion and fuel displacement. The physical model used is shown in Figure 1.2. Axial pressure gradients arise from the radial restraining force of the cladding which is imposed on the expanding solid-liquid fuel material. The fact of prime importance is that the driving force in this model is the solid fuel expansion and the fuel volume increase upon melting. The effect of fission gas, or even its presence, is not contained in SAS1A. Thus, if it is assumed that fission gas plays a major role in fuel motion, one could expect SAS1A to be applicable only to unirradiated pins. (Models

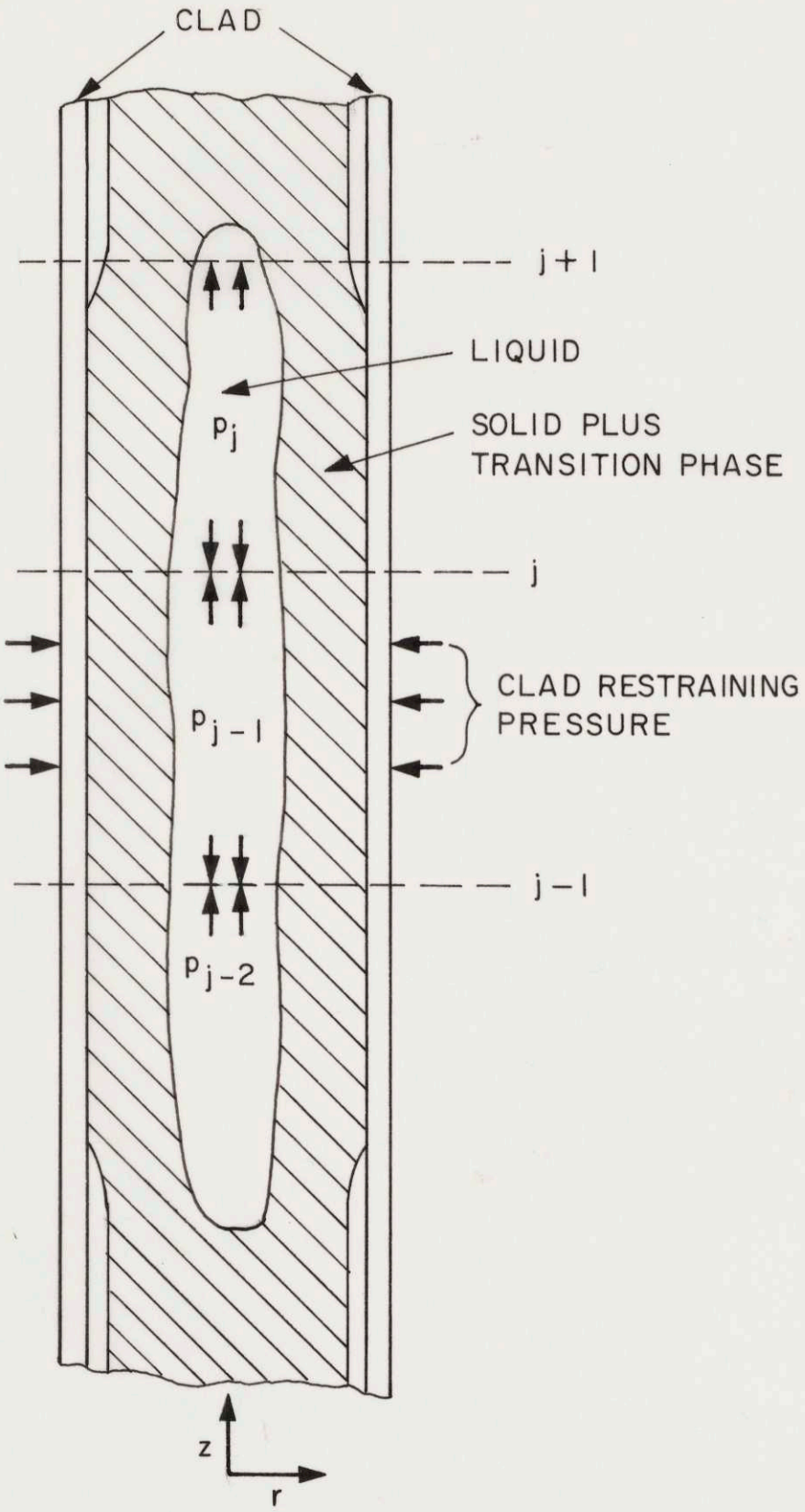

FUEL DYNAMICS MODEL (7)

FIGURE 1.2

incorporating fission gas effects are currently under development at A.N.L., however. (13))

The fuel dynamics module allows for pressure buildup to the point of cladding failure. One of the modules objectives was to estimate the fuel failure threshold. In addition, the module was to form a starting point for eventual further development of other modules attempting to describe fuel behavior after clad failure. In the fuel dynamics model, the axial pressure gradient acting on molten fuel causes axial motion.

The equation of motion of the fuel can be derived from the basic relation $ma = \Sigma F$, where the forces involved are friction, gravity and the axial pressure gradient. The force of gravity is mg, the mass times the acceleration of gravity. The friction force is, by definition of the friction coefficient F, $Fmv_z = Fm\frac{dz}{dt}$. The pressure gradient force per unit volume of fuel is simply $\frac{dP}{dz}$. Thus:

$$ma = m\frac{d^2z}{dt} = -mg - mF\frac{dz}{dt} - V\frac{dP}{dz}$$

where V is the volume. working with incremental axial segments, the equation of motion for a segment f is

$$\frac{d^2z}{dt^2} = \frac{-1}{\rho_f}\frac{dP_f}{dz} - F\frac{dz}{dt} - g$$

where P_f is the pressure on fuel segment f and ρ_f is the fuel density for segment f. In the model, P_f, the fuel pressure at any axial point is derived by calculating the cladding internal pressure required to produce the cladding strain. The final cladding strain previously calculated in the fuel deformation module is first used, and the strain increases as more fuel melts and expands (7).

J. Hanson and J. Field were the first to propose a model in which fission gas played a significant role in fuel movement (19). The model that they developed assumed that all fission gas trapped in an oxide region during steady state irradiation was released instantaneously when that region melts during a transient. Some earlier A.N.L. fuel dynamics experiments involving irradiated fuel showed that the trapped fission gas did not play a major role in cladding failure up to the point where the oxide started to melt (29). This substantiated the use of the melting point as the gas release point. The hypothesis, however, needs further verification as it still is not universally accepted (15).

G. E. next extended the theory by devising a molten fuel movement model to be used after an assumed instantaneous cladding breech. The model was designed to conservatively bound the problem. In addition to the use of the melting point as the gas release point, the model ob-

tained the driving force by calculating the pressure of the released gas corresponding to a constant temperature (assumed to equal the fuel melting temperature) of the gas and the volume which the gas occupies (the volume was assumed to be the fuel porosity volume).

The model was applied to the C5B test mentioned previously. The model is shown in Figure 1.3. An estimate of the driving pressure existing during the test was derived from the observed cladding deformation. The driving pressure was also calculated by the alternate method of finding the gas volume, the gas temperature, and the fuel expansion on melting effect. This alternate method, however, yielded an unrealistically high pressure and thus was disregarded. The pressure associated with the cladding deformation was used, with the assumption that the gas expanded isentropically. The result was the lower bound that if the fuel was assumed to displace a total of 10 inches, it would take only 20 milliseconds to completely displace with a maximum velocity of 52 ft./second occurring at 5.5 milliseconds (20).

A.N.L. has recently released SAS2A, on upgraded multichannel version of the SAS1A code. This version considers the effect of fission gas released from failed pins on coolant flow. A fuel-coolant interaction model is one aspect of the code. The effect of burnup in oxide fuels,

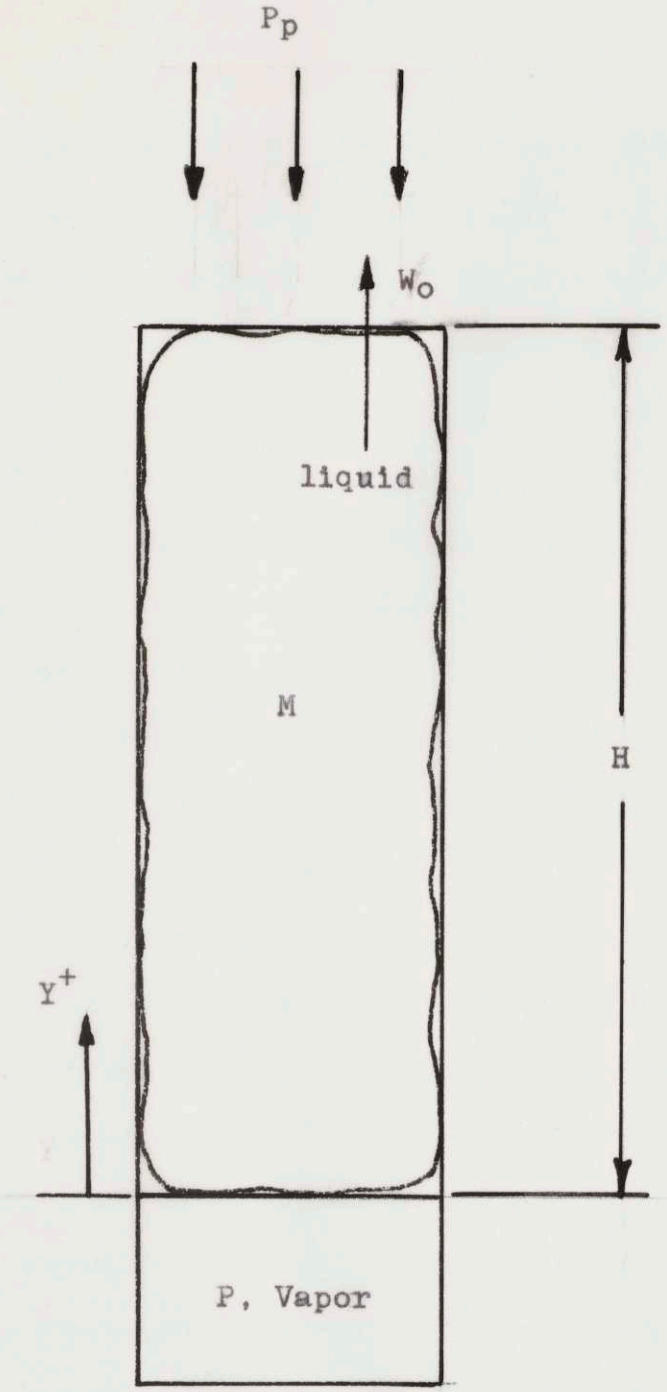

W_o=Outflow of Molten Fuel

M= Mass of Molten Fuel

P= Drive Pressure

P_b=Plenum Pressure

H= Displaced Fuel Length

FIGURE 1.3 (20)

to include the effects of fission products and restructuring, is the object of a further modification to be planned for SAS2A (13). The role of fission gas as the driving force in fuel movement has not yet been included in the code. Work at ANL is proceeding on an axial-squirting model which does consider the fission gas as the driving force in squirting a molten fuel-gas mixture from its position in the center of the pin. The work is currently being done in a study of an "inherently safe fuel element design," which allows for axial fuel movement much as was the case in C5B. It is expected, however, that the squirting model will eventually be implemented into SAS2A (4).

Carelli, from Westinghouse Advanced Reactors Division, has reported on other efforts to model fuel movement (6). At W.A.R.D., the FIDES codes is used to investigate molten fuel ejection from a failed pin. The physical model used is shown in Figure 1.4. It is assumed that only the molten fuel column length, Lm, above the location of the rupture takes part in the ejection. The driving force responsible for the motion is the fission gas plenum pressure, P_r.

In order for any fission gas released during the transient to fit this model, it must be assumed that this gas is able to vent to the plenum region during the tran-

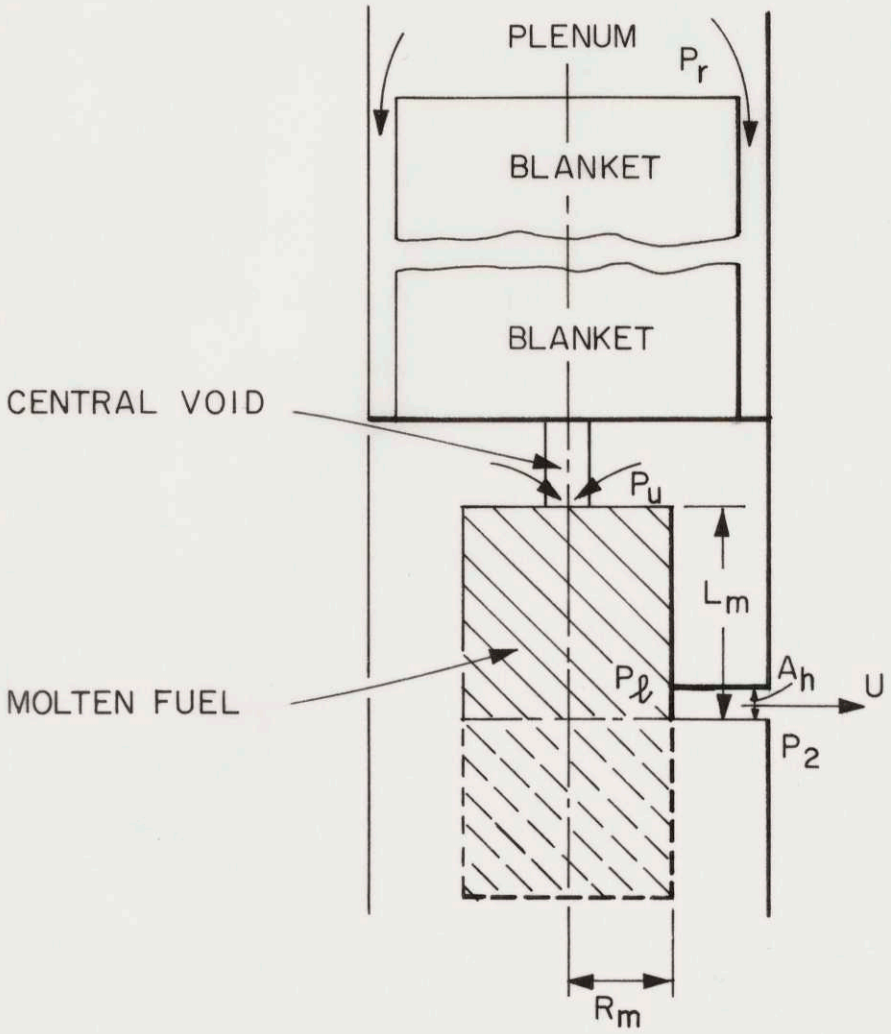
PLENUM
P_r
BLANKET
BLANKET
CENTRAL VOID
P_u
L_m
MOLTEN FUEL
P_ℓ
A_h
U
P_2
R_m

FIGURE 1.4

sient and before fuel motion. Experimental results have shown that this assumption is in error; gas cannot not vent to the plenum during a transient prior to fuel motion (30).

Thus the G.E. and W.A.R.D. models both assume that a pocket of gas behind the molten fuel column is the driving force for fuel motion, while the A.N.L. squirting model currently under development assumes that the fission gas is mixed with the liquid. This work attempts to use an approach similar to that of the A.N.L. model. This ANL specific fuel motion model is incorporated into a more comprehensive model including the different assumptions necessary to obtain the inputs to the specific fuel motion model. An attempt will be made to consider several factors which have not been considered in the analysis performed to date.

CHAPTER 2.

DESCRIPTION OF C5A AND C5B TESTS

2.1 Position in Test Series and Purpose

General Electric, in the program P.A. - 10, Task C, is conducting a series of experiments aimed at defining the failure mechanisms and thresholds of LMFBR fuel pins under severe overpower conditions. Series I test were directed toward development of fuel for the experimental fast ceramic reactor (SEFOR). Series II looked at the performance of the fuel and clad in zero burnup pins subjected to overpower transients. Series III irradiations investigated the effects of prior irradiation on transient performance. Series IV tests were planned to evaluate the effects of axial restraint, density, composition, and burnup.

Analysts comparing the results of Series II and Series III decided that a provision for molten fuel accomodation might relieve internal pressure and extend the transient failure threshold. Series V was designed to investigate the effects of molten fuel movement, fuel and blanket lengths, and fission product gasses on transient failure limits (20). Current G.E. transient tests are shown in Table 2.1. The Transient Reaction Test Facility at the National Reactor Testing Station, Idaho Falls, Idaho,

COMPLETED G.E. TRANSIENT TESTS

DESIG.	DIA. (IN.)	LENGTH (IN.)	SMEARED DENSITY	%UO_2	IRRADIATED	FAILED YES	FAILED NO
C4A	.250	14.2	90.4	80		X	
C4B	.250	14.2	91.2	80		X	
C4C	.250	14.2	80.4	80			X
C4D	.250	14.2	80.1	80			X
C4I	.250	13.5	83.5Pow.	80		X	
C4J	.250	13.5	83.5Pow.	80			X
PURPOSE: To determine transient failure threshold of zero burn-up fuel as a function of axial restraint, fuel density and form (pellet or powder)							
C5A	.250	24	90	100	20,000 MWd/Te	X	
C5B	.250	24	90	100	in GETR		X
PURPOSE: To study mobility of transient melted fuel							
C6A-1	.212	24	80	100			X
-2	.2208	24	80Pow.	100			X
-3	.212	24	80	100			X
C6B-1	.212	24	80Pow.	100			X
-2	.2203	24	80Pow.	100			X
-3	.212	24	80	100			X
PURPOSE: To evaluate transient performance of defected or sodium bended fuel. Powder fuel logged.							
C4X	.2186	13.48	91	100			X
PURPOSE: Checkout for C4E-H, K-L							

TESTS IN PROGRESS

C4E	.2159	13.46	80.5	72	
C4F	.2160	13.51	80.5	72	
C4G	.2154	13.50	90.5	72	60,000MWd/Te
C4H	.2152	13.45	90.4	72	in
C4K	.2205	13.5	84.1Pow.	72	EBR-II
C4L	.2206	13.5	84.2Pow.	72	
PURPOSE: To compare with C4A-D, I-J to evaluate effect of burnup.					

TABLE 2.1 (20, 33, 32)

(TREAT) is used for the transient tests, and the schedule of experiments for TREAT is shown in Table 2.2. Tests done by other facilities are included for comparison.

2.2 Testing Technique

Two oxide fuel specimens were manufactured and encapsulated. The pins were identical except that the 14 1/4 inch upper blanket of one (designated C5A) was composed of solid pellets, and the blanket of the other (C5B) was composed of annular pellots with a 0.070 inch inside diameter.

The pins were first irradiated at low power under steady state conditions at the G.E. test reactor (GETR) to a burnup of approximately 22,000 MWd/Te. The irradiation took place in four cycles and the peak power was approximately 12 KW/ft. The capsules were non-destructively examined after irradiation. The gamma scan and neutron radiograph showed the pins to be in good condition with no irregularities. A central void was lacking. Readings from thermocouples located in the coolant during irradiation were used to estimate fuel temperatures. The peak fuel temperature was estimated to be 2850°F. The lack of central void would indicate a peak temperature less than the sintering temperature (2912°F), so the calculations appeared to be accurate. Test parameters are shown in Table 2.3.

TABLE 2.2 (23)

	Tests	FY70	FY71	FY72	FY73
FEFPL	Checkout			CK	
	Fuel Element Failure Prop			P1 P4	
	Rate of Prop: Melting			P2 P5	
	Blockage			P3 P6 P8	
	Failure Propagation				P7 P9 P10
TREAT MK II	Fuel Move-Power Exeursion	E1 E2	E3 E4	E5 E6 E7	Continued FFTF Experiments or Demo Plant Simulation Tests
	Fuel Move-Loss of Flow		L1 L2 L3 L4 L5		
	Fuel Move-Slump		F1 F2	F3	
	Release of Small Amt. Molten Fuel		D1 D2	D3 D4 D5	
	Assembly Melt Thru			G1 G2	
	Trans Fail Threshold	H1 H2	H3		
TREAT STATIC	Molten Fuel Piston	S5 S6 S7	S8,9 S10 S11		
	Coolant Interaction	I1 I2 I3 I4	I5 I6 I7		
	Expulsion and Re-Entry			R1 R2,3 R4,5,6	
GE PA-10	Axially Res Fuel C4	A,B,C,I,J C4X	C4G C4H	C4E,F,K,L	
	Mobility of Molt Fuel	C5A,C5B			
	Defected-Bonded Fuel	C6A(1,2,3)	C6B(1,2,3)		
	Loss of Flow- Re-Entry	C10X	C10A,C10B		
	MK-II Failure Threshold		Plan Being Developed		
PNL Tests	Test Fuel Pins to Safety Limits		59-14,16 59-4		
	GETR-59		59-1,2		
	EBR-II-1,2		59-8,10		
EBR-II Project	EBR II Fuel Failure	Proposed to Test FFTF Fuel to Failure			
	Treat: Gas Release I		I		
	Fuel Motion		II		

TREAT TESTS

SUMMARY OF SERIES V EXPERIMENT PARAMETERS

GETR TEST DATA

	C5A	C5B
AVERAGE POWER (KW/FT)	9.7	9.4
PEAK POWER (KW/FT)	11.9	11.7
AVERAGE BURNUP (MWD/Te)	17,800	17,300
PEAK BURNUP (MWD/Te)	22,000	21,400

TABLE 2.3

SUMMARY OF SERIES V EXPERIMENT PARAMETERS

TREAT TEST DATA

	C5A	C5B
REACTOR PARAMETERS		
PERIOD (SEC)	0.131	0.137
REACTIVITY (%)	1.37	1.35
INTEGRATED POWER (MW-SEC)	309	310
PEAK POWER (MW)	520	505
FUEL PIN PARAMETERS		
PEAK SPECIMEN POWER (KW/FT)	160	155
TOTAL SPECIMEN POWER (CAL/GM)	338	339
% OF FUEL MELTED	30-37	30-37

TABLE 2.4

The entire test assembly as shown in Figure 2.1, was then placed in the TREAT reactor. Calibration transients were executed with both the C5A and C5B capsules, to verify physics and heat transfer calculations. Based upon the calibration data, transients were designed to result in the melting of approximately 40 percent of the fuel. Transient data is shown in Table 2.4. It can be seen that the two transients were similar.

During pretest it was found that the capsule thermocouples in C5A and C5B were not functioning. It was thus necessary to repeat the preheat procedures used in the calibration runs (when the thermocouples were working) and do the transient "blind". While there were thus no thermocouple results, by comparison with the calibration test and with the fuel microstructure in post-transient examination (i.e., molten fuel radius), a complete temperture histroy could be derived thru the use of a heat transfer code (20).

The detailed power profiles are shown in Figure 2.2 and 2.3. More detailed data on C5A and C5B tests is given in Appendix A.

2.3 Results

Following transient irradiation, the specimens were gamma scanned and neutron radiographed. Figures 2.4 and

FIGURE 2.1 (14)

TREAT TRANSIENT TEST ASSEMBLY - TASK C SERIES V

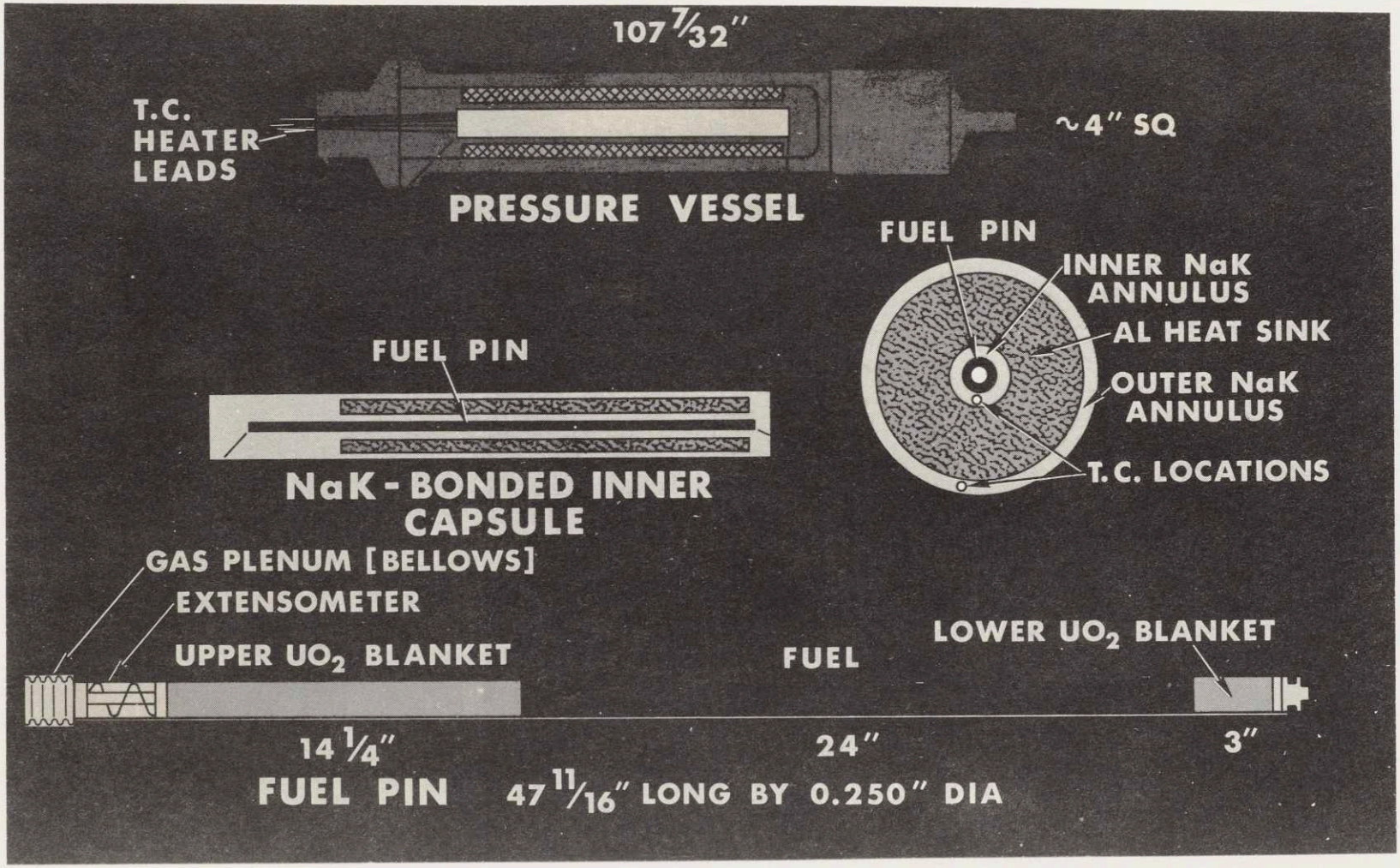

FIGURE 2.2 (17)

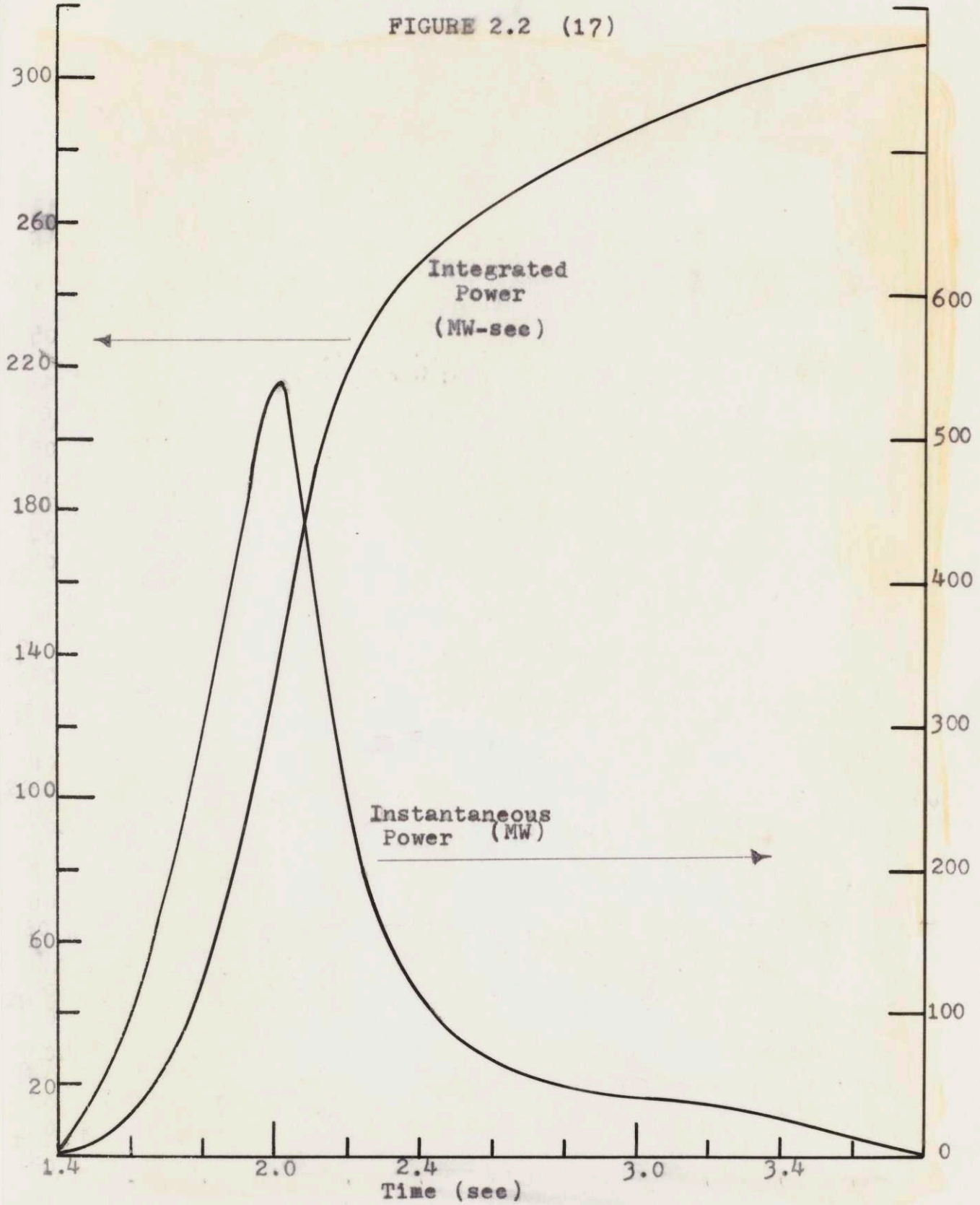
300
260
220
180
140
100
60
20
600
500
400
300
200
100
0
Integrated
Power
(MW-sec)
Instantaneous
Power (MW)
1.4
2.0
2.4
3.0
3.4
Time (sec)

FIGURE 2.3 (17)

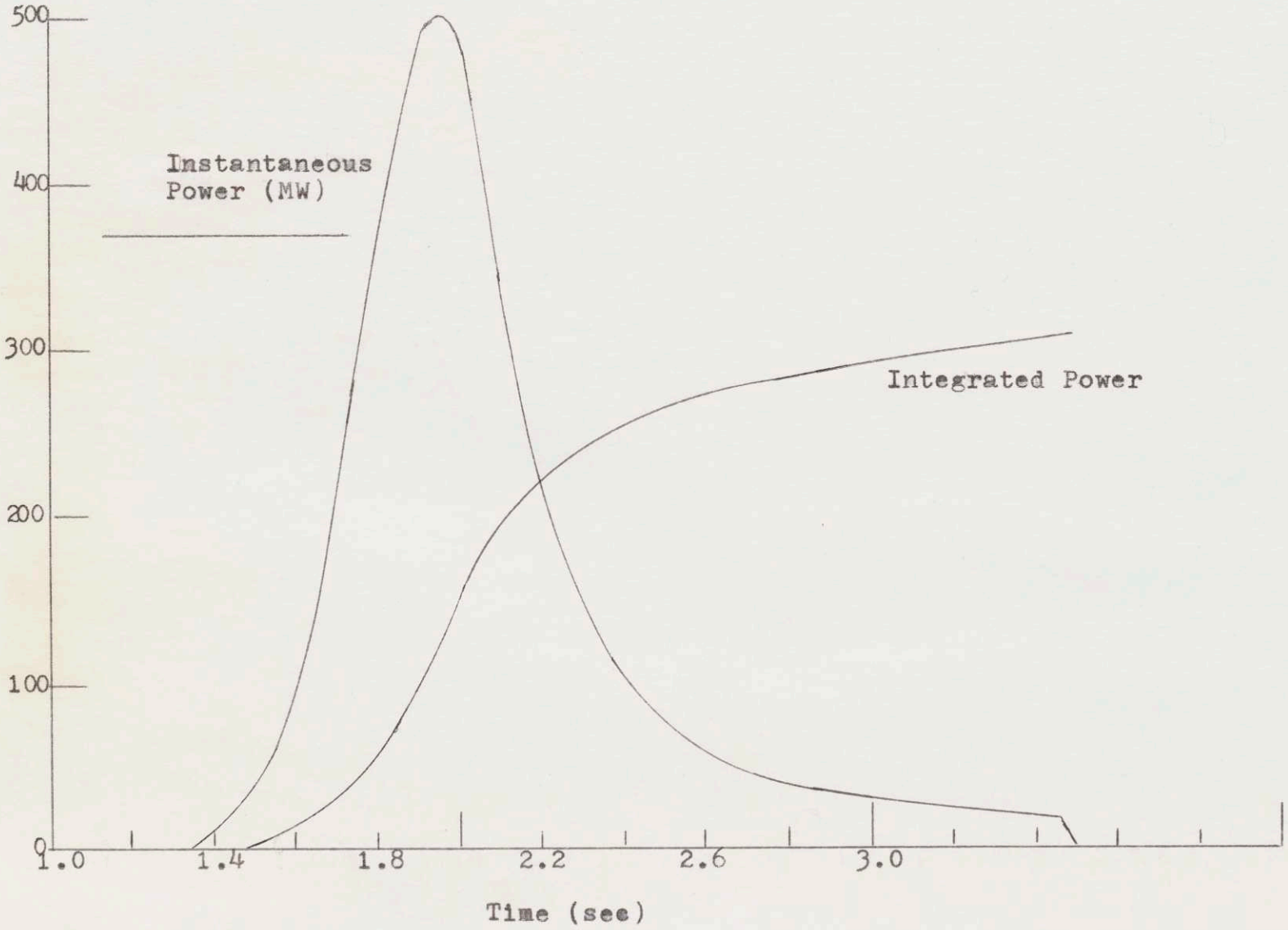
500
400
300
200
100
0
Instantaneous
Power (MW)
Integrated Power
1.0
1.4
1.8
2.2
2.6
3.0
Time (sec)

FIGURE 2.4 (14)

PIN C5A

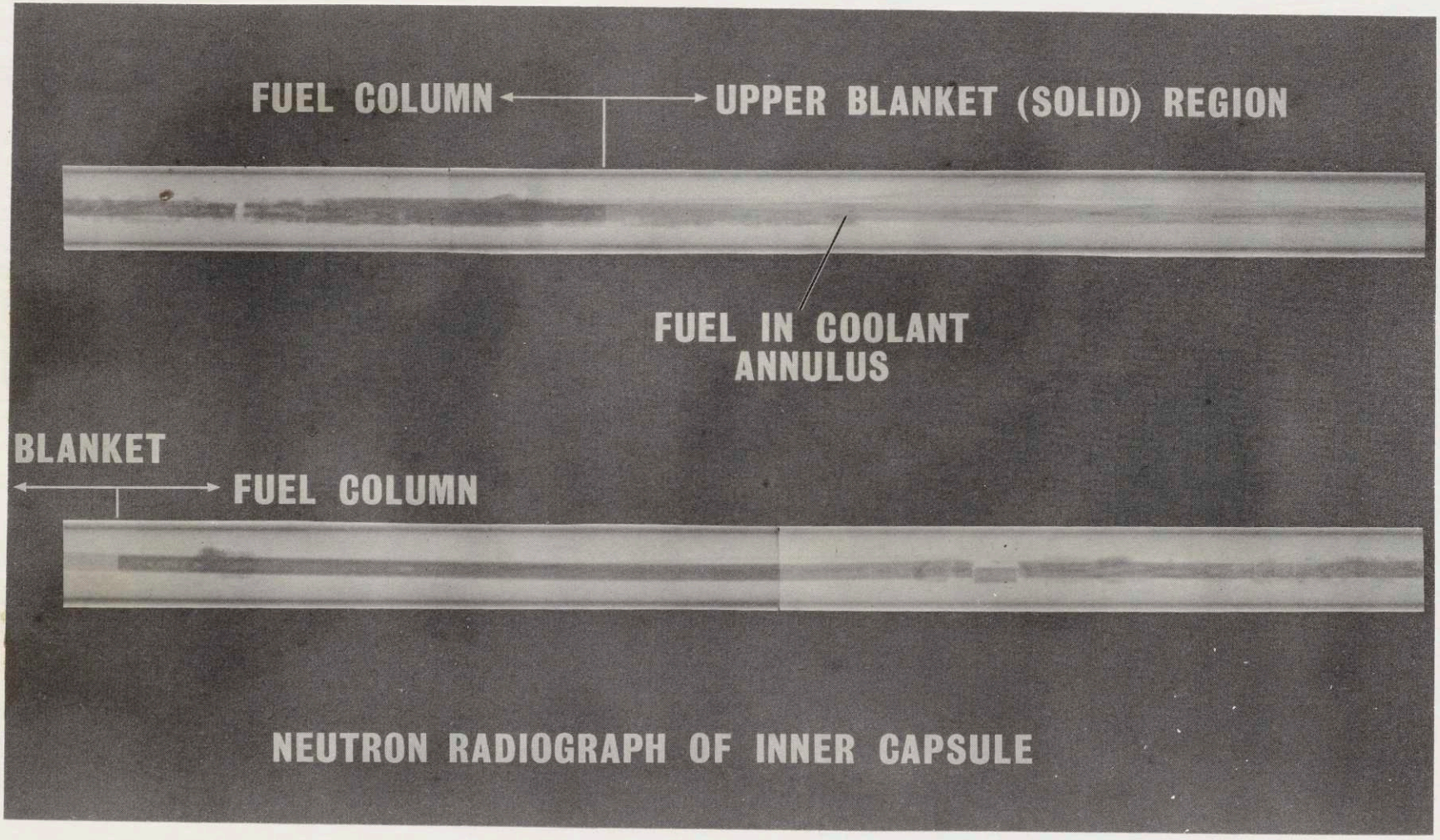

FIGURE 2.5 (14)

PIN C5A

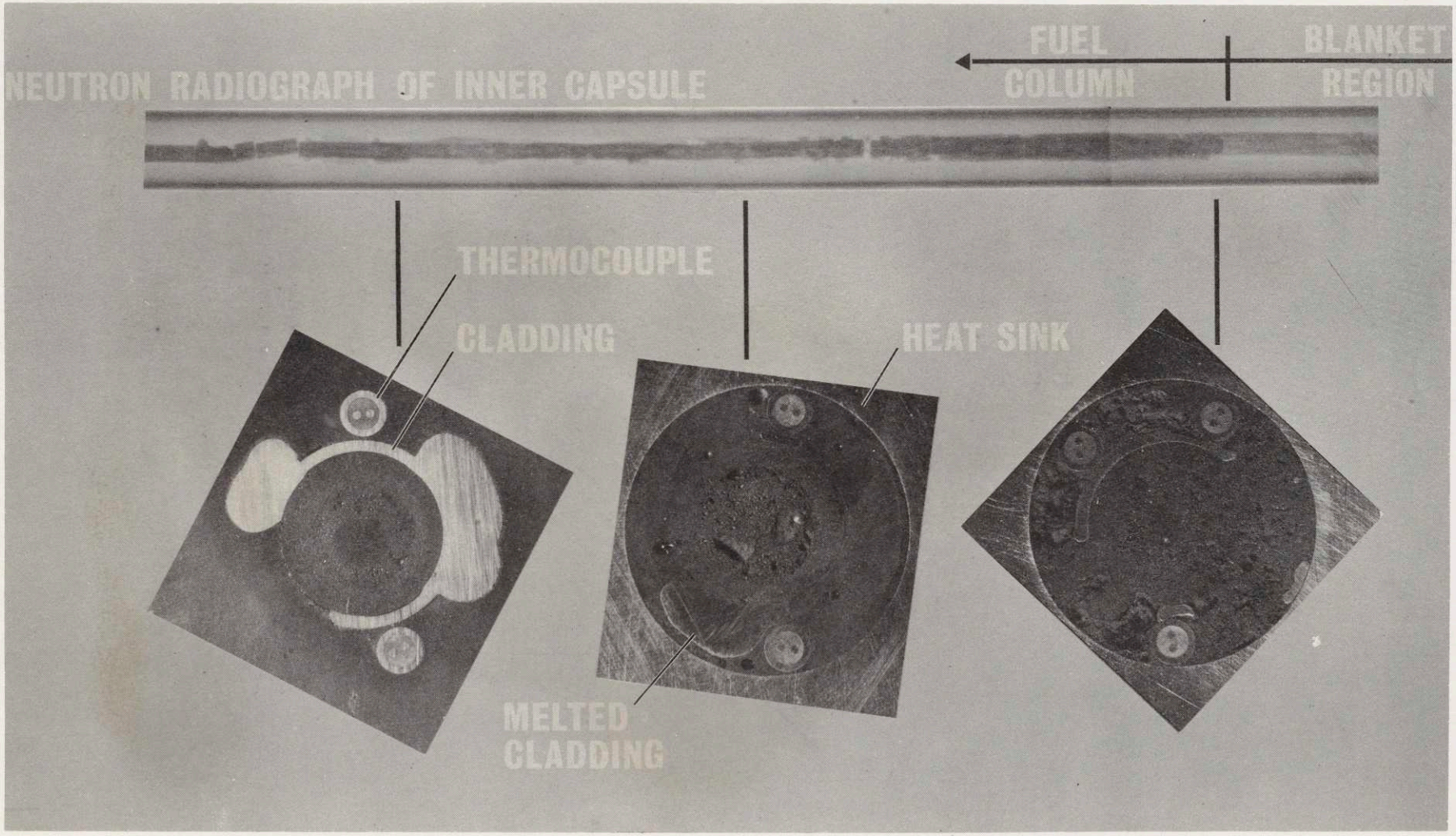

2.5 show the radio-graphs of the C5A inner capsule. The pin experienced gross failure with extensive fuel movement into the coolant annulus. The cladding melted in many places and the pin separated near the fuel midplane. The melted cladding is shown in Figure 2.6. Some cladding that remained showed a deformation of 3 to 4.5 miles.

The C5B radiograph is shown in Figure 2.7. The cladding was intact with no evidence of failure. A central void with plugs of fuel has formed in the upper half of the fuel, while the lower half is solid, apparently refilled with once-molten fuel. Fuel movement into the blanket region was obvious, with movement extending approximately 10 inches into the blanket (20).

The uppermost fuel pellet apparently "grew" 200 mils. Analysis reveals that molten fuel forced a separation between the fuel and blanket and filled the resultant void. Inspection of the cladding revealed only one defect: a bulge near the fuel blanket interface. This verifies the forced separation by molten fuel. Other task C experiments had the same occurrence: molten fuel coming into contact with caldding with only an increased cladding deformation observed (19). The C5B result is shown in Figure 2.8. The cladding elsewhere on the pin was deformed 2.5 to 4 mils.

FIGURE 2.6 (14)

PIN C5A

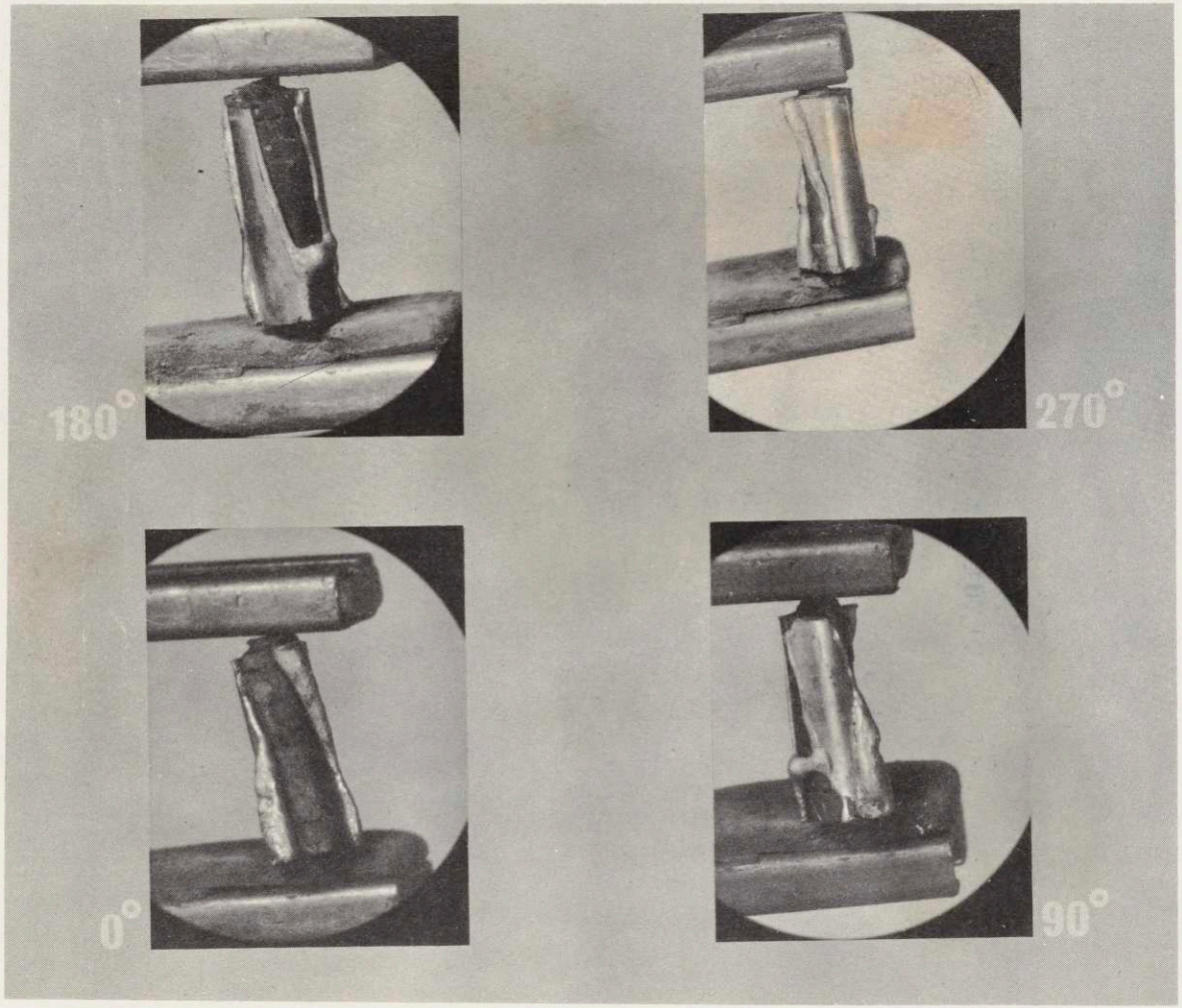

FIGURE 2.7 (14)

PIN C5B

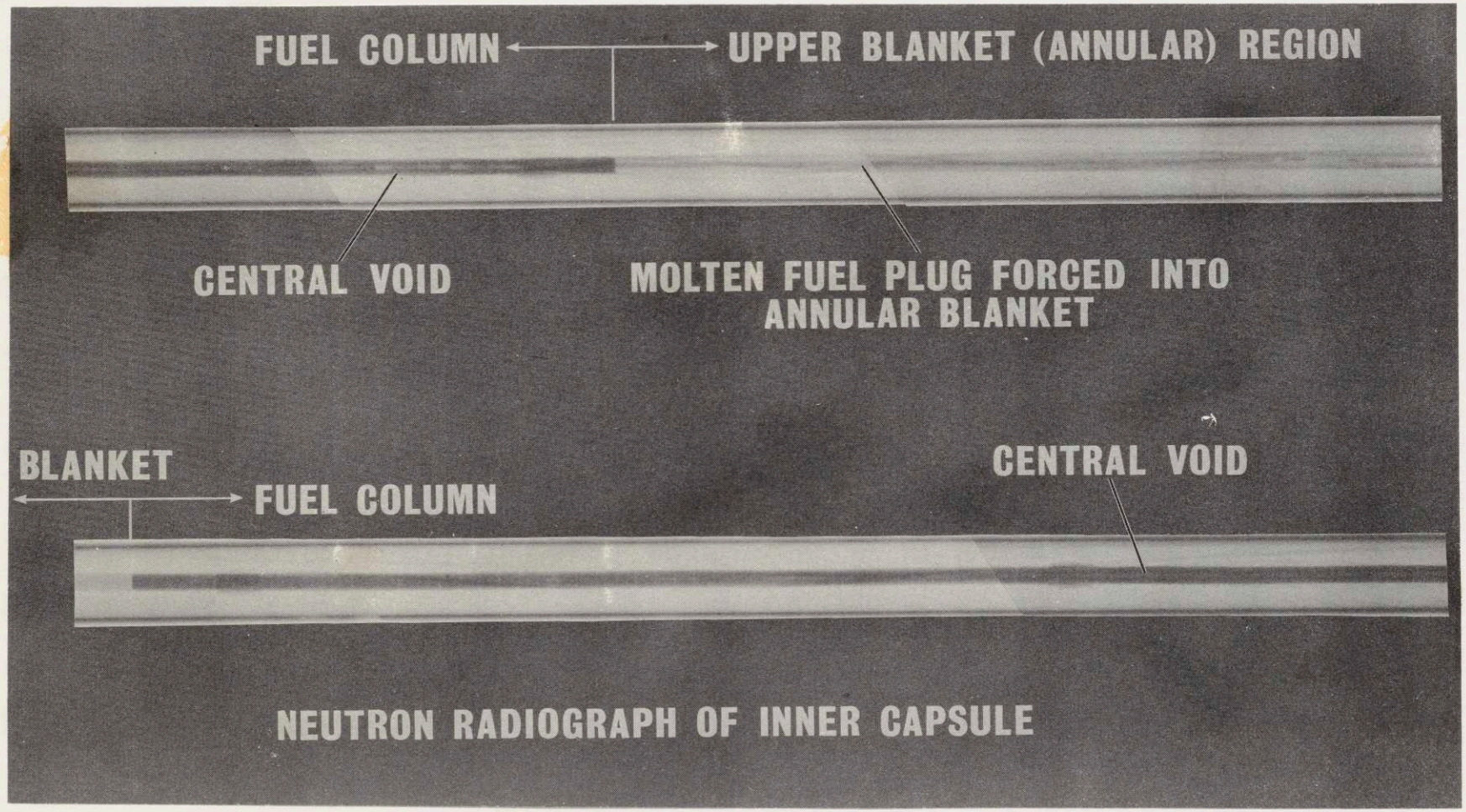

FIGURE 2.8 (14)

PIN C5B

Transient Initiated, Core Of Fuel Is Becoming Molten

Transient Progressing, Molten Fuel Forces Separation Between Fuel Column and Blanket

Molten Fuel Driven Up Blanket By Released Fission Gases

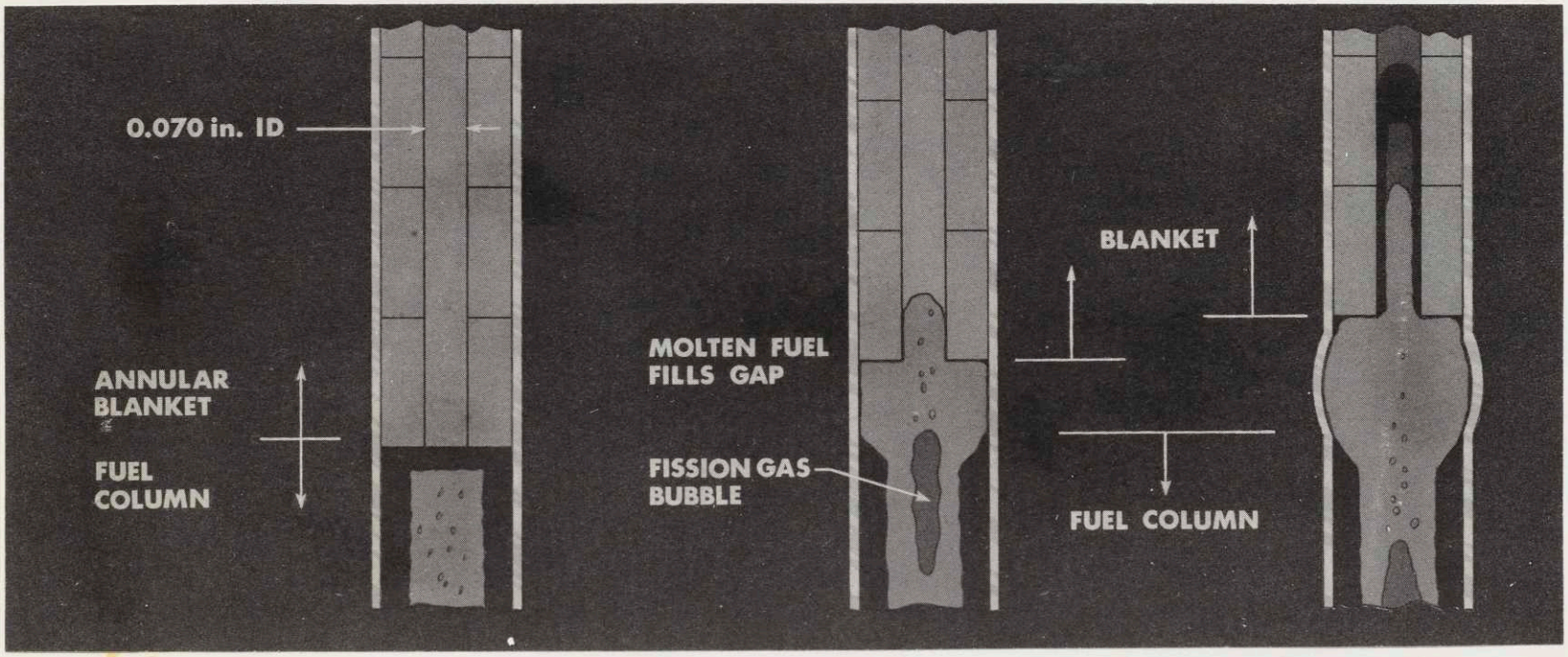

The C5B pin was destructively examined, with photographs taken of the sections. The results again verified the fuel-blanket separation theory as it was possible to easily identify the once-molten fuel by the bright spots interspersed in it. These bright spots were caused by metallic fission products which coalesced during fuel melting. The fuel melting, which was relative uniform axially, occurred to a radius of approximately .065 inches.

Figure 2.9 is a photograph of the fuel blanket interface area. Figure 2.10 is another photo showing three distinct fuel region. From the center they are:

1. fuel that entered heat of fusion
2. equialaxial grain growth region
3. as fabricated region (darkened area affected by high temperature, but remains with the as-fabricated grain structure).

Figure 2.11 shows once molten, sponge-type fuel in the annular blanket region. A fuel plug can also be seen filling the center hole of the blanket. The plug was approximately 6 1/4 inches above the fuel blanket interface. Figure 2.12 is a cross section view of the plug. The plug seemed to have 3 distinct layers:

1. a thin dense layer adjacent to the blanket pellets
2. a thicker layer with small to medium size poles
3. a center core with a spongy structure (large pores).

FIGURE 2.9 (17)

C5B Fuel-Blanket Interface Region

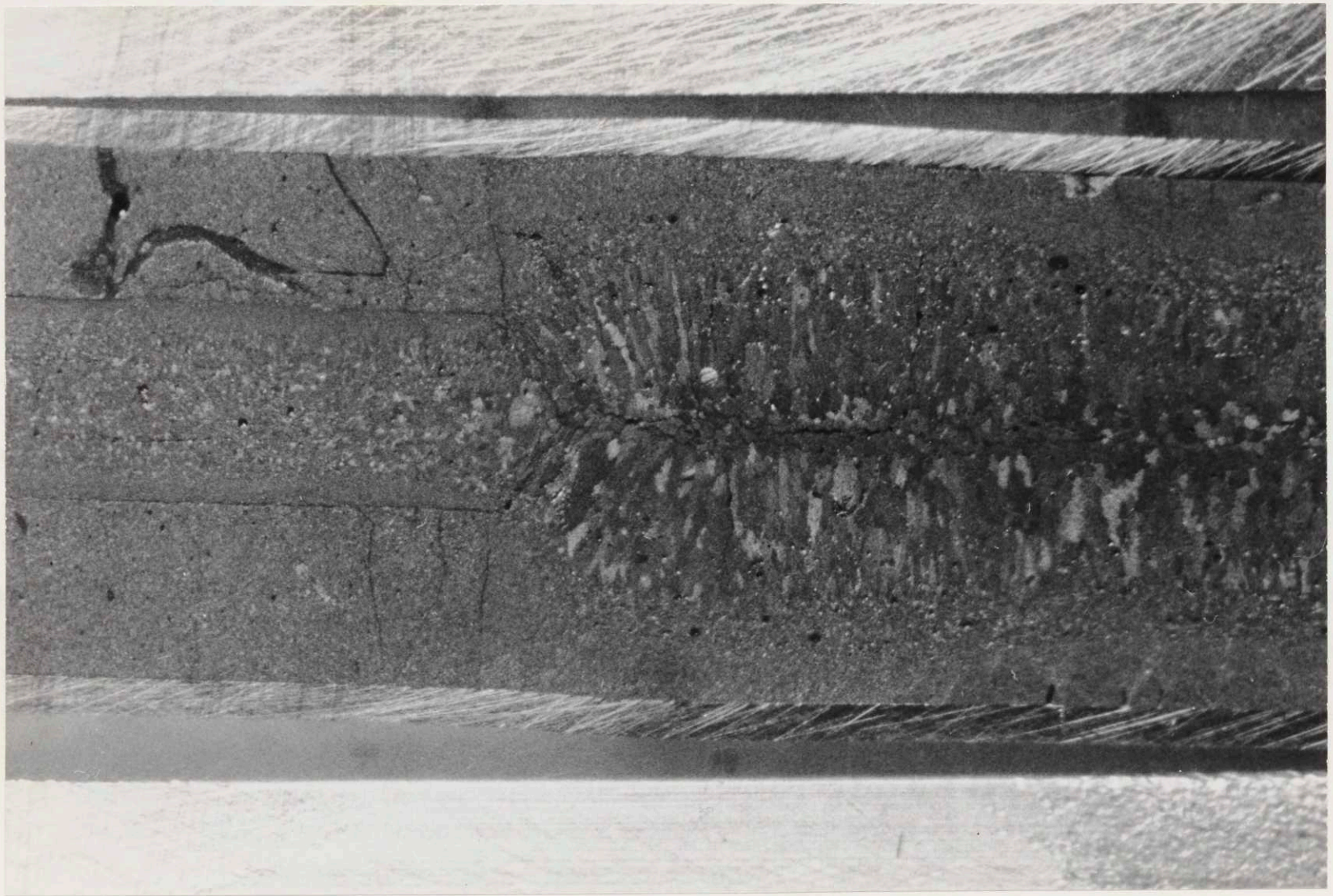

FIGURE 2.10 (17)

C5B Fuel Regions

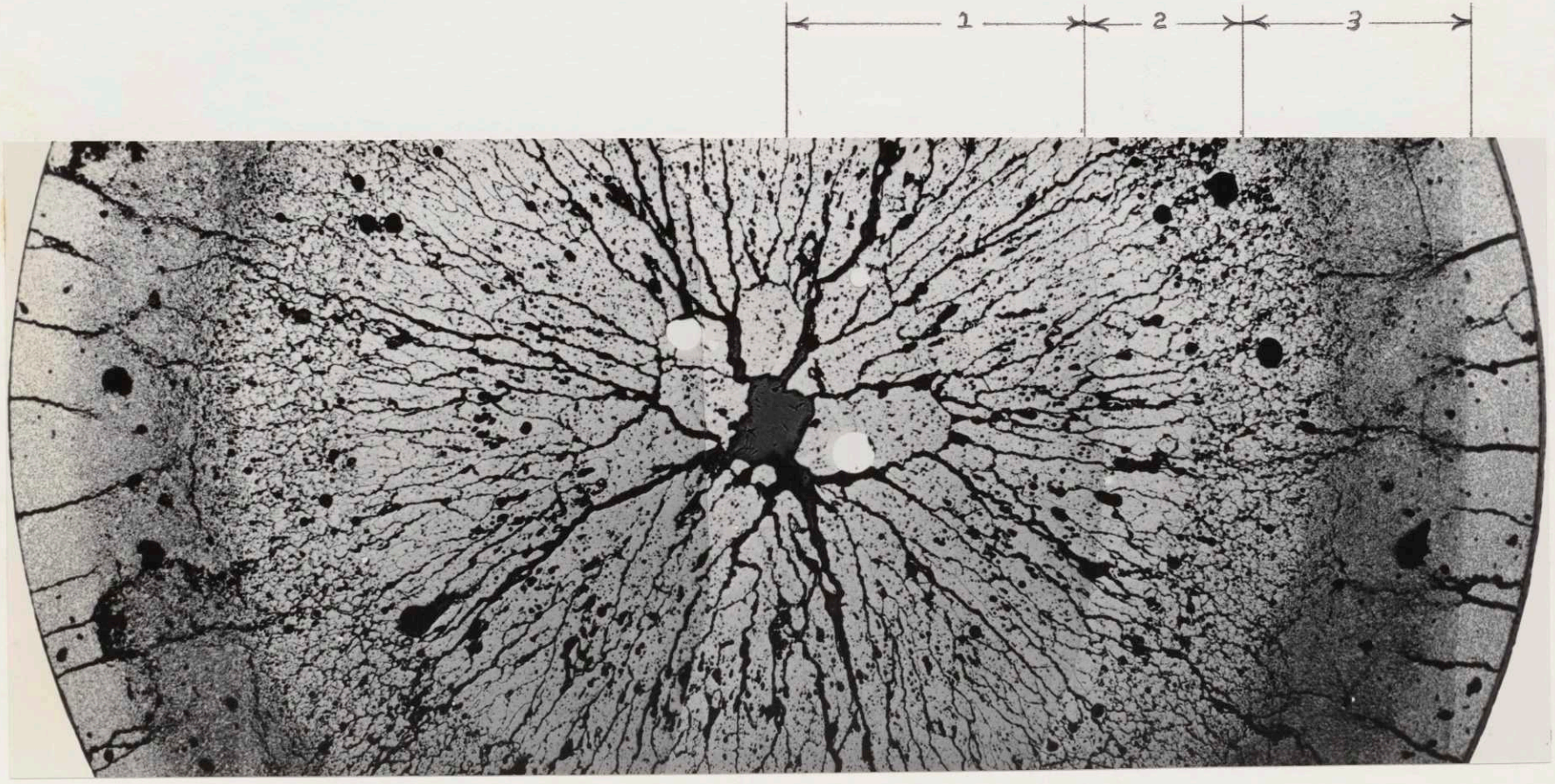

FIGURE 2.11 (17)

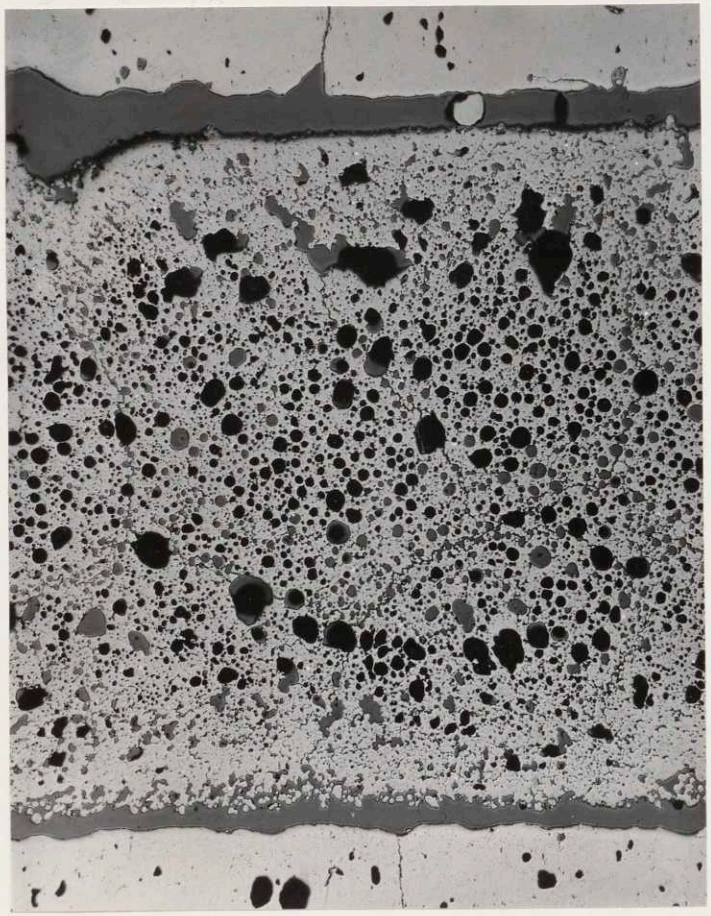

FIGURE 2.12 (17)

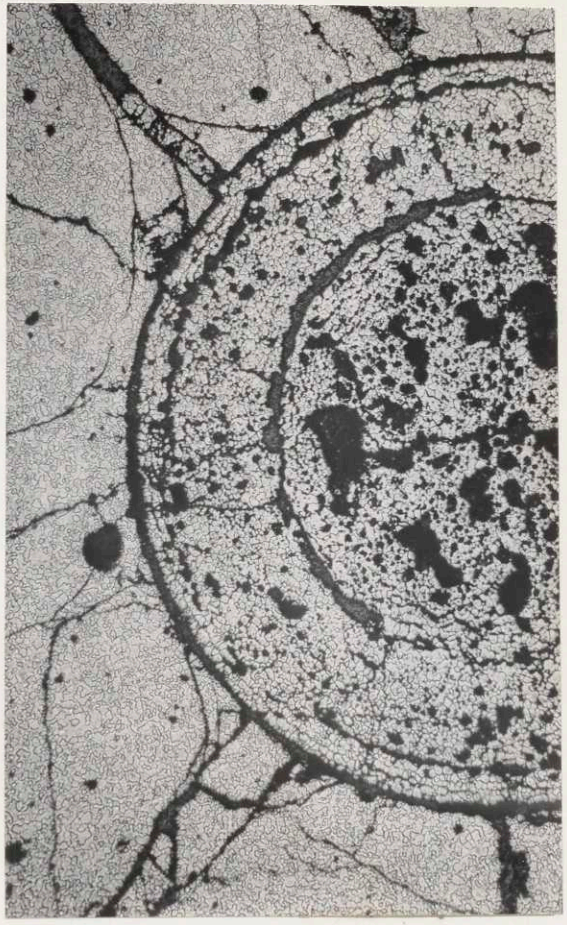

It has been postulated that the observed layering effect could have resulted from molten fuel initially driven by fuel-gas slugs, leaving layers of fuel on the blanket as the slugs moved upwards. This could then have been followed by a more homogeneous mixture of fuel and gas (porous structure in the center). A fuel bridge found across the void, shown in Figure 2.13, with sharp corners at the ends presumably indicating upward movement, could be explained by the fuel-gas slug concept (20).

Before being sectioned, the fuel pin was punctured and 38.8c.c. (at S.T.P.) of fission gas was collected (plus 6 c.c of the original fill gas). Analysis indicated that it was 83 percent xenon and 14 percent krypton (20).

FIGURE 2.13 (17)

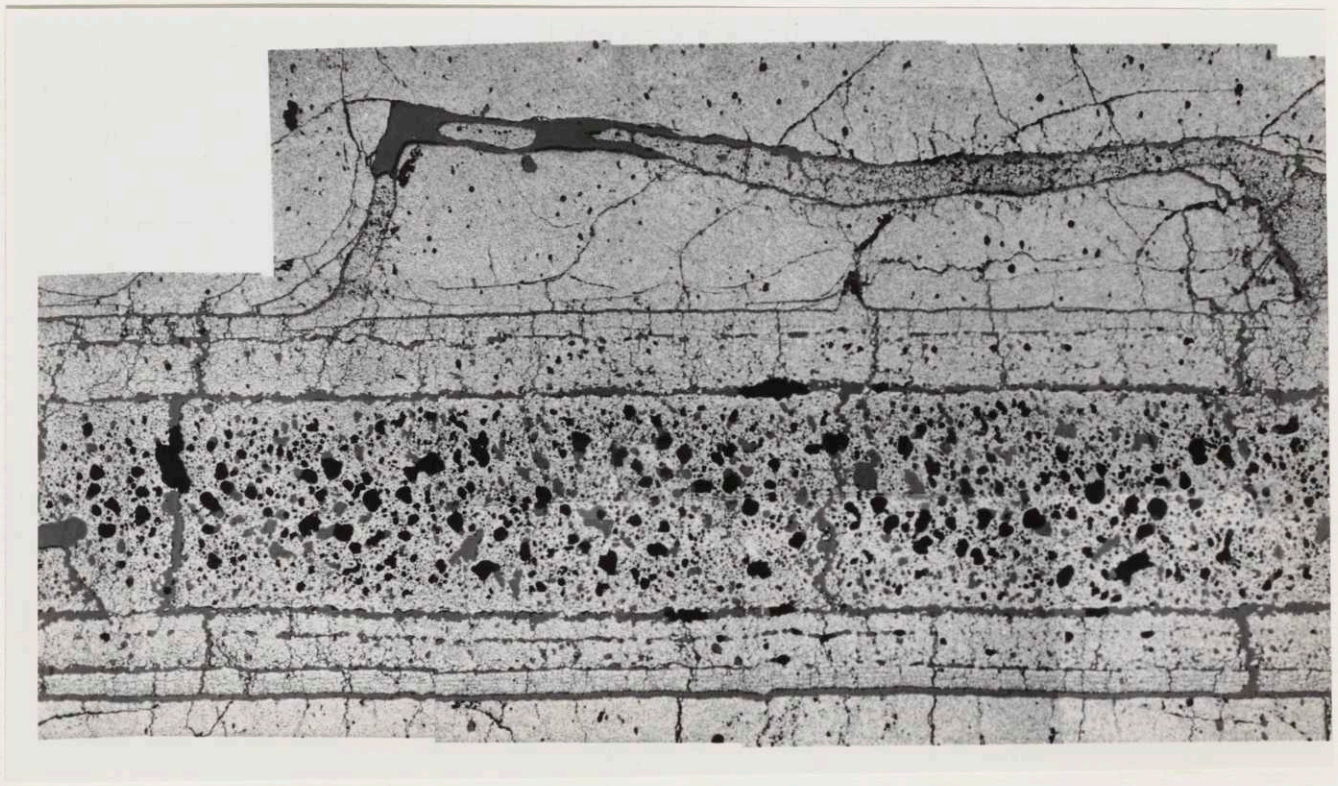

Chapter 3

MODEL FOR FUEL MOVEMENT

3.1 Explanation of Model

The model is in the form of a flow chart and is shown in Figure 3.1. Each block stands for one input or calculational procedure, and the entire sequence is based on the assumption that fission gas is the driving force behind fuel movement.

The primary purpose of the model is to correctly predict the fuel movement in an unfailed fuel pin, specifically the C5B pin. The model will be presented in general terms, however, so that it can be applied, with little modification, to standard LMFBR pins (i.e. without annular blanket pellets). Several assumption will be made in the model derivation. In the application to C5B, further simplifying assumptions will be made. These further assumptions are not part of the general model and would be replaced by other assumptions in the application of the model to other pin geometries.

The blocks enclosed in double lines indicate steps where known results are checked against theoretical predictions up to that step. In the C5B test, it was possible to observe many things about the pin. It was observed, of course, that the pin did not fail. Thus a

MODEL FOR MOLTEN FUEL MOVEMENT

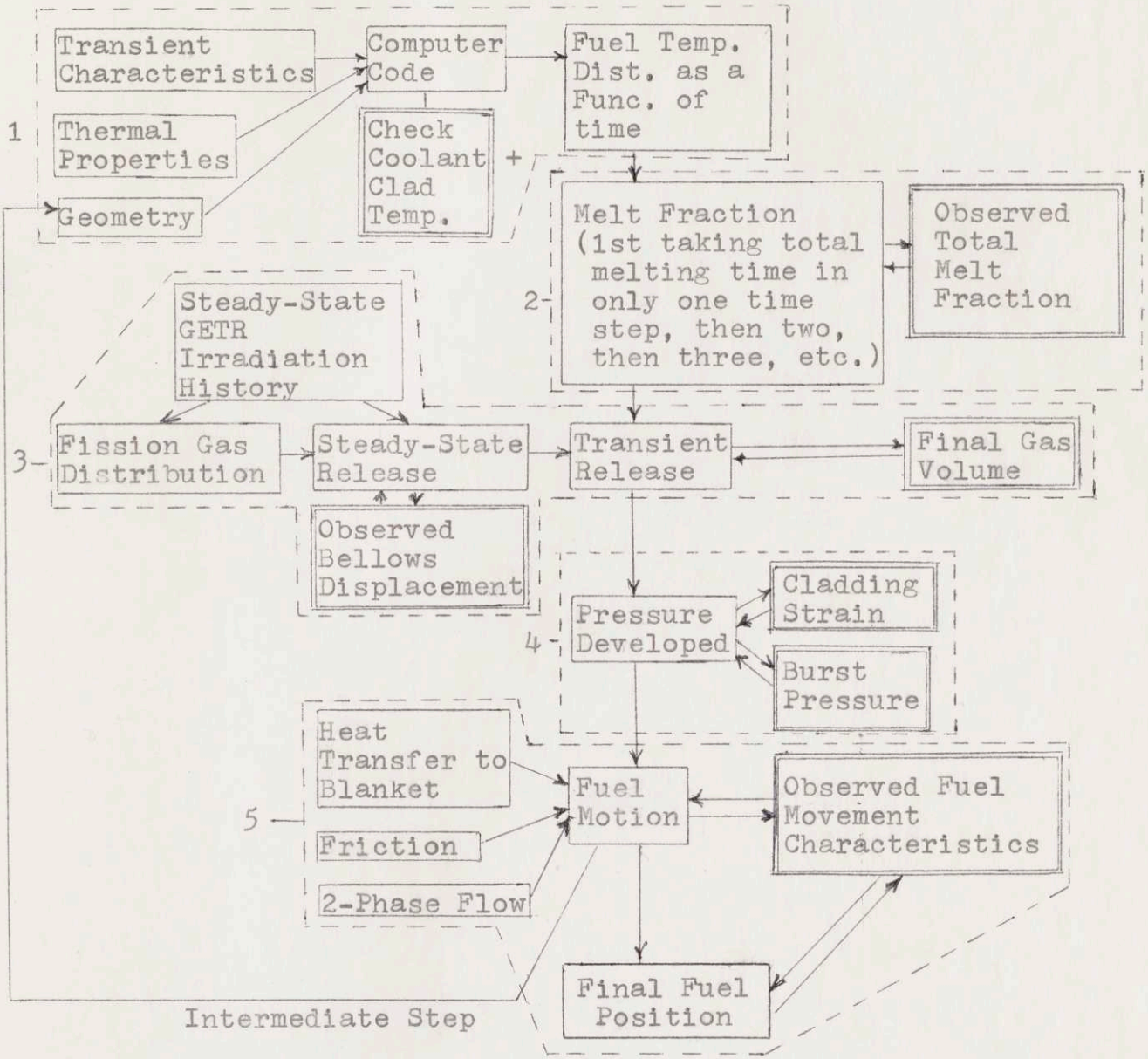

FIGURE 3.1

theoretical prediction of a pressure higher than the burst pressure would be suspect. These steps thus help to verify and keep accurate the model. It is important that these checks occur throughout the procedure, since each succeeding block is dependent on the precceding assumptions. The final check in the C5B case, of course, is to determine if the predicted fuel movement agrees with the observed movement. This check alone would not be valuable, in that it would be impossible to isolate the faulty assumption if the agreement was poor.

In application to another pin, some or all of the check blocks would not be used, since not all of the observable results would be known. It would still be possible to use the model with none of the check blocks, since the check blocks are not used as input for any later step.

3.2 Detail Model Description

The model can be divided into five distinct areas:

1. Temperature distribution of fuel and fuel melt front history.
2. Fraction of fuel melted
3. fission gas release
4. internal pressure developed
5. resulting fuel motion

3.2.1 Temperature Distribution of Fuel and Melt Front History

3.2.1.1 Procedure

The first area is relatively straight forward. A computer code is used, with the transient characteristics and the thermal properties of the assembly as input. The output is the fuel temperature distribution as a function of time (T(r,z,t)). A check on the cladding temperature is made to determine if there is any clad melting or possible boiling. This can be checked against observed results, if available.

The characteristics necessary for input include the normalized pin power as a function of time, the axial power shape, the radial power shape, the initial temperature distribution in the capsule, and the coolant pressure and flow rate. (In several experimental tests, including C5A and C5B, coolant flow rate was zero, since the capsule were designed with stagnant coolant). In the case of an experimental capsule in a test reactor, such as TREAT, the normalized pin power function was found through the use of two other inputs: the total reactor power as a function of time and the power factor (the calculated ratio of test specimen power to the test reactor power, watts/cm fuel/test reactor watt. The power factors

are calculated prior to the transient tests and their accuracy is checked through the use of calibration transients.).

The necessary thermal properties include the following material properties: the density, specific heat, and thermal conductivity, as a function of temperature, of all the materials involved. For the fuel, these three property functions must be available for the liquid, as well as the solid phase. The latent heat of fusion of the fuel is another input, and the phase change temperature of the clad and the coolant must be available for reference, as well as that of the fuel. In addition, the heat transfer coefficient across the gap must be determined. (Its initial value can be arrived at through the calibration transients, and its transient behavior is normally predicted through comparison with other tests, considering the pretransient gap size.)

The necessity of providing the capsule geometry is obvious. The geometry, however, should be that which exists at the start of the transient, as opposed to the original geometry (i.e., an attempt must be made to determine the fuel-clad gap dimension after steady state irradiation, either by comparison with other tests or through the use of the neutron radiograph.)

The computer code selected must be capable of transient heat-transfer analysis, at least two-dimensional, and must take into account phase change in the fuel. A code which accepts temperature dependent material data is also a necessity. It has been suggested that the THTD code is the most accurate and flexible code available for meeting these requirements (14). The Argus program and the TIGER 5 heat transfer code also meet the requirements and are possible choices. The heat transfer module of the SASlA code can also may be used, although it is designed for pins with small radial flux depressions (i.e. LMFBR pins in a fast flux). It can be used when corrections for the radial power distribution are made.

The output of the computer code is the transient capsule temperature distribution. This includes the melt fraction as a function of time (melt front history.)

3.2.1.2 Checks

At this point the clad temperature is checked to determine if there is any clad melting. The possibility of sodium boiling is also investigated, since it is assumed that if either of these phenomena occur, the fuel movement model will not be sufficient to describe the behavior. Both phenomena bring in many other considerations.

It also necessary to check the melt fraction results to insure that the particular case can be adequately treated by the fuel movement model. An inherent assumption in the model is that the fuel melt front moves radially outward. In other words, all the fuel melts between $r = a$ and $r = b$ before any melts between $r = c$ and $r = d$, where $d > c > b > a$. The output of area one, the melt front history, shows explicitly if the fuel melts "from the inside-out." If it does not, the calculations are discontinued as the particular model is not valid for any other case.

Although the fuel melts from the inside in most transient the fuel can partially melt accross the entire fuel radius (31). Or, in a very fast transient with an unusually large flux depression, it can melt away from the center while the center is still solid. The three cases are shown in Figure 3.2.

If the fuel does not melt from the inside, the fuel movement involves a mixture of solid fuel, liquid fuel, and gas. Major modifications in the model would be necessary to account for such phenomena.

If neither clad melting nor sodium boiling exists, and the melt front moves radially outward, the calculations continue into the second area.

FIGURE 3.2

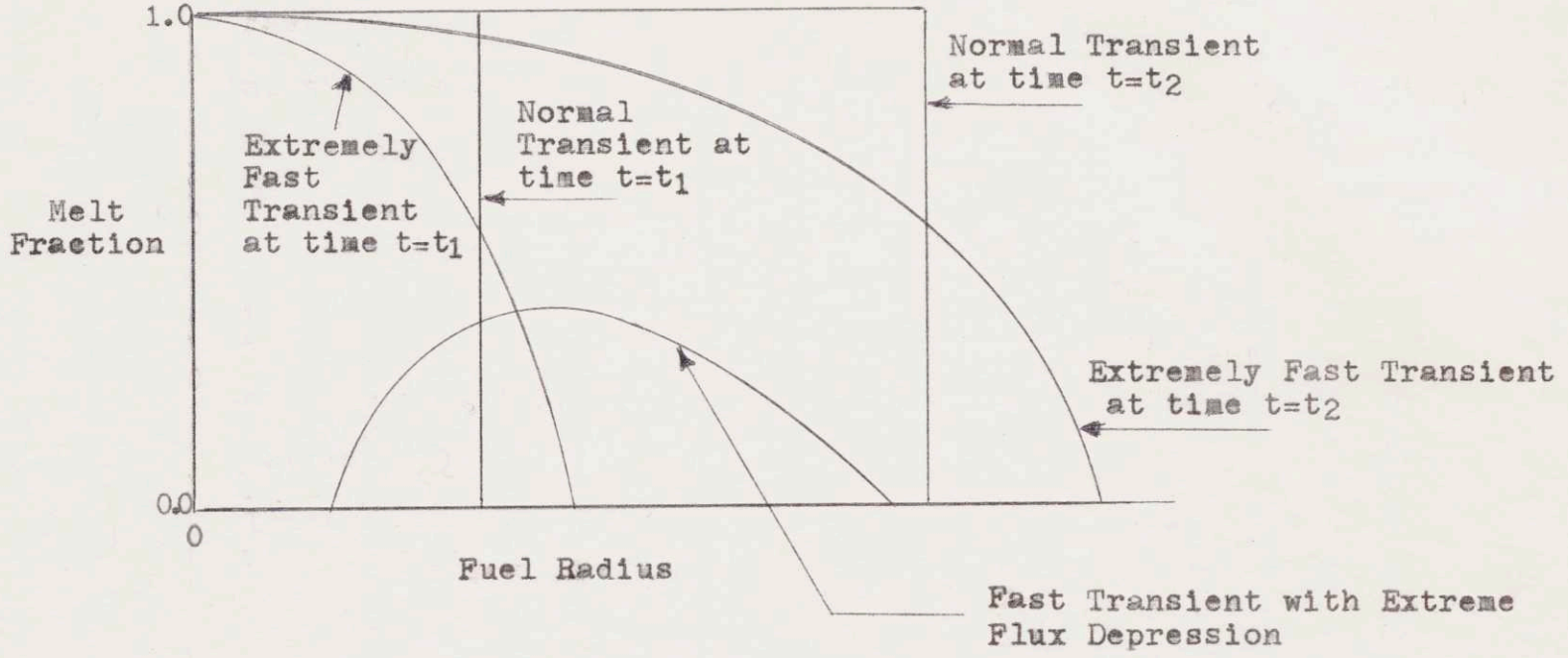
1.0
0.0
0
Melt Fraction
Fuel Radius
Normal Transient at time t=t2
Normal Transient at time t=t1
Extremely Fast Transient at time t=t1
Extremely Fast Transient at time t=t2
Fast Transient with Extreme Flux Depression

3.2.2 Fraction of Fuel Melted

3.2.2.1 Assumptions

In order to decide what particular melt fraction is to be used in later calcuations, one must make an assumption. The particular assumption can be selected from three alternatives.

3.2.2.1.1 The first alternative is that fuel melting is completed to the maximum value found in area one before any fuel motion occurs. (This is equivalent to saying, from the time of the fuel motion versus time of fuel melting standpoint, that the fuel melts instantaneously.) This assumption was made by G.E. (20) in their analysis of the C5B test and has been normally made in most fuel movement studies. In the G.E. analysis of C5B, however, only a conservative bound for the problem was desired, and the assumption was made to simplify a complex process. It was not first proven to be accurate for the C5B test (15). It has been suggested that the assumption should not be made exclusively, although it may prove to be an accurate assumption in some cases (11,31).

3.2.2.1.2 The second alternative is the opposite of the first. The assumption is that the fuel moves instantaneously, in comparison to the melt front motion. That is, for

a particular melt fraction, the subsequent fuel movement is assumed to go to completion before any further melting continues.

3.2.2.1.3 The third alternative is a combination of the first two. In this case, the fuel movement associated with a particular fraction of fuel melted is assumed to continue only for the time period associated with corresponding melt fraction. (The time period associated with a particular melt fraction is simply the time the fuel takes to melt to that fraction, with time beginning at the start of melting of the fraction of fuel under consideration). It is assumed that motion halts at the end of that time step and the geometry of the molten fuel remains fixed (is "frozen") until the next fuel melt fraction is calculated.

3.2.2.1.4 Another assumption is necessary. This concerns the effect on the heat generation function of changing the flux distribution. Fuel is moved out of the active core region and it is necessary to compute the effect of this change on the heat generation function. It is assumed that there is no change in the pin flux shape due to the movement of fuel, and thus changes in the heat generation rate will be made only thru changes in the distribution of fissile materials.

This assumption was made due to consideration of the fact that, especially dealing with a test pin such as a TREAT pin, the source of neutrons is virtually independent of the pin. The flux shape change due to fuel motion, but the changes are small. The changes are most pronounced for a pin with a central void (because, after melting, fuel is in the center), but they still can be ignored.

3.2.2.2 Procedure

The use of a particular alternative depends upon the conditions of the problem. The first step is to determine ΔT_1. This is the time step between the time of initiation of fuel melting and the time that the maximum melt fraction is reached.

As a starting point, alternative one is used in all cases. The total melt fraction (the maximum calculated in area one) is used as an input to area three. The calculation continues until the final movement is found. The time of completion of such motion, t_1, is noted, where t_1 is measured from the initiation of movement. Next t_1 and ΔT_1 are compared.

If $t_1 >> \Delta T_1$, the fuel moves much slower than the melt front. In this case alternate one will not be inaccurate and the fuel movement result already calculated will be accepted as the final result. (The result will

be taken as final unless a check at some later stage in the model indicates that a smaller time step is necessary. If this is the case, calculations will continue as in the case of $t_1 \simeq \Delta T_1$, discussed below).

A value of 10 has been arbitrarily chosen as the cut-off number for the ratio between t_1 and ΔT_1. Thus the criterion described above is $t_1/\Delta T_1 > 10$.

If $t_1 << \Delta T_1$, the melt front is moving much slower than the fuel. In this case alternative two is selected. More iterations are necessary.

The time step is divided in two ($\Delta T_2 = \Delta T_1/2$). The melt fraction at the end of the time step, ΔT_2, is used as an input to area three. (This melt fraction is less than the total melt fraction used in the first iteration). The calculations continue through all areas, until a final fuel movement is completed. The movement is assumed to be completed before more fuel is melted (i.e. it moves instantaneously). This final movement is used to change the capsule geometry. The new geometry is then a new input to area one, and the cycle is continued for the second ΔT_2 (and the corresponding second melt fraction).

The specific changes in the geometry for the second ΔT_2 calculation are a reduction in the fuel density and heat generation function for the inner region which now

contain a fuel-gas mixutre. This is a region that melted in the first time, plus the control void region, if any. Specifically, for the input to the heat transfer calculations in area one, it is assumed that a new material occupies this inner region. The new material is assumed to have the same characteristics as the original fuel, except for the density and the volumetric heat generation rate. For a solid pin, the density and heat generation functions are reduced in the region of fuel melting is reduced by a factor F_1, where $F_1 = V_{orig\ solid\ fuel}/V_{total}$, where the assumption that the flux shape does not change due to motion has been made. V_{total} is defined in Figure 3.3.

In the case of a pin that had a central void, the procedure is slightly more complicated, since the heat generation function was not defined for the void. To find the new heat generation function, one uses the relation that the heat generation function is equal to the fissile number density times the cross section times the flux, one again makes use of the assumption that the flux does not change due to motion. One then calculates the heat generation function for the region from the fuel center out to the melt radius by multiplying the flux distribution times the cross-section (constant also) times the new fissile number density. The new fissile number density is simply F_1 times the original fuel number density. This heat genera-

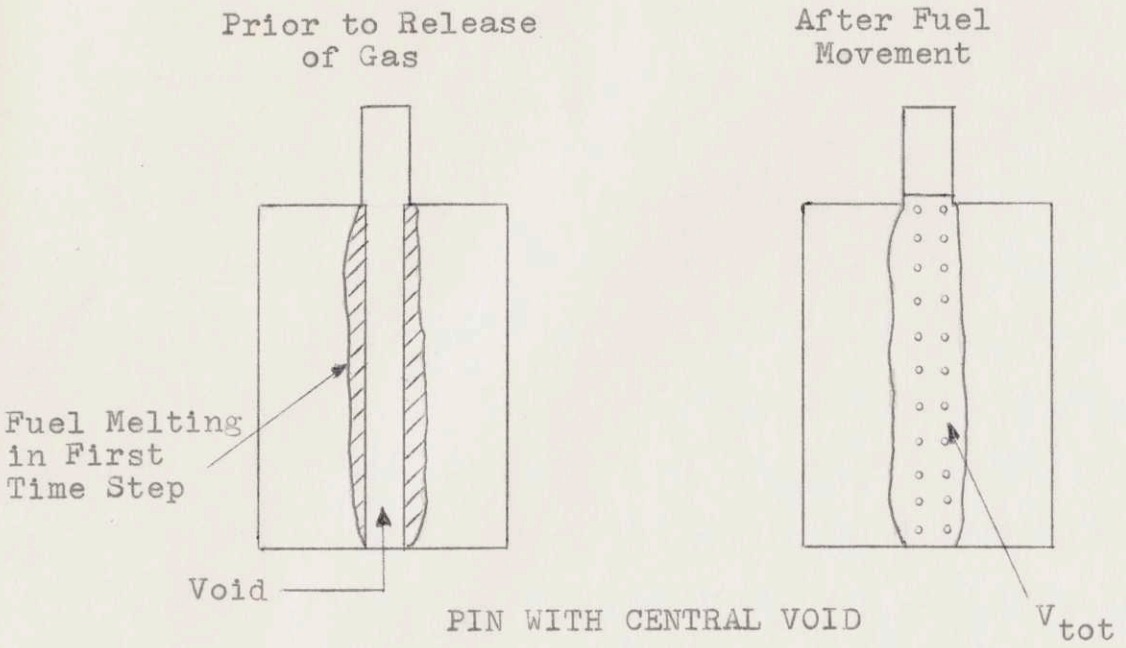
Prior to Release of Gas
After Fuel Movement
Fuel Melting in First Time Step
Void
PIN WITH CENTRAL VOID
V_{tot}

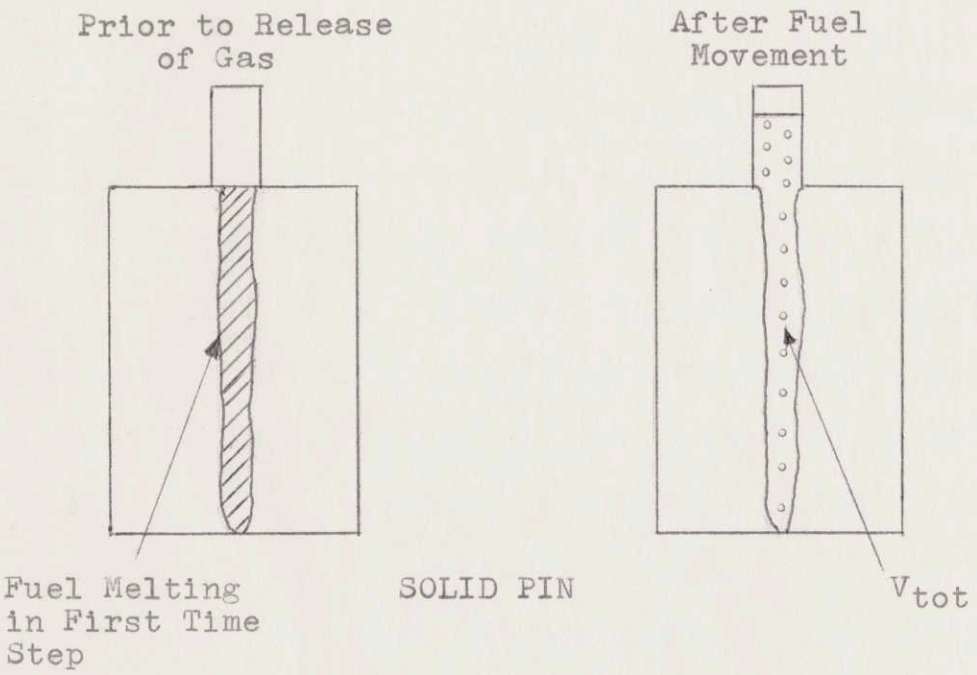
Prior to Release of Gas
After Fuel Movement
Fuel Melting in First Time Step
SOLID PIN
V_{tot}

FIGURE 3.3

tion rate for the "new" region is then used as an input to area one (the original heat generation rate is still used for the rest of the fuel-the part that hasn't melted). With these new inputs to the heat transfer calculations, a new temperature distribution is found. The transient calculations start at time $t_0 + \Delta T_2$, where t_0 is the time of initiation of melting. The input thermal properties are taken as those existing at $t_0 + \Delta T_2$, according to the temperature distribution results from the first (or preceding) cycle. The fraction of fuel melted in the second ΔT_2 is computed, and the result is used in the next area. The cycle continues through area five, where a final fuel movement is calculated. If this result is very different from the very first result, obtained through the use of the complete melting before motion assumption, further iterations should be made, until the results of the last iteration do not differ appreciably from the preceding results and all checks in different stages of the model indicate accuracy. In the case of $t_1 << \Delta T_1$, it might be apparent after the first two interations that a very small ΔT_1 is necessary and then one could jump to a division of ΔT_1 into ten equal steps, for example. (This specific method is addressed mainly to axial movement, i.e. movement to an annular blanket, and to find the final extent of fuel movement. In other model applications,

the technique would vary slightly. If the fuel moved outside the pin through failure, for example, the new density mentioned would have to be calculated on a mass basis: P_{new} = (original mass - expelled mass)/volume.) Again the cutoff number is arbitrarily set at 10 in this alternative. Assumption two is thus used when $t_1/\Delta T_1 < 0.1$. When t_1 is close to ΔT_1, the process is more complicated. In actuality, of course, the process is continuous under all conditions. That is more fuel is melting and adding to the driving force, while the fuel that first melted is in motion. Stepwise calculations, however, are used to simplify the problem.

If $10\ \Delta T_1 \geq t_1 \geq 0.1\ \Delta T_1$, alternative three is selected. This means that the fuel is assumed to melt and move in small time steps. The fuel only moves far as long as the time step. Then the geometry is frozen until the melting for the next time step is calculated. Iterations continue until all checks indicate that the results are accurate.

The procedure is shown in Figure 3.4.

3.2.2.3 Checks and Comments

In some cases, it is possible to check the results of this area with known results. In the C5B test, for example, the final fraction of fuel melted is known from observations (20).

Determine

from heat transfer code output

from completion of one iteration of model - i.e. make assumption one - that the fuel melts instantaneously, and calculate the time needed to complete movement

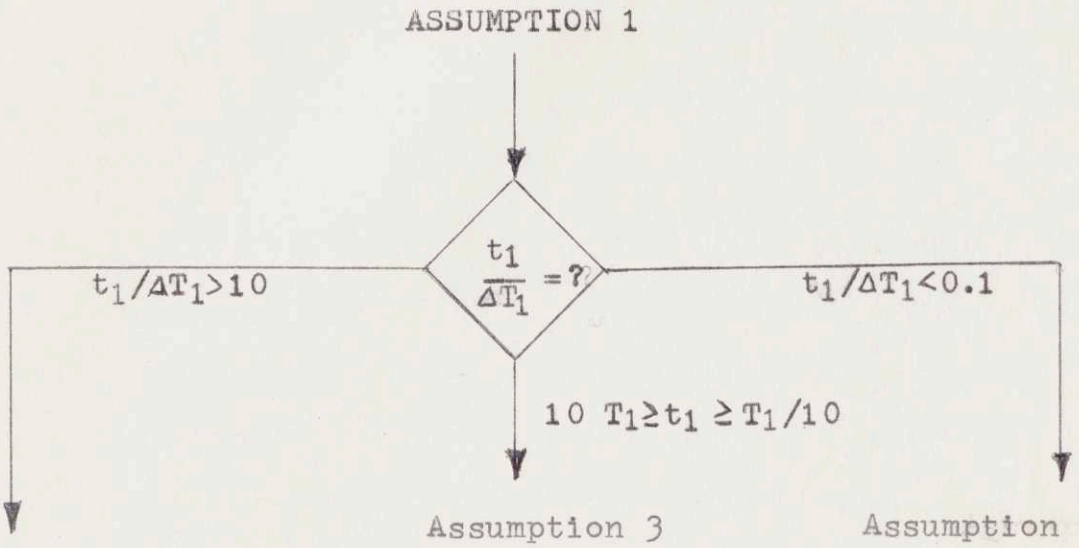

First interaction is final result - Assumption 1 (that fuel melts instantaneously) is accurate.

Assumption 3

divides time of melting into increments and do step-by-step calculations. In each step, the extent of fuel melting is calculated and then the resulting fuel movement is calculating, assuming the fuel moves only as far as it can in that The liquid fuel is then frozen in that position for the next melting calculation, etc.

Assumption 2

divide time of melting into increments and do step-by-step calculations - assuming that the fuel moves instantaneously.

Figure 3.4

In considering fuel movement after melting, the liquid fuel follows a path to the relief area. In a normal pin (i.e., solid) the relief area would be the coolant channel and the fuel forms its own path by widening a crack or forming a new crack in the solid fuel. In considering axial movement, this model inherently assumes that their is a path to the relief area that the molten fuel can follow. This case is shown in Figure 3.5a. In Figure 3.5b, there is no path to the relief area and the molten fuel must either push a solid fuel plug up the blanket or form a crack in the solid fuel surrounding it. Again this case considering solid fuel cannot be adequately described by the current model, and a different method must be used. Normally, the existence of a central void guarantees a path to an axial relief area. If there is no central void, a relatively flat axial power profile (such as in C5B) or the existence of the hotter coolant at the top of the pin can insure that melting at the top occurs soon after melting at the axial centerline. Thus it is seen that the number of cases to which the current model cannot be applied is low. (Even if there is not a path to the relief area, the basic theoretical assumptions about the driving force in the model will hold. Modifications for the existence of solid fuel segments or cracking must be made, however.)

PATH FOR FUEL MOTION

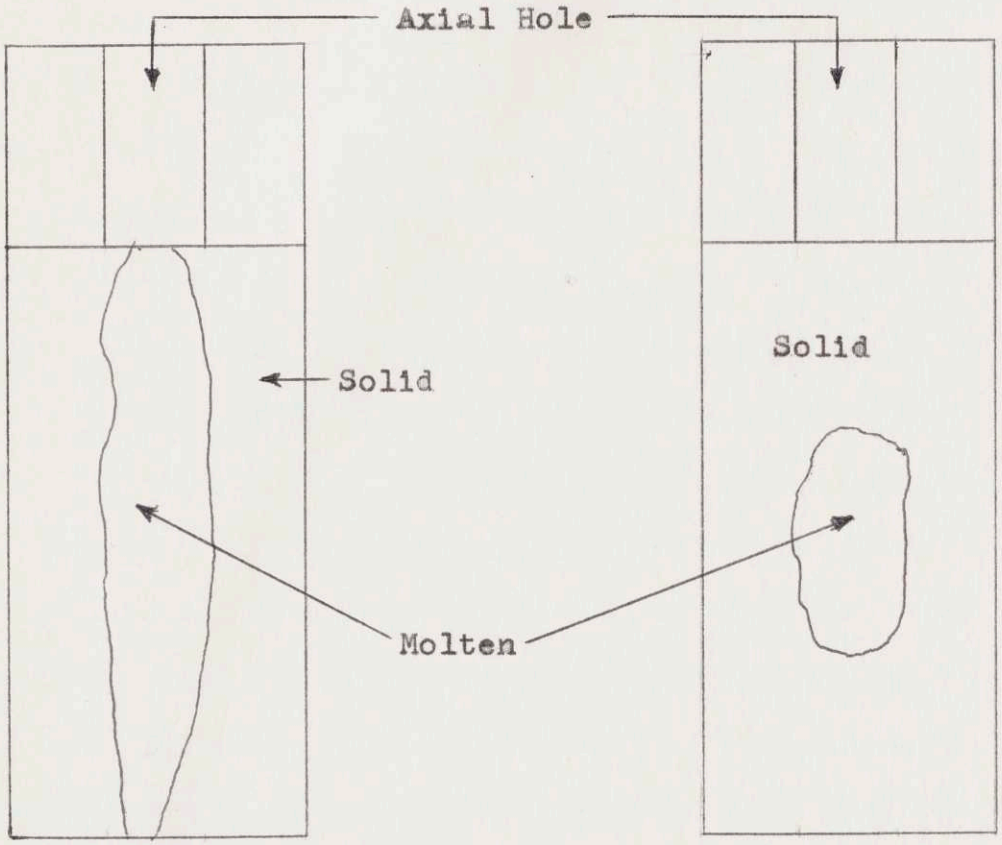

FIGURE 3.5

3.2.3 Area 3: Fission Gas Release

3.2.3.1 Assumptions

3.2.3.1.1 The first assumption of area 3 is that the steady state release rate of the fission gas trapped in the fuel can be related to the fuel temperature by the Lewis model (22), Figure 3.6.

Although the fuel temperature has been shown to be the main factor (26), the release rate is actually dependent on many other factors. It has been shown, for example, that a disproportionate amount of fission gas release can be associated with major reactor power changes (24). No numerical relation for this dependence, however, is available. Due to the importance of the many factors, a complete steady-state irradiation history is necessary for a truly accurate determination. This model will assume, however, that the Lewis temperature relation will suffice. Although developed for Xenon, the behavior is the same for Kryton (26), for example, and the Lewis model is used for all fission gas. Whenever another factor is extremely atypical, (such as a test involving an unusually large number of start-ups and shut-downs), the user can make corrections in the application of the Lewis model, in accord with the experimental experience concerning the factor involved.

GAS RELEASE MODEL

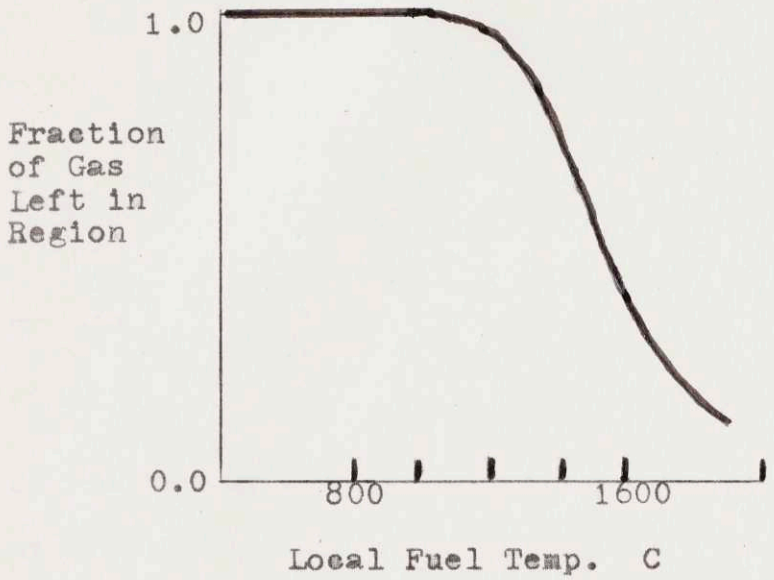

FIGURE 3.6

3.2.3.1.2 The second assumption of area 3 is the central assumption of this thesis: that the fission gas trapped in the fuel is released when the fuel melts.

It has been suggested that the trapped fission gas can be possibly released and start fuel motion before the particular fuel region has completely melted, i.e., gone through the heat of fusion. Some investigators have suggested that the gas could possibly be released when the melting temperature is reached (31). Figure 3.7 represents the difference in the amount of fuel into heat of fusion, and through heat of fusion, according to THTD calculations for a typical TREAT transient (C4A). It can be seen that the difference is great. In this model it will be assumed that gas release only occurs after the fuel is through heat of fusion, since this assumption has been used, with success, in the past (30). Actually, the gas is probably released at some intermediate stage. If this intermediate stage is closer to the "gas released upon reaching the melting temperature" assumption, the model will underestimate the intensity of fuel motion. (This is because more pressure would be developed, at an earlier time, than would be calculated according to the "release upon melting" assumption.)

FIGURE 3.7

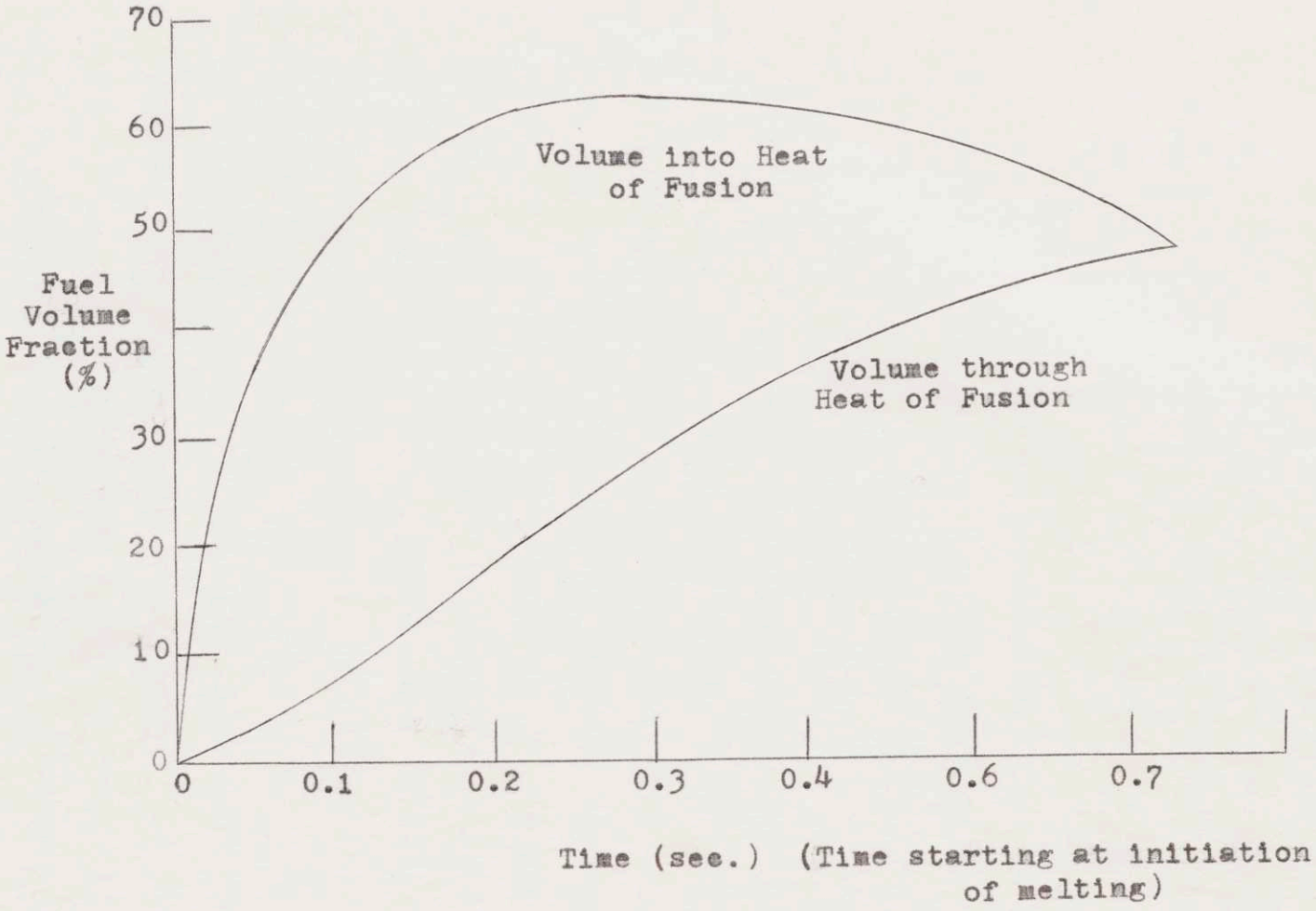
70
60
50
30
20
10
0
Fuel Volume Fraction (%)
Volume into Heat of Fusion
Volume through Heat of Fusion
0
0.1
0.2
0.3
0.4
0.6
0.7
Time (sec.) (Time starting at initiation of melting)

3.2.3.1.3 One further assumption is that a negligible amount of fission gas is generated during the short time of the transient. It is assumed that only the fission gas already existing in the fuel will affect fuel movement.

3.2.3.2 Procedure

First one must determine the distribution within the pin of the fission gas produced during steady state operation. The amount of fission gas is determined from the burnup. (The amount of gas is proportional to the number of fissions. Approximately 15 percent of the fission products are gases (26), and there are 2 atoms per fission. Thus there approximately .30 gas atoms produced for each fission. The number of fissions is directly proportional to the burnup.) The distribution of the gas in the fuel pin is simply equal to the radial flux distribution for the steady-state irradiation. Most of the fission gas produced remains trapped within the fuel structure, but some is released.

To determine the amount that is released, assumption 1 (the Lewis relation) is made. The specific procedure is to divide the pin into radial segments, compute the average temperature in each segment (from the calculated steady-state temperature distribution), and compute the release rate associated with the particular segment. The

amount of fission gas trapped in that segment is found from the fission gas distribution discussed above, and the product of the two factors (release rate times amount of gas) yields the fission gas release for that segment. The exact size of the segment is arbitrary and is determined in each individual case so as to insure the degree of accuracy required.

Assumptions two and three are now employed. Assumption two states that all the fission gas trapped in the fuel is released upon the melting of the fuel and three states that only the fission gas generated prior to the transient is involved. The amount of gas originally trapped in the fuel is known. The amount released is known. The difference is the amount still trapped (as a function of r), and by the use of the melt fraction output of area two, one determines the amount of gas released in the transient.

3.2.3.3 Checks and Comments

In some cases, one can check the value for total steady-state fission gas release against observed results. In C5B, for example, the bellows was calibrated so that the pin internal pressure could be derived from the position of the bellows in the pre-transient neutron radiographs.

The sum of the transient release and the steady-state release represents the total of "free" fission gas in the pin. If it is assumed that very little gas is retrapped, one could expect to remove the total amount of "free" fission gas from an unfailed pin after the transient. This represents another possible check on the model.

3.2.4 Area 4: Internal Pressure Developed

3.2.4.1 Assumptions

3.2.4.1.1 The first assumption is that the fission gas released during the transient cannot vent to the plenum during the time of the transient. This assumption has been experimentally verified (30).

The second assumption is that the temperature of the transient released gas remains constant, at the fuel melting temperature. This appears to be accurate in that further heat normally would go to melting more fuel on the surface of the molten mass (although the gas in the center of the molten fuel might increase in temperature slightly).

The third assumption concerns the volume that the fission gas occupies when it is released. In most cases the gas occupies whatever volume is left in the active fuel region, after the increase in molten fuel volume takes place. This is normally a substantial volume due to the existence of a central void. In pins without a central void, the volume left could be very small or non-existent. Obviously some lower limit must be set to give a realistic volume for initial pressure calculations. It has been suggested that the fuel porosity be used as this lower limit (2)), and this model will make use of that suggestion. The volume must exist, so an inherent related assumption is

that the fuel-gas mixture moves instantaneously out of the active fuel region to a level to allow the gas to occupy the fuel porosity volume. The problem is again that the process is continuous. The fuel-gas mixture moves as soon as the first fuel is melted.

The pressure as the driving force is the prime consideration in this model, and thus the third assumption is necessary to allow a calculation of the pressure in some cases (a volume must exist in order to calculate the pressure of a gas). The assumption is expected to result in incorrect prediction of the fuel motion near the time that motion commences. Later in motion, however, it is felt that the pressure effect will override the volume increase effect so greatly that the prediction will not be inaccurate.

The fourth assumption states that all the gas situated in the natural voids (fuel porosity) in the active fuel region, and one half of the gas in the central void (if any), is unable to reach the plenum region upon the melting of the fuel (i.e., it is surrounded by molten fuel before it can "escape" and it joins with the released gas to pressurize the mixture). It is expected that the gas located in the pores would have no chance of escape during melting. In the case of a central void, however, some portion of the gas would be expected to escape and reach the plenum. The

value of one half was chosen arbitrarily to signify the probability of escape. Depending upon the melt front motion axially, however, this value could be adjusted for a specific case. (If the fuel melted near the bottom first, as an extreme example, the initial pressure would drive most of the gas in the central void to the plenum region before the upper fuel could melt and trap the gas.)

3.2.4.2 Procedure

The procedure in this area is to make assumptions one and two and use the perfect gas law to find the pressure of the gas. The total void space in the active fuel region is calculated, and the volume increase of the melted fuel is subtracted from this, and the remaining volume is taken as the volume available to the gas. If this calculated volume is less than the original fuel porosity, assumption three is made so that at least the original fuel porosity is available for the gas to occupy. Assumption three assumes instantaneous movement (due to fuel expansion) before the fuel movement is commenced. The extent of this initial movement should, of course, be small compared to the expected final fuel movement. (If the final movement calculated from using this method is not much greater than the initial movement, a smaller time step for melting is used and thus the initial movement is reduced).

The entire problem exists only for the first iteration for any size time step. In subsequent iterations (i.e., when a second layer of fuel is assumed to melt) the existing gas already occupies a volume. The gas just released is assumed to occupy the same volume, and the volume is decreased due to the instantaneous volume increase accompanying the last layer of fuel melting. The error associated with the instantaneous melting assumption, of course, will be reduced as the time step is reduced.

In any case, the gas temperature, amount of fission gas released, and volume are known. Now it is only necessary to apply assumption four, which states how much of the gas already in a free state in the active care region must be used in the determination of pressure.

To apply assumption four, the amount of gas in the active fuel region must be known. This is found by first calculating the pre-transient pressure. The pre-transient pressure is just the new volume of gas in the total pin void space over the original volume of gas in that void space, times the original pressure, this is simple

$$P_{new} = \frac{V_{new}}{V_{orig}} P_{orig} \quad \text{with} \quad T = \text{constant}$$

an expression of the ideal gas law.

For example, if the original pressure in a pin was one atmosphere, there were originally 5 c.c. of cover gas (at S.T.P.), and 5 c.c. of fission gas (at S.T.P.) was released during steady-state irradiation, the pre-transient pressure would be

$$P_{new} = \frac{5 \text{c.c.} + 5 \text{c.c.}}{5 \text{ c.c.}} (1 \text{ atmosphere}) = 2 \text{ atmospheres.}$$

Using the pre-transient pressure, one can calculate the amount of gas in the voids in the active fuel region. At one atmosphere pressure 10 c.c. of gas would occupy 10 c.c. of volume. At two atmospheres, according to the ideal gas low, 10 c.c. would only occupy 5 c.c. of volume (the temperature is considered to be contant here). Thus the volume at S.T.P. of a gas is simply the pressure that it is under times the volume that it is occupying.

For example, if there are 5.0 c.c. of void space in an active core region (and thus 5.0 c.c. of gas, at the existing conditions), and the pressure is 2.0 atmospheres, the amount of gas is simply 2.0 x 5.0 = 10.0 c.c. of gas at S.T.P.

The amount of gas in the active fuel void can thus be calculated and assumption four can be applied, yielding the amoung of pre-transient gas that will help to pressurize the fuel.

The total of this last calculation and the fission gas released in the transient is the amount of gas that will be pressurized. Since the total amount, the temperature, and the volume occupied is known, the pressure can be found from the ideal gas law.

3.2.4.3 Checks

The internal pressure can possibly be checked again against observed results. A uniform clad deformation can be related to a corresponding internal pressure, and also the clad burst condition can be related to an internal pressure. Obviously the model should not predict a pressure greater than the clad burst pressure if the pin is known not to have failed. If such is the case, a smaller time step must be used. Likewise the pressure can be compared to a uniform clad deformation, if one exists, to test the model accuracy. It is not normally known, however, at what time in movement deformation occurred.

3.2.5 Fuel Motion

3.2.5.1 Assumptions

3.2.5.1.1 The first assumption is that for the purposes of fuel motion, the fuel gas mixture is treated as a homogeneous, compressible, fluid.

3.2.5.1.2 The second assumption is that the temperature of the mixture does not change appreciably during movement. This assumption should not be very inaccurate, for the reasons discussed previously. As the mixture moves outside the active fuel region into a colder region (the blanket, for example), the effect of the colder region is to solidify part of the molten fuel, rather than to lower its temperature. Again the very center of the fuel could increase in temperature (if heat generation continued).

3.2.5.1.3 The third assumption is that heat transfer and two-phase flow considerations are negligible. The assumption is employed in order that initial calculations can be made. The accuracy of the assumption is checked at a later stage and corrections due to the heat transfer and two-phase flow effects are possible.

3.2.5.1.4 The fourth assumption is that the analysis of the velocity distribution can be accomplished in a one-dimensional study. The model deals only with the velocity

in the z direction (for assumed axial movement). In cases where two-dimensional effects are involved, suitable corrections could be made.

3.5.2 Procedure

Assumptions one, two, and four are made and the continuity and momentum equation for a compressible fluid are written (considering only the axial velocity distribution).

The continuity equation is

$$\frac{-\partial \rho}{\partial t} = \frac{\partial}{\partial z}(\rho V_z) \ .$$

The momentum equation reduces to

$$\frac{\partial}{\partial t}(\rho V_z) = - \frac{\partial(\rho V_z^2)}{\partial z} - \frac{dP}{dz} - f(V_z) - \rho g$$

where $f(V_z)$ is the friction surface force per unit volume.

Combining the continuity equation with the momentum equation results in

$$\rho \frac{\partial V_z}{\partial t} = - \rho V_z \frac{\partial V_z}{\partial z} - \frac{dP}{dz} - f(V_z) - \rho g \qquad (5.1)$$

To solve the equation, the finite difference method can be used. Rearranging equation (5.1),

$$\frac{\partial V_z}{\partial t} = - V_z \frac{\partial V_z}{\partial z} - \frac{1}{\rho} \frac{dP}{dz} - \frac{f(V_z)}{\rho} - g \qquad (5.2)$$

For a solution of this problem, several other relations are needed. The friction force can be tabulated as a function of velocity. (It has been suggested that the rough pipe correlations be used (34).)

Since the liquid fuel in the mixture is assumed incompressible, the mixture pressure can be obtained thru considerations of the fission gas only. Assuming that the fission gas in the mixture obeys the ideal gas law, P can be written as a function of ρ and T. Using assumption two, T is constant so P is known as a function of ρ.

$$P = \rho RT = \rho \bar{R} T/M \qquad (5.3)$$

where R is gas constant for fission gas

$\bar{R}$ is the universal gas constant

M is the molecular weight of the fission gas.

Now ρ_i, the density at one node in a finite difference scheme, can be related to the velocity (V_z will be written here simply as V).

The mass at a particular node at then end of time step t_n is equal to the mass at that node at the end of time step t_{n-1}, plus the mass that has moved into that node in time step t_n minus the mass that moved out of that node in time step t_n. Using subscripts to refer to the nodes in the axial direction and superscripts to

refer to the time steps; writing the mass as the density times the volume; and using $G = VA$; one has has:

$$\rho_i^n A_i \Delta_z = \rho_i^{n-1} A_i \Delta_z + \rho_{i,i-1}^{n-1} G_{i,i-1}^{n-1} \Delta t - \rho_{i,i+1}^{n-1} G_{i,i+1}^{n-1} \Delta t \tag{5.4}$$

where ρ_i^n is the density at node i at time t_n and $\rho_{i,i-1}^{n-1} = (\rho_i^{n-1} + \rho_{i-1}^{n-1})/2$. To simplify,

$$\rho_i^n = \rho_i^{n-1} + \frac{\Delta t}{A_i \Delta z}\left(\rho_{i,i-1}^{n-1} G_{i,i-1}^{n-1} - \rho_{i,i+1}^{n-1} G_{i,i+1}^{n-1}\right) \tag{5.5}$$

Now equation (5.2) can be written in finite difference form. Specifically:

$$\frac{V_i^{n+1} + V_i^n}{\Delta t} = -V_i^n\left[\frac{V_{i,i-1}^n - V_{i,i+1}^n}{\Delta z}\right] - \frac{1}{\rho_i^n}\left[\frac{P_{i,i-1}^n - P_{i,i+1}^n}{\Delta z}\right] - \frac{1}{\rho_i}\left[F_{i,i-1}^n - F_{i,i+1}^n\right] - g$$

Solving for V_i^{n+1},

$$V_i^{n+1} = V_i^n - \Delta t\, V_i^n\left[\frac{V_{i,i-1}^n - V_{i,i+1}^n}{\Delta z}\right] - \frac{\Delta t}{\rho_i}\left[\frac{\rho_{i,i-1}^n - \rho_{i,i+1}^n}{\Delta z}\right] - \frac{\Delta t}{\rho_i^n}\left[F_{i,i-1}^n - F_{i,i+1}^n\right] - g\Delta t \tag{5.6}$$

where ρ_i^n is a known function of V_i^n (equation (5.5), and ρ_i^n is a known function of ρ_i^n (equation (5.3) and thus also a function V_i^n .

The specific finite difference scheme is shown in Figure 3.8. First calculations of V_i^1 are made for each axial node. Then calculations are made for V_i^2 at each axial node. The calculations continue with the result being the velocity at each axial point as a function of time.

There are several problems associated with the application of the finite difference method to this problem. First, there is a velocity discontinuity at the cavity mouth (the point that the fuel moves from the active core). This must be remembered in the application and a nodal point should <u>not</u> be placed on the fuel mouth boundary (two different velocities would then be associated with one nodal point).

One further problem is associated with the finite difference application: the interface between the fuel-gas mixture and the plenum gas is moving. This means that the interface can be inside a node. In this case the use of the surrounding nodal values to calculate a particular variable value would not be accurate, due to the extreme density differences. It is necessary to set boundary conditions which enable a different method to be used at the

FINITE DIFFERENCE SCHEME

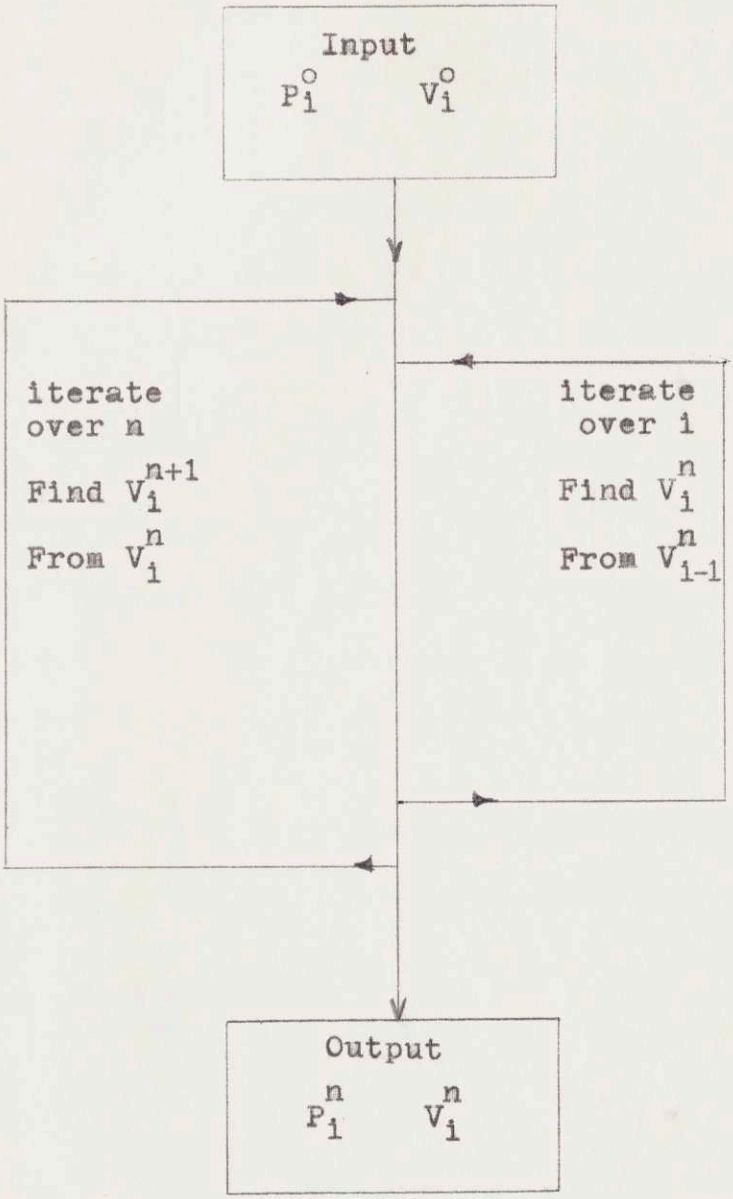

FIGURE 3.8

interface. Or, it has been suggested that the application be made using a Lagrangian, or moving, coordinate system.

Due to the computer needs and the problems associated with the application of the finite difference method, a different, simplified method will be used to solve the governing equation for the motion of the mixture. The finite difference method should be used, however, when possible, in order to insure the accuracy of the solution.

3.2.5.3 Simplified Method

The method used in this model follows from the axial squirting model under development at A.N.L. Equation (5.1),

$$\rho \frac{\partial V_z}{\partial z} = - \rho V_z \frac{\partial V_z}{\partial z} - \frac{dP}{dz} - f(V_z) - \rho g \qquad (5.1)$$

serves as the starting point. An integral method is used, so it is necessary to assume an axial velocity distribution. As in the A.N.L. squirting model, only the velocity distribution up to the cavity mouth (the point where the fuel leaves the active core and enter the blanket region) is considered. Obviously the velocity of the fuel of the extreme bottom of the pin is equal to zero. Also, considering only the active fuel region, the maximum velocity will occur at the uppermost part of the region. A polynomial expression thus seems valid and A.N.L. has suggested

$$\frac{V_z}{V_{mouth}} = \left(\frac{z}{L}\right)^n .$$

In the use of the squirting model of A.N.L., Travis (34) has determined that $n = 4$ was an appropriate value for axial squirting in most pins. The determination was semi-empirical, with the geometrical equations representing the shape of the cavity yielding the theoretical basis. Since this determination was based on other theoretical assumptions (amount of fission gas, etc.), other values of n will be tried in this work.

Using this velocity distribtuion and assuming that the fuel velocity does not change past the mouth (that is no velocity changes other than area related ones; the assumption actually being that $V_z A$ does not change past the mouth), one integrates the equation from $z = 0$ to $z = Z + L$, where Z is the distance that the uppermost part of the fuel has moved, and L is the length of the fuel column.

The assumption that the velocity does not change (except for area related changes) past the mouth was used as an approximation because the pathway past the mouth is normally small in diameter, compared to the fuel region; because one is principally concerned with how much fuel exits the mouth; and because in other than axial fuel motion cases the velocity after the mouth is affected by so many different factors (such as the effect of coolant flow on the exiting fuel-gas mixture in a pin failure

test). At any rate, it appears necessary to remain with this approximation. Integration of equation (5.1) yields

$$\int \rho\left(\frac{dV_z}{dt}\right)dz = -\int \rho V_z \frac{dV_z}{dz} + \int f(z)dz - \int \frac{dP}{dz}\,dz - \int \rho g dz$$

Assuming $V_z = V_m\left(\frac{z}{L}\right)^4$ and differentiating to obtain

$$\frac{\partial V_z}{\partial t} = V_m\, 4\left(\frac{z}{L}\right)^3 \frac{dz}{dt} = V_m\, 4\left(\frac{z}{L}\right)^3 V_z = V_m^2 \left(\frac{z}{L}\right)^7$$

One can substitute the above expression for $\frac{\partial V_z}{\partial t}$.

Integration yields

$$V_m^2 \frac{\rho L}{2}\left(\frac{Z}{L}\right)^8 = P_0 - P_z - \int f(z)dz - \rho g(Z + L) \qquad (5.7)$$

where the expression $z = Z + L$ has been used and $\int f(z)dz$ is simple the total pressure drop due to friction. ($\frac{dV_m}{dt}$ has been set equal to zero. The reason for this will be discussed later.)

The squirting model only deals with the friction forces outside the active core fuel region (i.e. in an axial problem only the friction with the blanket). The model assumes that the normal friction factors for flow in closed conduits apply, although it is suggested that the correlations for rough pipe be used. The friction factor can then be determined, as a function of the Reynolds number (a function V_m). The corresponding pressure drop per unit length, times the

length, Z , that the fuel has moved yields the total friction force. The pressure difference is also a function of the length the fuel has moved. For example, in the case of the mixture moving up an axial hole, with a plenum pressure resisting motion, the pressure driving force term is simply the internal gas pressure minus the plenum gas pressure.

The plenum pressure is

$$P_b = P_{bo} \frac{V_{bo}}{V_{bo} - AZ}$$

where the o subscripted variables are simply the original values of the plenum pressure and the volume that the plenum gas occupied, and A is the area of the hole.

The internal gas pressure is

$$P_a = P_{ao} \frac{V_{ao}}{V_{ao} + AZ}$$

Thus the general equation can be rewritten as

$$\frac{V_m^2 \rho}{2} \left(\frac{Z}{L}\right)^8 = - g(Z,V_m) + h(Z) - \rho g(Z + L)$$

where $g(Z,V_m)$ is the total friction force function and $h(Z)$ is the pressure difference driving force function, $P_b - P_a$, $g(Z,V_m) = (\Delta P_{fric}/L)\ (Z)$, with ΔP_{fric} a function of the Reynolds number.

Also, ρ can be replaced in the equation by

$$\frac{\text{Total Mass}}{V_{ao} + ZA}$$

Thus the result is a transcendental equation in Z and V_m. These two variables can be related by $Z = \int_0^t V_m dt$ and thus the equation can be solved by taking infinitesimal time steps, and finding the Z corresponding to a V_m at each times step. It is assumed that V_m is constant, for a particular time step. A value for V_m is suggested a corresponding Z is calculated and the values are tried in the equation. The V_m value is then corrected and the procedure is repeated until the two sides of the equation agree.

3.2.5.4 Checks and Comments

The simple method described computes fuel movement without consideration of two-phase flow or heat transfer to the blanket. The characteristics of the motion obtained are used to evaluate the heat transfer and two-phase flow effects, and these effects are then applied to obtain updated fuel movement characteristics. The approximation leaves much to be desired, since an incorrect "answer" is used in the computation of factors needed for the calculation of the correct "answer". It has been suggested, however, that the two-phase flow and heat transfer corrections

will be minor in most cases. When large corrections are necessary, an iterative solution technique can be employed. (The corrected fuel movement result used to recalculate the heat transfer and two-phase flow effects, etc.).

The effects of two-phase flow are numerous. The effect of the gas bubbles on friction and heat transfer is important. The mechanism for two or more smaller bubbles to form larger bubbles is also important. Perhaps the most important quantitative effect on fuel motion is the slip velocity. This is the difference in the velocity of the liquid fuel and the gas bubbles. The gas bubbles, due to their buoyancy, move up a channel faster than the liquid. The importance of this is shown in Figure 3.9. Once a fission gas bubble moves past the surface of the fuel mixture, it is no longer driving the fuel-gas mixture from the core. Instead it is retarding the motion. Thus the expressions for P_a and P_b described previously (the difference in P_a and P_b being the driving force) must be modified so that as gas "slips" out of the fuel-gas mixture, P_b goes up and P_a goes down accordingly.

The amount of gas "slipping" out is then the important variable. To find this the model calculates a bubble rise velocity. This velocity is then compared to the average fuel movement velocity (for a time step or for the entire time of movement) to determine if the effect can be neglected.

THE IMPORTANCE OF SLIP VELOCITY

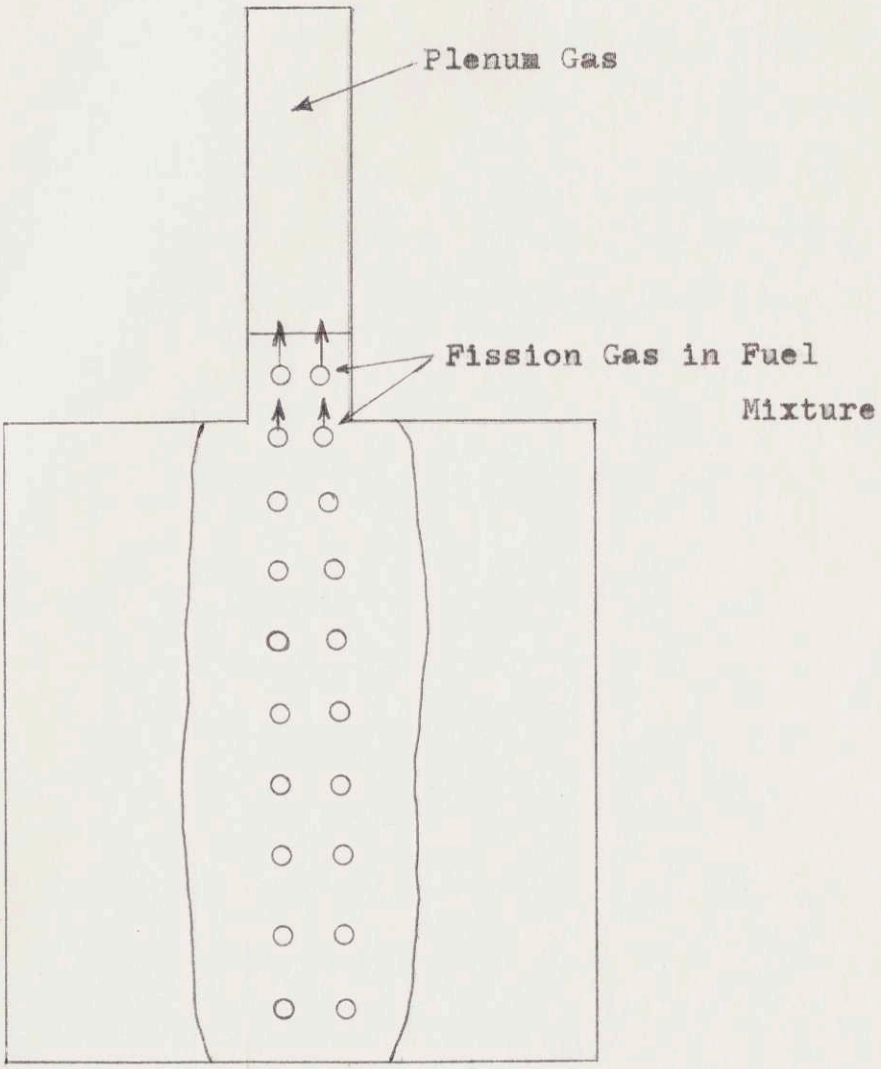

FIGURE 3.9

If it is determined that the effect is not negligible, one can calculate, for each time step, the amount of gas which has "slipped" out. An appropriate modification is then made in the driving force for the next time step. Different expressions for the bubble rise velocity can be obtained, each valid in a particular region. The highly turbulent region gives the highest velocity, so the expression will be used here, as the most conservative case. The expression (35) is:

$$V_\infty = 1.18 \left[\frac{\sigma g g_c}{P_\ell}\right]^{2.5} \qquad (5.8)$$

where σ is the surface tension

g is the acceleration of gravity

g_c is the gravitation constant

P_ℓ is the density of the liquid

The fuel movement model considers that the fuel gas mixture remains at a constant temperature--the fuel melting point. Since the fuel is in a liquid state heat transfer from the blanket would solidify some of the fuel, rather than lower the temperature. The effect of the colder blanket will be offset by one factor heretofore unmentioned: the liquid fuel will continue to generated some heat. The amount of heat generated, of course, is dependent on the power profile outside the active fuel area.

As an approximate method for determining the amount of heat that can be lost to the colder blanket, one can use the thermal boundary layer.

Assuming that the blanket is at a uniform temperature, T_0 , and that the moving fuel is at a constant temperature (the melting temperature), T_1 , the thermal boundary layer in the blanket is defined such that, past the boundary layer, there is no significant heat flux due to the molten fuel.

For a boundary layer that is small compared with the cylinder dimensions, the thermal layer can be approximated by (25):

$$\sigma = \sqrt{6\alpha t}$$

where α is the thermal diffusivity

The heat transfer can be related to the thermal boundary layer:

$$Q = \frac{k(T_1 - T_0)A}{\sigma}$$

Now the boundary layer must be calculated as a function of z . The time, t , that the molten fuel is in contact with the blanket at a particular z can be related to V_z . The axial blanket can be sectioned into nodes, and the time that the molten fuel reaches the centerline of

that node can be found. $Z = \int_0^t V_z dt$ where Z is measured from the fuel blanket interface. In this way a time, t, for heat transfer can be found for each axial node (t is the measured from the time that the molten fuel reaches that node until the completion of fuel movement). A Q for each node can then be found and the total heat transferred can be found by summing the nodal values. This can be compared to the heat being generated in the fuel.

If more heat is lost than is generated, some of the liquid fuel will be solidified. Assuming that no gas is trapped, the effect will be reduce internal pressure (and thus the driving force) by allowing more volume for the gas (since solidification means a decrease in liquid fuel volume). An increase in friction would probably result from the solidification and constriction of the fuel pathway. No quantitative discussion of this effect will be attempted, however.

If more heat is generated than is lost through conduction, an increase in gas pressure and the driving force will result.

3.3 Comments

The method of solution of the fuel movement equation, of course, depends upon the time steps being small. This, coupled with the fact that a transcendental equation must be solved, makes it very desirable that all calculations be performed on the computer. In fact due to the existence of the iterative steps in considering the melting of fuel, it would be practical to put the entire model in computer format. It is quite possible that the time steps in the two iterative areas (fuel melting + movement) can be linked, and the model thus simplified. The codifying of the model, however, is not including in the scope of this work.

In order to simplify the discussion of the model, basic geometries were often exploited. In the expression for internal gas pressure, for example, it was assumed that the axial hole was of a constant dimension. A hole of varying size, however, could be dealt with-without any changes in the theoretical format. It would only be necessary to express the acial variation of the cavity diameter as a function of Z. This function would then replace ZA in the pressure expressions.

CHAPTER 4.

RESULTS OF APPLICATION OF MODEL TO C5A-C5B

4.1. Comparison with Observed Results

The model results were calculated area by area for both C5A and C5B. In area one, it was first decided that the problem could be treated by a one-dimensional heat transfer study. The justification for this was the fact that the axial power shape was almost flat, having a peak to average ratio of only 1.08. In addition, the post-transient destruction of C5B showed that the melt radius was essentially constant for the length of the pin.

4.1.1. C5A Results

The C5A case is first examined. In that test, the temperature distribution was calculated and the maximum clad temperature was 1425°F. The maximum coolant temperature was 870°F. With the melting point of the clad being 2500°F, and the boiling point of the coolant set at 1400°F, it can be seen that neither clad melting nor coolant boiling was a problem.

The temperature distribution yielded the following results in area two:

The melting began at 2.48 seconds and the peak melting radius of 0.068 inches was reached at 2.66 sec.

Since there is no place for the fuel to move to (it must be remembered that this fuel movement model only deals with movement prior to failure), there was no need to divide the time of melting into time steps. Thus the melting radius of 0.068 in. was an input to area three.

Considering the inputs to area three, the average burnup for C5A was 17800 MW_d/T_e. This yields a total fission gas generation of 2.105 $X10^{21}$ atoms, or, at S.T.P., a volume of 78.29 c.c.

The distribution of fission gas is represented in Figure A.1, and the steady state temperature distribution is shown in Figure A.2. From Figure A.1, it was determined that 38% of the fission gas generated is located within the melted region. ($(r/R)^2 = .382$)

Using the temperature distribution in Figure A.2, Figure A.1, and the relation shown in Figure 3.4, it was calculated that 27.8% of the gas in that area was released during steady state operation. (No observed bellows displacement was recorded for C5A and therefore only the steady-state release within the melted area is important. If a bellows displacement were known, one would find the total release and then check against the observed result.) Thus the area three result is that 21.53 c.c. of gas, at S.T.P., were released in the melting of the fuel.

Area four next calculated internal pressure. The fuel porosity for C5A was 0.73 c.c. First the amount of gas occupying this space before the transient begins must be calculated. Using the observed pre-transient pressure of 2.20 atmospheres, the volume of gas in the voids was 1.606 c.c., at S.T.P. Using the value of 21.53 c.c. as the transient release, one has a total of 23.14 c.c., at S.T.P., occupying a volume of 0.73 c.c. at 5610°R. The calculated pressure was 361.4 atmospheres or 5312.9 psia, which was greater than the burst strength (20) of the clad, 3812 psia.

The pressure was calculated without the effect of the increase in volume of the melting fuel. Thus failure definitely takes place. This, of course, agrees with experimental observations.

In this case, where there was no room for fuel movement, the model can do no more than show the obvious: the pin will fail. If, however, there was a central void (and still no axial hole), the model could be more useful. The volume left for the gas after fuel expansion and cladding deformation could be determined, and a more exact determination of failure could be made. If the calculations indicated failure, one could revert to area two and work with .9 or some other fraction of the time step. In this

way one could determine what melt fraction was necessary to just cause the clad to exceed the failure limit. The time corresponding to each melt fraction is known, and therefore one could arrive at the time of failure. R. Stuart and G. Thomas applied a similar model (the starting point for their work: a less complicated model, but also based on the assumption that fission gas is prime driving force behind fuel motion or failure) to a TREAT pin and were able to predict clad failure to within 0.1 seconds of the actual failure time. (30)

4.1.2 C5B Results

In C5B, it was first calculated that the maximum clad temperature was 1395°F. The maximum coolant temperature was 855°F. Again neither clad melting nor sodium boiling was a problem. According to the area two results, the melting began at 2.40 seconds and the peak melting occurred at 2.59 seconds, with the maximum melt radius being 0.066 inches. This was used as the initial input to area two.

Alternative one (all fuel melts before any moves) is first used and thus the value of 0.066 inches was the initial input to area three.

The average burnup for C5B was 17900 MW_d/T_e. This yields a total fission gas generation of 2.0349 x 10^{21} atoms, or, at S.T.P., a volume of 75.68 c.c.

The distribution of fission gas and the steady state

temperature distribution for C5B is shown in Figures A.1 and A.2. From Figure A.1, it was determined that 36% of the fission gas is within the melted region. Using the Lewis relation of Figure 3.4, it was calculated that a total of 8.5% of the total fission gas, or 6.44 c.c., at S.T.P., was released during steady-state operation.

The calculated steady-state gas release can be compared with the observed bellows displacement. The bellows displacement indicated a pressure of 30 psia, or 2.04 atm. (The bellows was calibrated, so that pressure could be determined from it.) (20) The total void volume in the pellet was 6.41 c.c., so a pressure of 2.04 atm. would mean that the gas volume was 2.04 (6.41 c.c.) = 13.08 c.c. at room temperature. At S.T.P., the volume is 13.08 (273°C/293°C) = 12.19 c.c. The original cover gas was 6.05 c.c., so that the volume of steady-state release gas associated with the bellows displacement was 12.19 - 6.05 = 6.14 c.c.

Taking 6.14 c.c. as the correct answer, the model result of 6.44 c.c. represents an error of 4.9%.

Next the transient release is calculated. With the melt radius of .066, it was calculated that 21.00 c.c. of gas, at S.T.P., was released during the transient. (27.2 c.c. was originally produced in this area, but 6.2 c.c. was released during the steady-state irradiation). This can be compared to the final gas volume removed from

the pin as another check.

The final gas volume removed from the pin after the transient was 38.8 c.c. at S.T.P. Subtracting from this the cover gas volume, 6.05 c.c., and the steady state release, 6.44 c.c., yields an expected value of 26.31 c.c. of gas. Taking this as the standard, the model calculated value of 21.00 c.c. represents a difference of 20.2%.

Now the pressure is calculated. Assuming that the gas takes up the fuel porosity of 0.71 c.c., one first finds the mass of the gas already occupying the pores. This is simply 2.04 (the pressure, in atmospheres, taken from the observed bellows displacement) times the fuel porosity volume, 0.71 c.c. The result is a volume of gas of 1.45 c.c., at S.T.P. Thus it is necessary to calculate the pressure developed by 22.45 c.c. of gas at 5610°C, occupying a volume of 0.71 c.c. The result is a pressure of 362 atmospheres, or 5320 psia. This is above the burst strength of the cladding, and the result indicates that more than one time step must be used (i.e., alternative one is incorrect here in that fuel motion occurred, and relieved the pressure before the total melt fraction (and the 5320 psia pressure) was reached). Note that this conclusion did not result from the t_1 versus ΔT_1 comparison, as t_1 has not yet been computed.

The calculations will be continued, however, to find a t_1, in order to decide between alternatives two and three on the next iteration.

Continuing to area five, one can first make an estimate of the extent of fuel motion, based on an isothermal expansion of the gas in the fuel gas mixture.

Assuming that the plenum gas and the fuel-gas mixture remain at constant temperature, one has $PV = RT = \text{constant}$ for both the plenum gas and the gas in the fuel-gas mixture. Using $(P_{\text{fission gas}} - P_{\text{plenum gas}})A = Mg$ as the equilibrium position one can derive an expression for $V_{\text{fission gas-final}}$ in terms of known original quantities. (Derivation given in Appendix B.)

The result of this application gives a final fuel movement of 11.42 inches (into the blanket), as compared to the 10 inch observed result. (This calculation was intended only to be rough check on the amount of gases present.)

The movement due to the volume increase alone (that has been assumed to take place instantaneously), was calculated to be over 8 inches. Since it was assumed that this initial motion would be small compared to the final motion, again it is noted that more time steps are necessary (i.e., use an alternative assumption rather than assuming that all fuel melts before any moves.)

The integral method was than applied to find the time or fuel movement. A time step of 10 milliseconds was used, as the calculations were done by hand. Results were obtained for the case of $n = 3$, $n = 4$ (A.N.L.'s suggested value) and $n = 5$. The results were, for $n = 5$, a final movement of 11.33 inches in a time of 36 milliseconds; for $n = 4$, a final movement of 12.36 inches in a time of 41 milliseconds; and for $n = 3$, a final movement of 13.51 inches in a time of 44 milliseconds.

In all cases, t_1 can be seen to be greater than $0.1 \Delta T_1$, so alternative two is used in the next cycle.

Looking at two phase flow effects, the bubble rise velocity was estimated to be less than 0.623 ft./sec. by equation 5.8. In the time of motion, the gas bubbles could slip at most 0.623 ft./sec. Taking 41 milliseconds as the time of motion, the gas bubbles could move at most 0.0262 ft.

Thus the only gas that could slip through to the plenum region was that which was located less than .0262 ft. from the blanket. For the two foot pin, this means that, at most, 1.31% of the gas could escape. Thus, as was suggested, the effect is unimportant.

In the second cycle of the model, $\Delta T_2 = 0.095$ seconds. At the end of the first 0.095 seconds, the melt radius is .053 inches.

Moving to area three, the transient release was calculated as 13.85 c.c., at S.T.P. In area four, it was calculated that the corresponding internal pressure developed is 3418 psia. This pressure was below that of the cladding burst.

The pressure was compared to the observed cladding deformation. The average cladding deformation of 3 mils in C5B was calculated to have resulted from a pressure of approximately 3000 psia, so the internal pressure of 3418 psia calculated for this cycle was close to the maximum pressure that apparently was developed.

Movement was calculated for this first time step to be a total of 7.32 inches up the axial hole, completed in 16 milliseconds (motion is assumed to go to completion because .016 sec $< \Delta T_2$). The initial motion due to fuel volume increase, however, was 4.3 inches.

In the second cycle, the fuel movement of 7.32 inches was used in the calculations to reduce the effective density and heat transfer rates. The result was that the heat transfer calculations yielded a melting during the second time step out to radius .063. This was calculated to produce an additional gas release of 5.21 c.c. of gas, at S.T.P. The additional gas and volume increase was calculated to yield a new internal pressure of 1320 psia. The ensuing fuel motion yield an additional fuel movement of only 2.14 inches, for a total movement of 9.46 inches.

The fuel movement results are shown in table 4.1.

4.2 Comparison with G.E. Preliminary Results

The G.E. preliminary analysis (20) was designed only to set conservative bounds for the fuel movement problem, so a detailed comparison of results with the calculations in this work is unwarranted. Several theoretical comparisons can be made, however.

The G.E. analysis (20) used the peak burnup values to calculate total fission gas generation and therefore yielded a greater amount of fission gas than the model of this work, which used the average burnup. In addition, the G.E. 4% gas release assumption (assuming that 4% of the fission gas was released in the steady state, at all radial pts.) appears to be a major source of difference between the G.E. results and those of the current model. For example, it was impossible to correlate the 4% gas release rate with the amount of gas calculated from the bellows displacement (7.2%, as calculated by G.E.). (20) It appears that the Lewis relation used in the model in this work increases the accuracy of the prediction. Using the Lewis model, a gas release rate differing by less than 5% from the rate related to the observed bellows displacement was obtained.

In the fuel motion itself, the disregarding of two-phase flow effects does not seem to be inaccurate. The friction effect, however, is definitely important and should continue to be used in further analysis. Table

TABLE 4.1

FUEL MOVEMENT -FINAL FUEL POSITION RESULTS

(Movement measured in inches from fuel-blanket interface.)

Observed Result	Isothermal Expansion Calculation	Squirting Model: (one step) n=1	n=4	n=5	Squirting Model (two steps) n=4
~10.00	11.42	13.51	12.36	11.33	9.46 (First Step Result: 7.32)

4.2 compares the model results with those of G.E.

4.3 Conclusions

Although the hand calculations and the integral methods yielded at best a rough approximation to the actual fuel movement equations, the close agreement between the model and the observed results at the intermediate checking stages (steady-state gas release, final gas content, internal pressure developed) seem to indicate that the theoretical basis of the model was sound. It is expected that this basis will be valuable after the development of more accurate calculational methods. (A computer code employing finite different methods, for example).

In the case of two phase flow considerations, it is expected that the effects will not be important in most cases of interest, as was the case for C5B.

The theoretical basis of the model, namely the consideration of the fission gas that is mixed with the liquid fuel as the primary driving force for motion, is expected to be useful in applications to fuel pin failures and subsequent fuel ejections.

TABLE 4.2

COMPARISON WITH G. E. RESULTS

	Model Result	G. E. Result	Observed Result
Fission Gas Generation (c.c. at S.T.P.)	75.68	87.50	-
Steady-State Release (c.c. at S.T.P.)	6.44	3.50	6.3
Agreement with Observed Result (from Bellows Displacement)	4.9%	41.7%	-
Transient Release (c.c. at S.T.P)	21.0	29.4	32.75
Agreement with Final Gas Volume	20.2%	10.7%	-
Calculated Pressure Maximum (psia)	5320 (1-step) 3418 (2-step)	7200	(Clad did not burst. Burst pressure=3812. Pressure related to observed deformation= 3000)
Final Fuel Movement (inches)	9.46		~10.00

CHAPTER 5

THE RELEVANCE OF C5A-C5B ANALYSIS TO LMFBR SAFETY

5.1 C5A-B Tests vs. Overpower Transient in LMFBR

The C5A and C5B tests were not designed to exactly duplicate "standard" LMFBR overpower transients. The power transients were selected to produce substantial fuel melting, based on earlier TREAT experiments. The TREAT reactor is thermal, and therefore the flux for the C5A and C5B tests was not representative of a fast reactor. In addition, the experimental test capsule consisted only of a single pin, with stagnant sodium as the coolant. Thus the effect of flowing sodium and possible rod bundle effects were absent from the experiment. The C5A and C5B pins were also 100% UO_2, while LMFBR designs call for a mixed plutonium and uranium oxide.

5.1.1. Radial Flux Differences

The thermal flux spectrum in TREAT results in flux depression in the pins. This accounts for the radial power shape for C5A and C5B shown in Appendix A. The result is a radial transient temperature profile quite different from a typical LMFBR accident pin. A comparison of the C5B results with the calculated results for the FORE-II ramp insertion accident (designed as a representative accident for a large LMFBR core) is shown in Figure 5.1.

FIGURE 5.1 (14, 20)

Time Starts When First Fuel Has Reached Melting Temp.

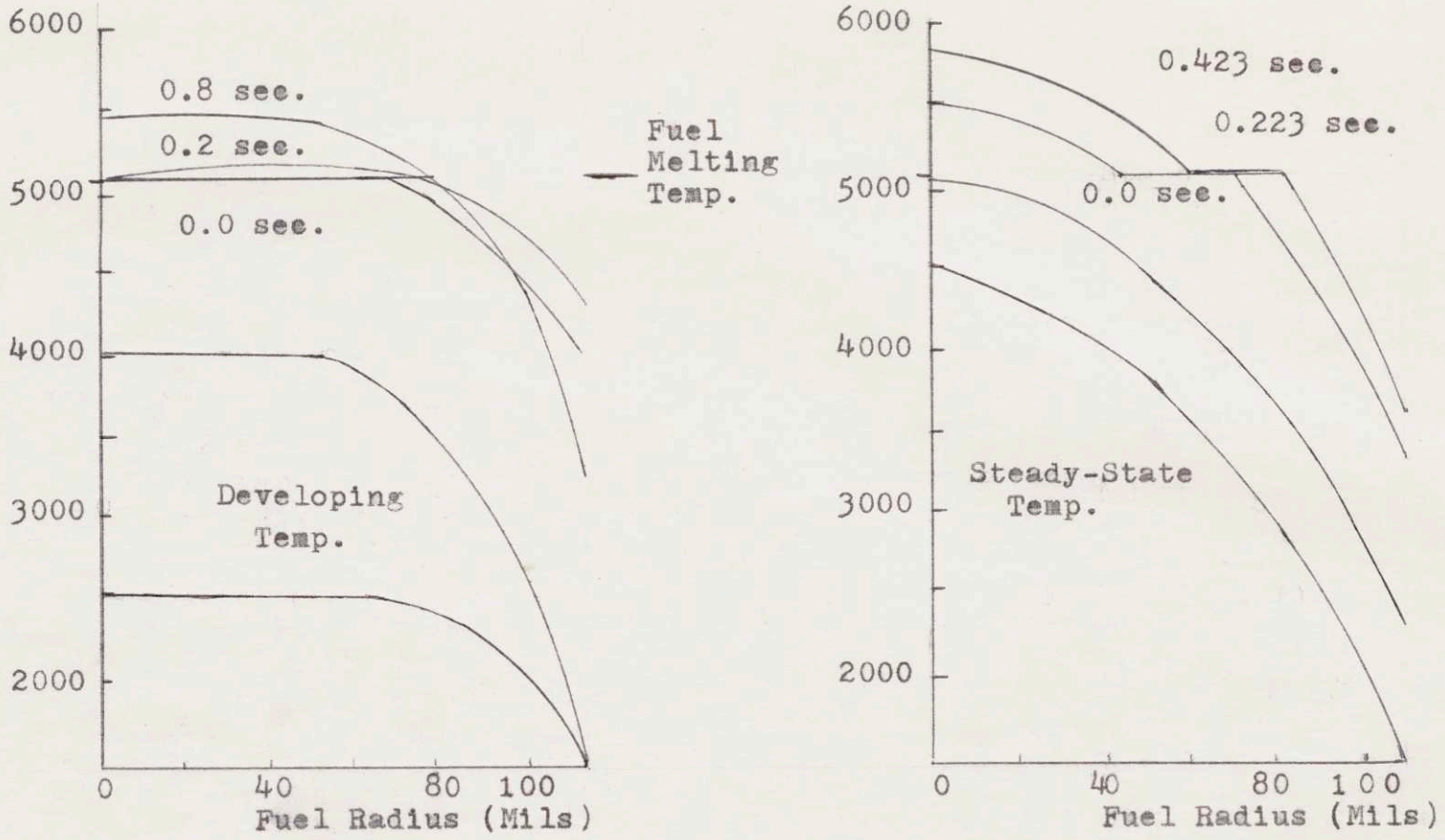

The figure illustrates the flatter temperature profile due to flux depression. (The calculations in both cases do not account for fuel movement.)

In some TREAT experiments, a thermal flux shield (a thin cadmium sheet) was used with some highly enriched fuel segments to eliminate the thermal flux and thus prevent the extreme radial power gradients. (10) This method was not used in the Task C series tests, however.

Although the flux depression causes TREAT pins to have a temperature profile somewhat different from LMFBR pins, it is possible to counteract the effect. C4A was a TREAT test, using a mixed oxide (80% UO_2) pin, which was subjected to a transient very similar to the C5A and C5B transients. (Actually the C4A transient served as a model for the series V tests). Figure 5.2 compares the total energy generation and retained energy distribution calculated for C4A and FORE-II. Figure 5.3 compares the amount of fuel into and through heat of fusion in C4A and FORE-II. The close agreement between TREAT test and hypothetical accident calculations led to the conclusion "... that the TREAT experiments provide an adequate simulation of the hypothetical accident, in terms of the amount of fuel reaching the melting point in a given period." (14)

TREAT REACTOR vs. SEVERE LMFBR ACCIDENT

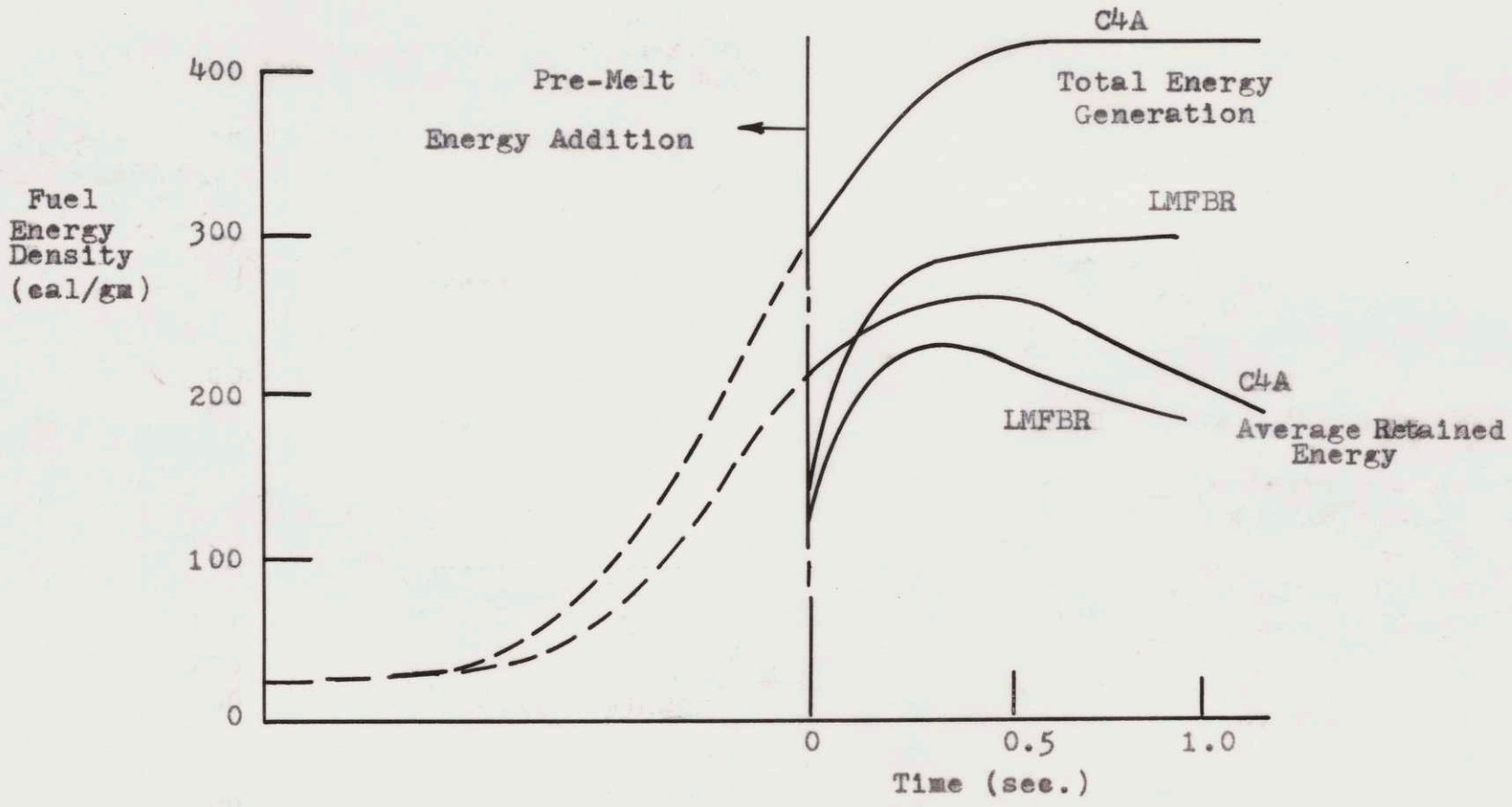

FIGURE 5.2 (14)

FIGURE 5.3 (14)

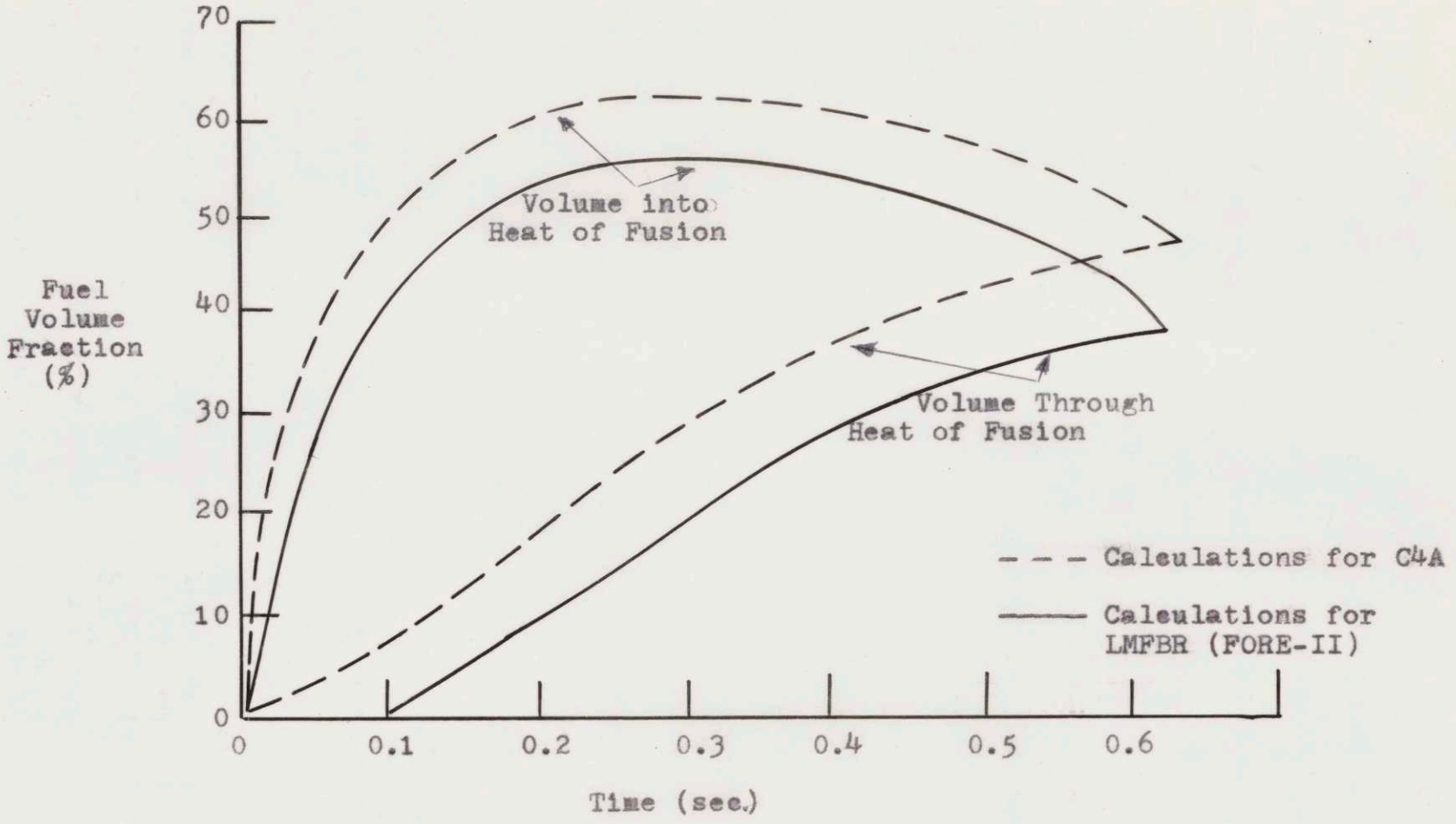
70
60
50
40
30
20
10
0
Fuel Volume Fraction (%)
Volume into Heat of Fusion
Volume Through Heat of Fusion
0
0.1
0.2
0.3
0.4
0.5
0.6
Time (sec.)
- - - Calculations for C4A
——— Calculations for LMFBR (FORE-II)

5.1.2. Axial Power Profile Differences

The axial power shape could greatly affect fuel motion. The axial power shape in the C5B pin was almost flat. The peak to average axial flux ratio was only 1.08, while the peak to average axial flux ratio is normally 1.2 or greater in an LMFBR design.

This difference could be important. In a pin with an axial relief column like C5B, for example, axial power peaking could mean that the fuel in the axial center would melt and cause a pressure buildup before the upper fuel melted. If the upper fuel has not melted, there is no path to the relief area (assuming that there is no central void). This effect would be reduced somewhat by the effect of the flowing coolant, which is hotter nearer the top of the core resulting in a rise in fuel temperature in the upper regions.

5.1.3. Other Differences

The rod bundle effects do not seem to be relevent to a fuel movement analysis, so a single encapsulated pin like C5B should be sufficient. The use of a stagnant coolant only serves to yield a more uniform axial temperature gradient. Flowing coolant would mean that the coolant would cool the top of the pin less than the bottom and center (because the coolant is hotter at the top). The fact that the pin is UO_2 instead of a mixed oxide is not known to have a significant bearing on fuel movement results,

although little work has been done in this area, and some further investigation is needed.

5.2. Comparison of Radial versus Axial Fuel Movement

The model described in this work is designed to apply towards axial movement in a fuel pin that does not experience failure. Axial movement was chosen for analysis because it is a simpler problem free of many of the uncertainties associated with radial fuel movement and subsequent failure. The latter more complicated problem, however, is what must be solved and used as an input for fuel-sodium interaction studies. The question, then, is how the axial model can be applied to the radial problem.

The axial model described in this work gives relations for the basic forces that expell liquid fuel, fission gas, and solid fuel from the active fuel region (It has been postulated that the basic forces result from the fission gas pressure and the volume increase of molten fuel). The driving forces are the same, regardless of whether the fuel is expelled axially or radially. As mentioned previously, the path that the fuel uses to move outwardly depends greatly on the fuel structure. Cracks in the fuel or weak spots in the cladding near the point of highest pressure would be the first to yield. For analysis, it would probably be necessary to assume a specific size pathway to the clad, and a specific size hole in the

cladding. The energy to first deform and then break the clad must also be considered in the analysis. Once the fuel breaks through the cladding, the force of the coolant must be considered. The driving force is the difference between the pressures within and on the outside of the fuel, so the effect of the coolant on the pressure at the fuel ejection must be determined. In short, the problem is a complicated one. A model accurately describing axial movement, however, is a necessary beginning in the assault on the task.

Chapter 6

SUGGESTED AREAS FOR FURTHER STUDY

6.1 General Areas for Further Study

6.1.1 Further Experimental Efforts to Follow Fuel Motion-Hodoscope

In the application of the fuel movement model to C5B, the main observed result is the final extent of fuel movement. In failed pins, even this evidence is difficult to obtain. In order to have complete confidence in a fuel movement model, a designer would like to show that the model describes fuel motion accurately in all the stages. To do this, one must experimentally determine the position of the fuel at the different stages. The hodoscope recently installed at TREAT can provide such information. The hodoscope represents two-dimensional "motion pictures" of fuel meltdown phenomena during transient experiments (9).

To use the hodoscope, the TREAT core is loaded with a test capsule at the center and an open slot running through the reactor. The hodoscope consists of a collimator with 334 slots, an array of fast neutron detectors (one at the end of each slot), and electronic equipment to collect and store the data. The configuration is shown in Figure 6.1 .

The data from the hodoscope is recorded on high speed film (the overall time resolution of the hodoscope can be

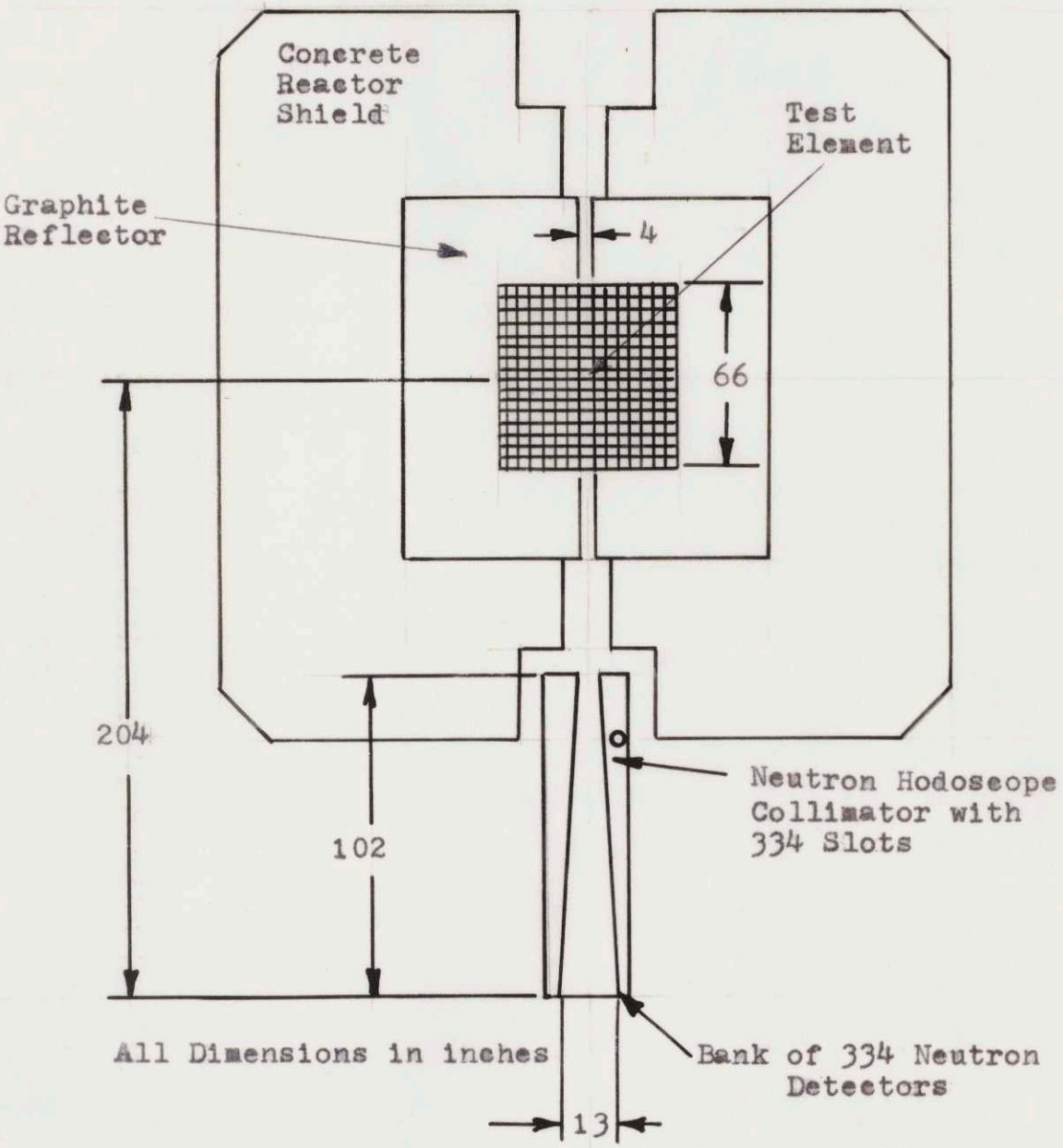

HODOSCOPE CONFIGURATION

FIGURE 6.1 (9)

set to a minimum of 1.2 milliseconds) in digital format and is later interpreted by an electronic scanner.

The hodoscope has been successfully used to monitor several A.N.L. tests and the results agreed well with the postmortem inspections. Figure 6.2 shows a reference row of detectors (monitoring an area with no fuel movement). The ordinate is the normalized count rate difference, using the center of the power peak as the reference point. If there were no fuel motion, the ordinate would be zero throughout the remainder of the transient (the plot starts at the time of the power peak). A positive difference means a count rate greater than that at the peak, a negative value would mean a count rate less than that at the peak. The plot in Figure 6.2 shows the statistical spread to be expected.

Figure 6.3 is a plot of the 7 detectors at the topmost active row. The middle three detectors in this row (7,8,9) cover the fuel region. The others cover only the cladding, sodium, etc. The three covering the fuel go well above the baseline indicating upward movement of fuel into the space above the original fuel top.

In order for fuel to expand past the top position, it must have been depleted somewhere else. Figure 6.4 is a plot of 9 detectors in row 11, which is halfway down the fuel element. Again the center three detectors cover the fuel region and there is unmistakable evidence of a de-

REFERENCE PLOT

(No Possible Motion)

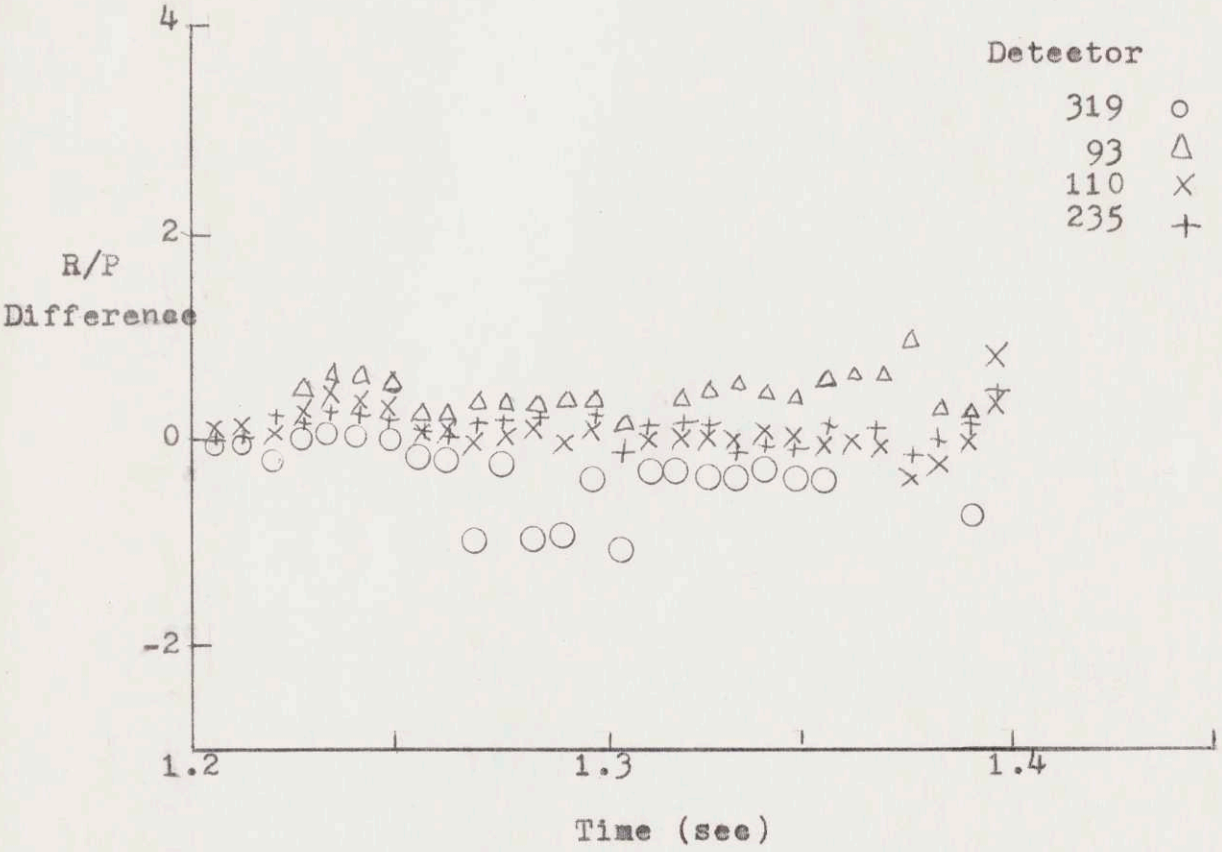

FIGURE 6.2 (9)

TOP ROW

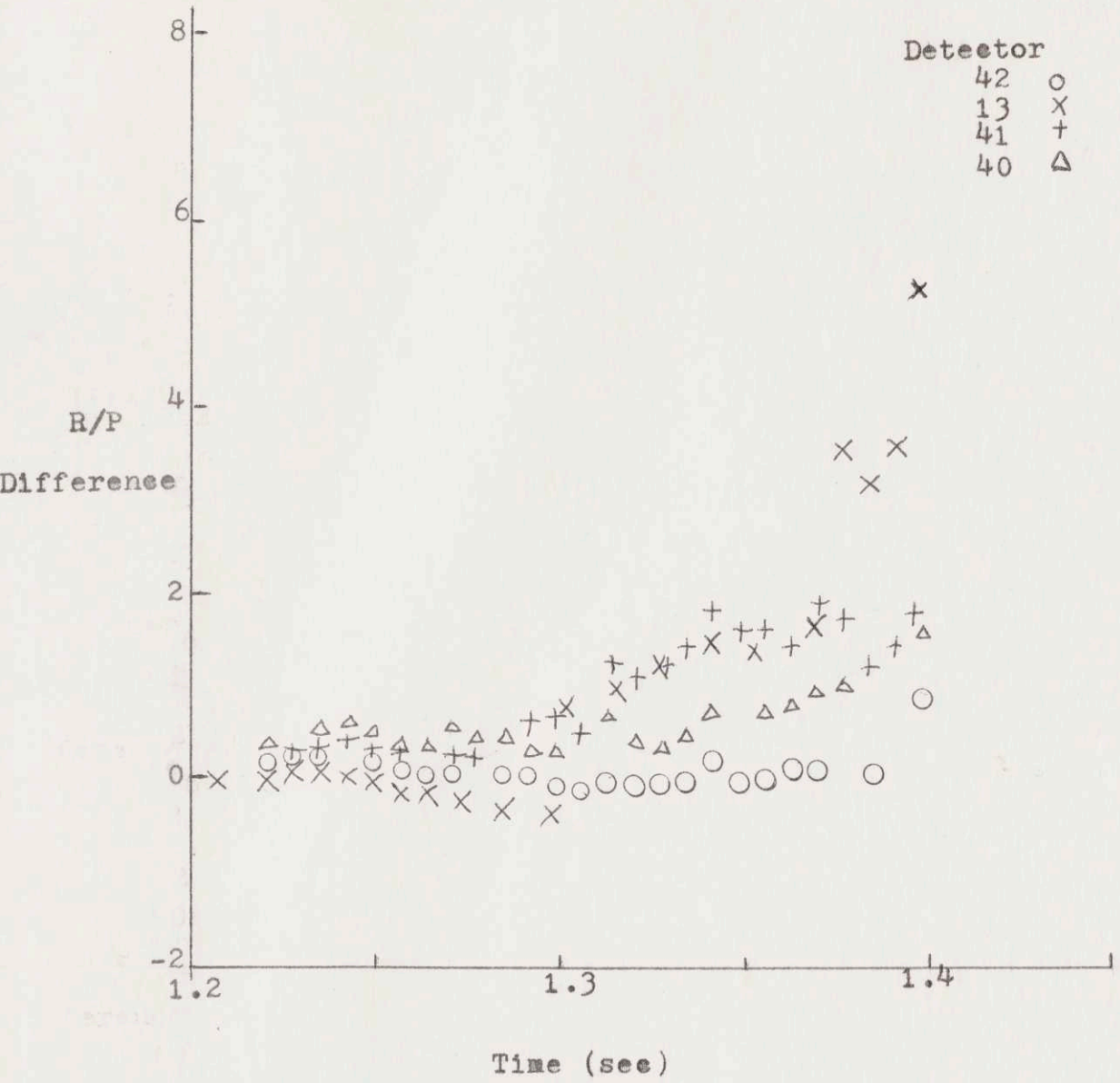

FIGURE 6.3 (9)

BOTTOM ROW

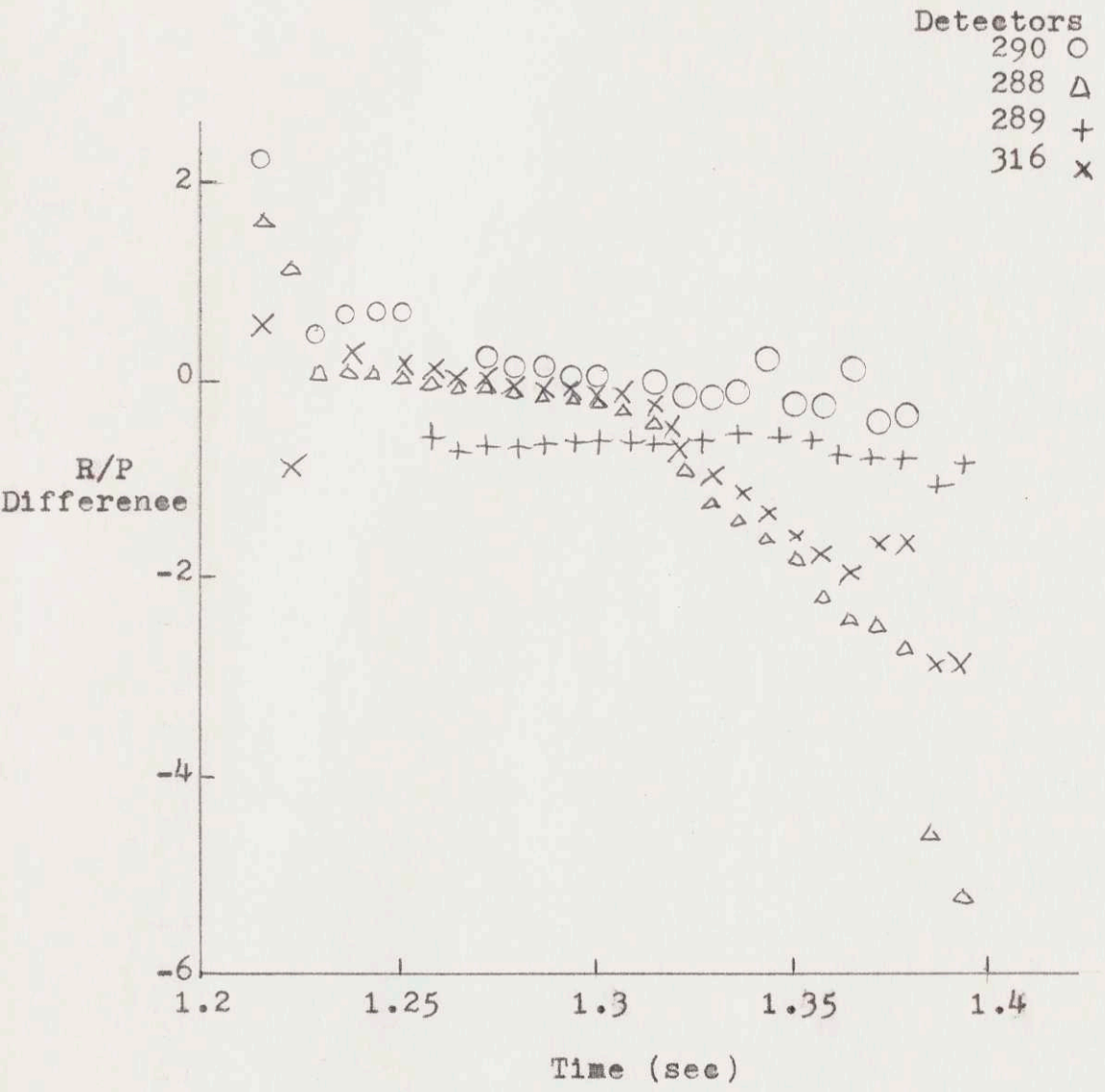

FIGURE 6.4 (9)

crease in fuel density at this position. Postmortem inspections supported these hodoscope observations (9).

The hodoscope could thus be of great help, both in the specific assumptions of examining a fuel movement model and in stage-by-stage testing of such a model. A later A.N.L. test, transient 1317 (Pin H2), has reached an advanced stage of analysis and is an example of the possibilities of the hodoscope. The pin was not irradiated before the test and displayed a non-typical oscillatory behavior (2). The use of the hodoscope in conjunction with other tests, especially with test pins which have undergone steady-state irradiation and subsequent fission gas buildup, is definitely an area valuable for further study. The hodoscope has been used in many tests, but the current problem is that the complete deciphered hodoscope data has not been available until long after the test dates, due to a backlog on the scanning equipment.

6.1.2 Use of Partially Hollowed Blanket to Raise Failure Threshold

In the analysis of the G.E. C5B test, one conclusion was that a provision for the accomodation of the volume increase of molten fuel and for the relief of internal pressure might increase the transient failure threshold (20). That is, a higher energy transient could be withstood in a pin provided with space for such a relief. A study of the

value of such a technique is definitely an appropriate area for further study. It must be determined if the advantages, from both an economic and a safety standpoint, outweigh the disadvantages associated with a blank space in the pin. The removal of material from the blanket makes it a poorer reflector. This means that breeding will be lowered and more critical mass will be required.

A.N.L. has started work on an "inherently safe" fuel element design, which relies on axial movement of fuel to prevent failure. A.N.L. made a preliminary evaluation of three concepts. The three concepts were 1. a partially annular axial blanket, 2. an axial enrichment zoning scheme to guarantee that movable molten fuel exists at the ends of the fuel column, and 3. a nozzle and shelf arrangement at the top of the fuel column to intensify axial squirting and prevent the downward return of fuel (3).

The first concept is similar to the G.E. proposal made after analysis of C5B . The second consists of using higher enrichment pellets over a finite length at the ends of the column. This is to guarantee a flatter power profile, thus enhancing fuel melting at the ends of the fuel column during a power transient. This insures that molten fuel in the center of the pin will not be denied access to the blanket. The third concept is shown in Figure 6.5. The nozzle enhances squirting, while the shelf attempts to prevent the downward return of the fuel.

NOZZLE AND SHELF CONCEPT

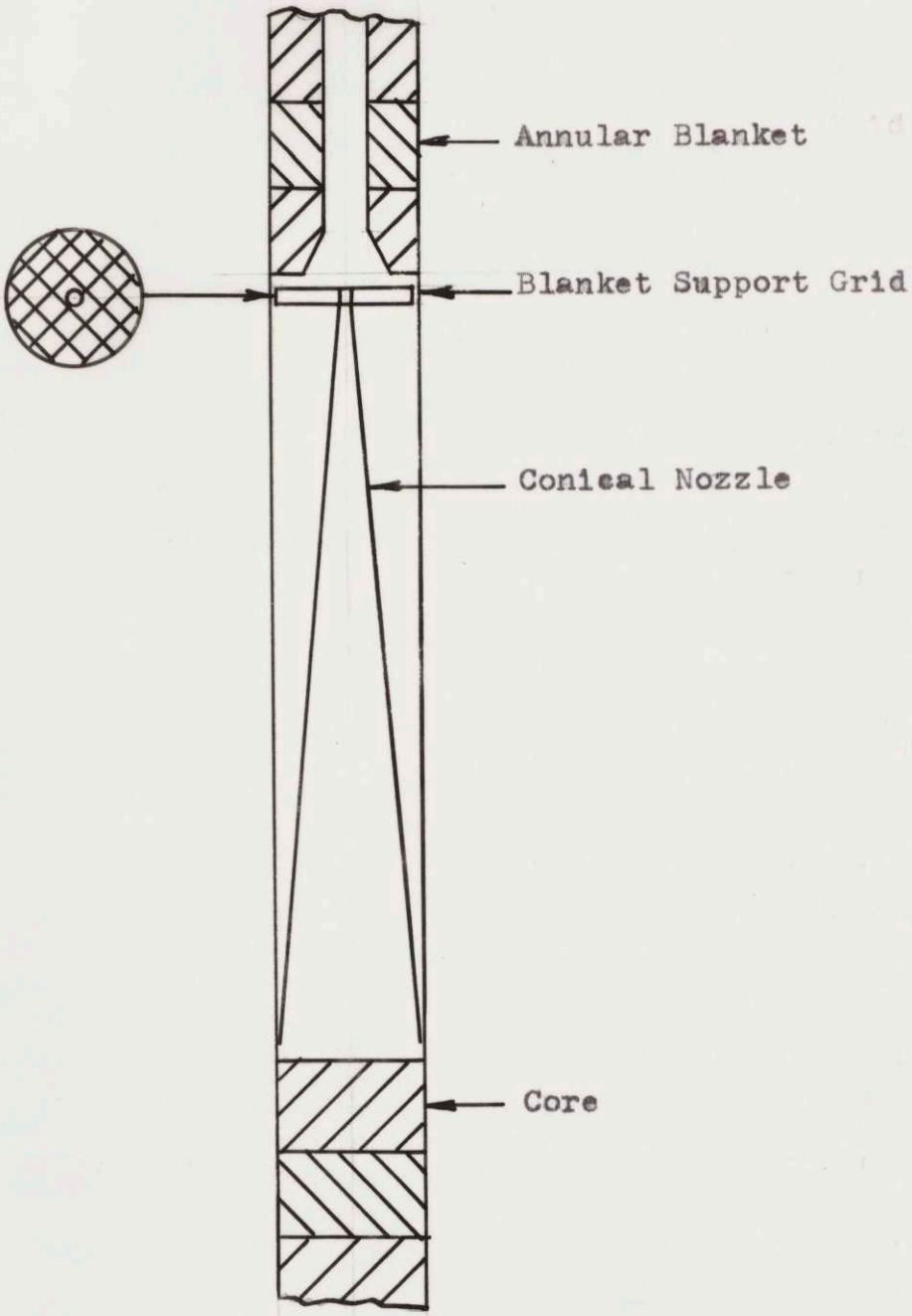

FIGURE 6.5 (3)

The concepts deserve further study. A.N.L. has noted that the first concept, besides lowering breeding, would bring an economic penalty associated with fabricating and handling two types of blanket pellets. The second concept also involves the penalty of having two types of pellets (two different enrichments). Slumping of the higher enriched fuel in a loss of coolant accident must also be considered. The third concept would also bring a breeding loss, since the blanket would be separated from the fuel (3). In examining the concepts, a more thorough knowledge of fuel movement mechanisms is a prerequisite.

6.1.3 Reactivity Effect of Fuel Motion

The safety advantage of having molten fuel move into an "accommodation" space instead of forcing a breech in the clad has already been discussed. Another safety question is connected with fuel movement, however. That is the reactivity effect of having active fuel moving away from the core. Wolfe, for example, has stated: "... there is no doubt that in the presence of the large Doppler effect characteristic of large LMFBR's even relatively small forces and resulting fuel motion within the fuel clad can terminate large reactivity accidents with little damage, except to the fuel itself (37)." Wolfe was not speaking only of pins that have a space for accommodation. In a solid pin, there would still be expansion and it has been

estimated that an upward expansion of the fuel only one quarter inch would decrease reactivity close to one dollar (37).

The study of the reactivity effect in both types of pins (the standard LMFBR pin and the "inherently safe" design) is definitely an area ripe for further study. The density distribution in the moving fuel would have to be known, of course, since this is a principal parameter in reactivity studies. A necessary area for further work is the slumping phenomena. It must be determined under what conditions, if any, fuel melting will result in motion of the fuel toward the center of the core. Due the high fuel inventory in an LMFBR, this is definitely a sensitive and important issue.

6.2 Suggested Areas for Further Study at M.I.T.

6.2.1 Coding of Model

The iterative nature of the model for molten fuel movement developed in this work, and the dependence on the use of small time step to achieve greater accuracy mandates that the model be put in a computer code format. This would enable the model to be applied to other tests pins with greater simplicity and greater accuracy.

No major changes in the model are necessary for coding, but the investigation of a possible linkage of the two time steps involved (the time steps for the melting of the fuel and the time steps for the fuel motion) is a necessity.

6.2.2 Finite Difference Techniques to Obtain Detailed Behavior of Moving Fuel

As was stated previously, to have complete confidence in a fuel movement model, one would like to show that the model describes fuel motion accurately in all stages. The fuel motion model used in this work must be improved to accomplish this objective. The integral technique was used to arrive quickly at an approximate answer, and it was necessary to postulate an axial velocity distribution. A more satisfactory model would calculate the actual velocity distribution and the density distribution resulting.

This density distribution is especially important for reactivity considerations.

Some work at A.N.L. has been done using finite difference techniques to solve the equation of motion (34). The work was attempted in order to show the validity of the squirting model and it has not been completed. The work took into account friction forces, but two-phase flow and heat transfer to the blanket have not yet been included, as is the case in the A.N.L. squirting model.

The basic finite difference format for the solution of the fuel motion equation was presented in Chapter 3. The movement of the boundary between the fuel-gas mixture and the plenum gas presents the main difficulties in the analysis.

Another objective for further study is the inclusion of all factors in the governing equations for the fuel-gas mixture. Currently, the heat transfer to the blanket, the heat generation in the molten fuel in the blanket region, and the effects of two-phase flow are not considered in the equations for the system. The inclusion of these factors in the basic equations would be an advantage over the current practices of neglecting the effects or treating them separately.

6.2.3 Study of the Point of Gas Release

The fission gas is assumed to be the prime driving force for fuel motion. This means that a knowledge of the exact time of release of trapped fission gas is of utmost importance. The model described in this work assumed that the gas was released only after the fuel had gone through the heat of fusion. It is suggested that further study is needed to determine if any gas is released while the fuel is into, but not through, heat of fusion.

REFERENCES

1. Argonne National Laboratory, "Fuel Dynamics Workplan", ANL-RAS 71-18, 1971.
2. Argonne National Laboratory, Reactor Development Program Progress Report, April-May, 1971, ANL-7825.
3. Argonne National Laboratory, Reactor Development Program Progress Report, Dec. 1971, ANL-7900.
4. Argonne National Laboratory, Reactor Development Program Progress Report, Jan., 1971, ANL-RDP-1.
5. Arpaci, Vedat S., Conduction Heat Transfer, Addison-Wesley Pub. Co., Reading, Mass., 1966.
6. Carelli, M. D., "Fission Gas and Molten Fuel Ejection from Failed Fuel Rods in an LMFBR," Proceedings of Conference on New Developments in Reactor Mathematics and Applications, March 29-31, 1971.
7. Carter, J. C., et. al., "SAS2A, A Computer Code for the Analysis of Fast-Reactor Power and Flow Transients," ANL-7607.
8. Chawla, T. C. et.al., "Heat Transfer Coefficient Correlation for Liquid-Metal Spray Cooling Relative to Fission Gas Jet Impingement in LMFBR Subassemblies, Trans. A.N.S., 15(1), 1972.
9. De Volpi, A. and C. E. Dickerman, "Fast Neutron Hodoscope Observation of Fuel Meltdown Experiments at Treat: Transients 1255 and 1281," Paper for A.N.S. Meeting, June 1971.

10. Dickerman, C. E. et. al., "Behavior of Th-20 wt% U Fast-Reactor Fuel Under Transient Heating to Failure", Nucl. Appl., 3 (1), 1967.

11. Dickerman, C., Personal Communication, August 1971.

12. Dickerman, C. E., "Studies of Fast Reactor Core Behavior Under Accident Conditions", Nuclear Safety, 11 (3), 1970.

13. Dunn, F. E., "The SAS2A LMFBR Accident Analysis Code," Proceedings of Conference on New Developments in Reactor Mathematics and Applications, March 29-31, 1971.

14. Field, J. H. and G. R. Thomas, "Transient Overpower Tests and Thermal Analysis for Sodium-Cooled Reactor Fuel", ASME-AIChE 11th National Heat Transfer Conference, August 3-6, 1969.

15. Field, J. H., Personal Communication, May 1972.

16. Freeman, D. D., "Nuclear Analysis for Task C Series V Experimental Design", Memo to T. Hikido, G. E. B.R.D.O., 1967.

17. General Electric Co., B.R.D.O., C5A-C5B Transient Data, received May 1971.

18. General Electric Co., B.R.D.O., G.E.T.R. C5A-C5B Capsule Power Summary, received May 1971.

19. Hanson, J. E. et. al., "Experimental Studies of Transient Effects in Fast Reactor Fuels. Series III," July 1969, GEAP-4469.

20. Hikido, T. and J. Field, "Molten Fuel Movement in Transient Overpower Tests of Irradiated Oxide Fuel," Sept., 1969, GEAP-13543.

21. Kelber, C. N. et. al., "Safety Problems of Liquid-Metal-Cooled Fast Breeder Reactors," Feb. 1970, ANL-7657.

22. Lewis, W. B., et.al., "Fission Gas Behavior in UO_2 Fuel," 3RD. U.N. Int. Conf. on the Peaceful Uses of Atomic Energy, Geneva, 1964.

23. McWethy, L. M., et. al., "Core Design Development Needs in Relation to Fuel Failure Propagation, Sodium Boiling and CLAD/Fuel-Sodium Thermal Interaction," 1970, GEAP-13639-2.

24. Nutley, M., et. al., "The Effect of UO_2 Density on Fission Product Gas Release and Sheath Expansion", Trans. A.N.S., 8(2), 1965.

25. Ozisik, M. Necati, Boundary Value Problems of Heat Conduction, International Textbook Company, Scranton, Pa., 1968.

26. Robertson, J. A. L., Irradiation Effects in Nuclear Fuels, Gordon and Breach, N.Y., 1969.

27. Rohsenow, W., Heat, Mass, and Momentum Transfer, Prentice-Hall, Englewood Cliffs, N.J., 1961.

28. Shames, I., Mechanics of Fluids, McGrow-Hill, New York, 1962.

29. Steart, R. R., et. al., "Studies of Fast Reactor Fuel-element Behavior under Transient Heating to Failure, II", ANL-7552 (1969).

30. Stuart, R. C. and G. R. Thomas, "Effects of Fission Gas on Transient Overpower Fuel Rod Failure", Trans. A.N.S., 13(2), 1970.

31. Stuart, R. C., Personal Communication, May 1972.

32. Thomas, G. R., and J. H. Field, "Transient Overpower Irradiation of Axially-Restrained Zero-Burnup, Fast Reactor Fuel Specimens", Sept. 1969, GEAP-13562.

33. Thomas, G. R., Personal Communication, June 1971.

34. Travis, R., Personal Communications, May 1972 & August 1972.

35. Wallace, G. B., One-Dimensional Two-Phase Flow, McGraw-Hill, New York, 1969.

36. Wilson, R. E. et. al., "Experimental Evaluation of Fission Gas Jet Impingement in LMFBR Subassemblies", Trans. A.N.S., 15(1), 1972.

37. Wolfe, B., "Liquid Metal Fast Reactor Accidents", Proceedings of Conference on New Developments in Reactor Mathematics and Applications, March 29-31, 1971.

APPENDIX A
C5A-C5B TEST DATA

The distribution of fission gas in C5A and C5B is shown in Figure A.1. (Distributions assumed identical). The steady-state temperature distribution for both pins is shown in Figure A.2.

The axial power distribution for the transient test is shown in Figure A.3. (Again identical for C5A and C5B). The radial power distributions for the transient tests are shown in Figures A.4 (C5A) and A.5(C5B).

The exact TREAT capsule geometry is shown in Figure A.6.

The power factors for the test were $.5810 \times 10^{-4}$ watts per c.c. fuel/treat watt for C5A and .5846 watts per c.c. fuel/treat watt. (16)

G.E. calculations and the results of the calibration transient suggested a value for the fuel-clad gap coefficient of 2000 BTU/hr.ft.^{2} F. This value was used in the analysis in this work.

FIGURE A.1 (20)

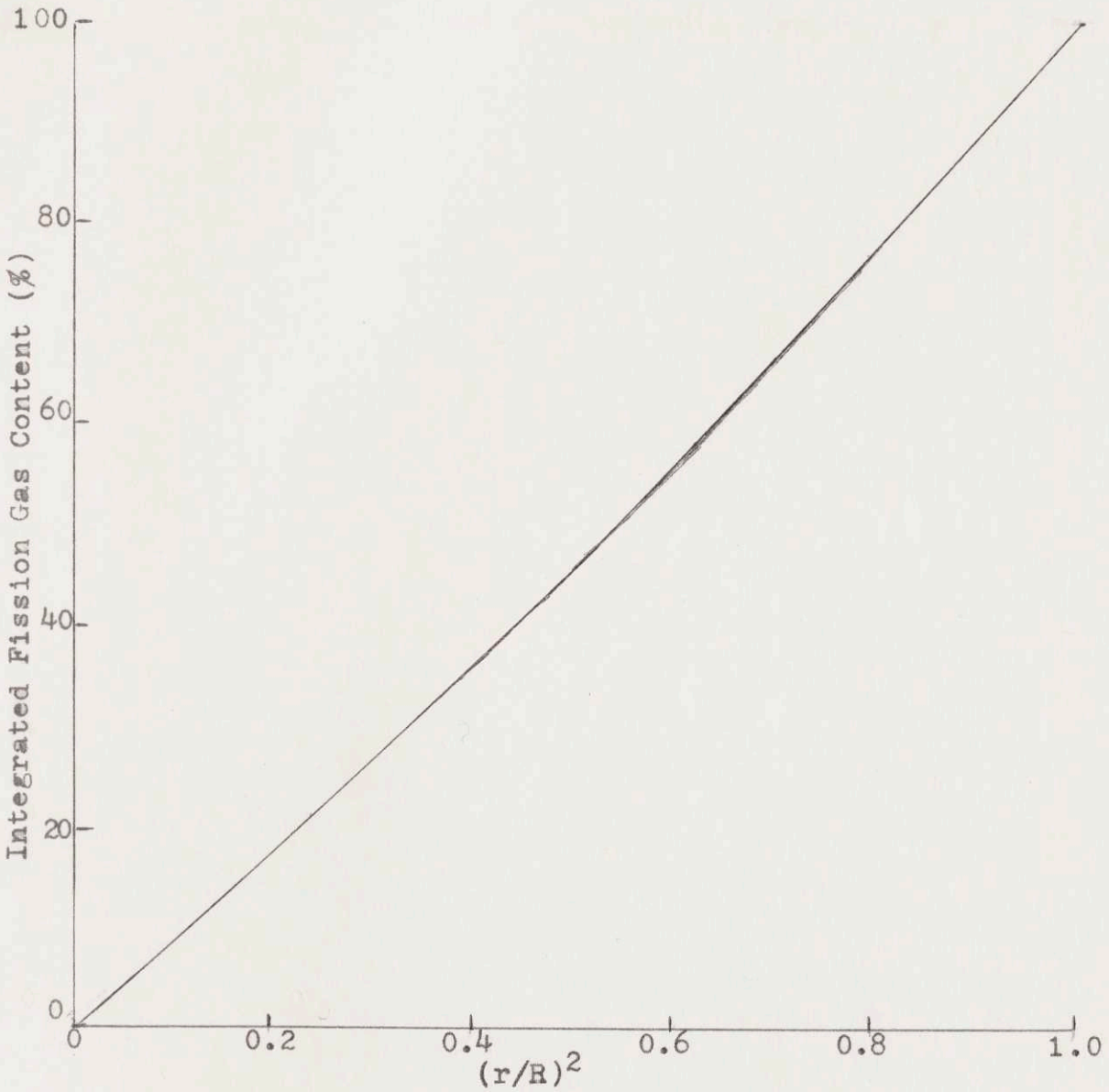
100
80
60
40
20
0
Integrated Fission Gas Content (%)
0
0.2
0.4
0.6
0.8
1.0
(r/R)2

FIGURE A.2 (20)

STEADY-STATE TEMPERATURE DISTRIBUTION

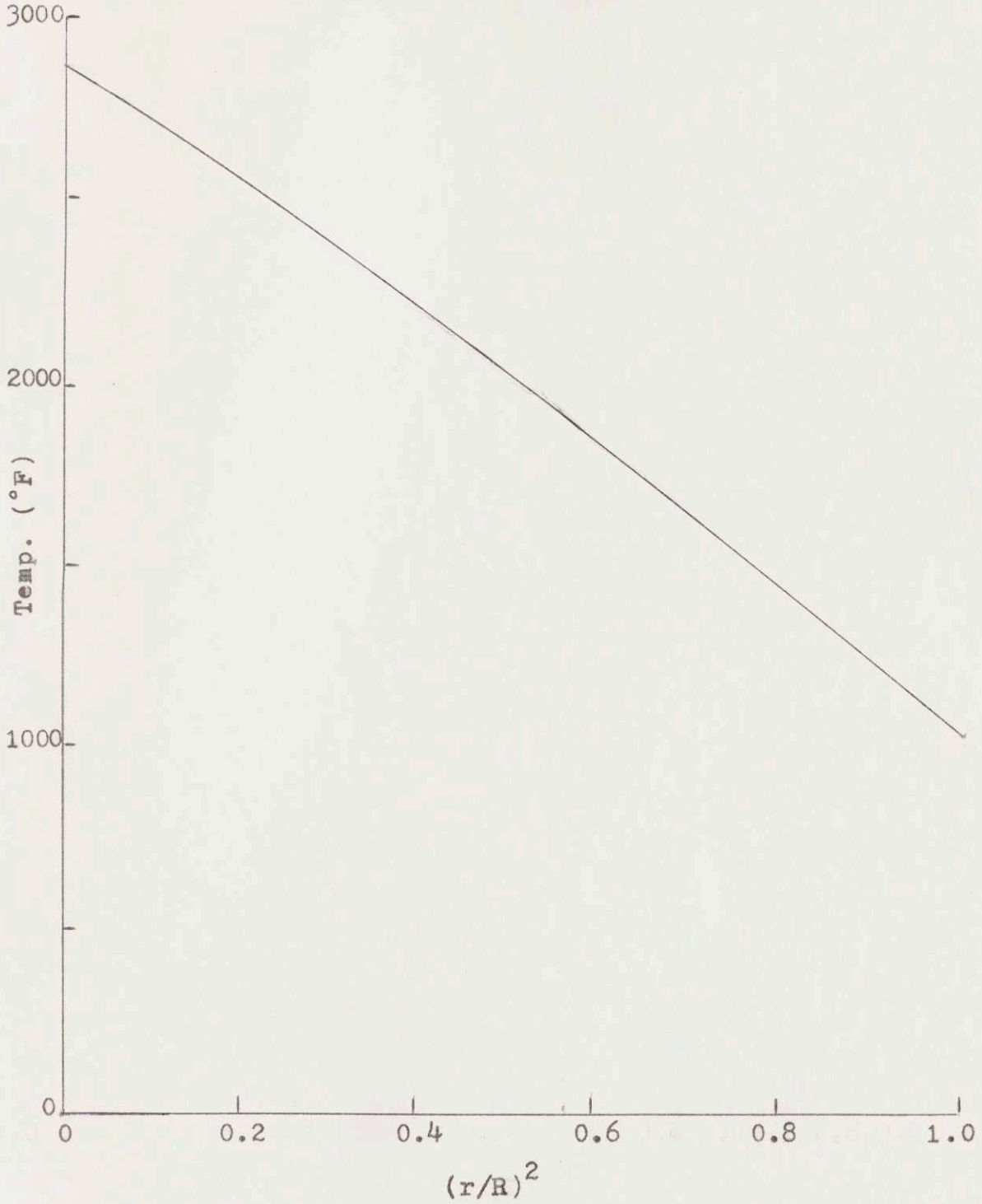

FIGURE A.4 (17)

RADIAL POWER PROFILE FOR C5A

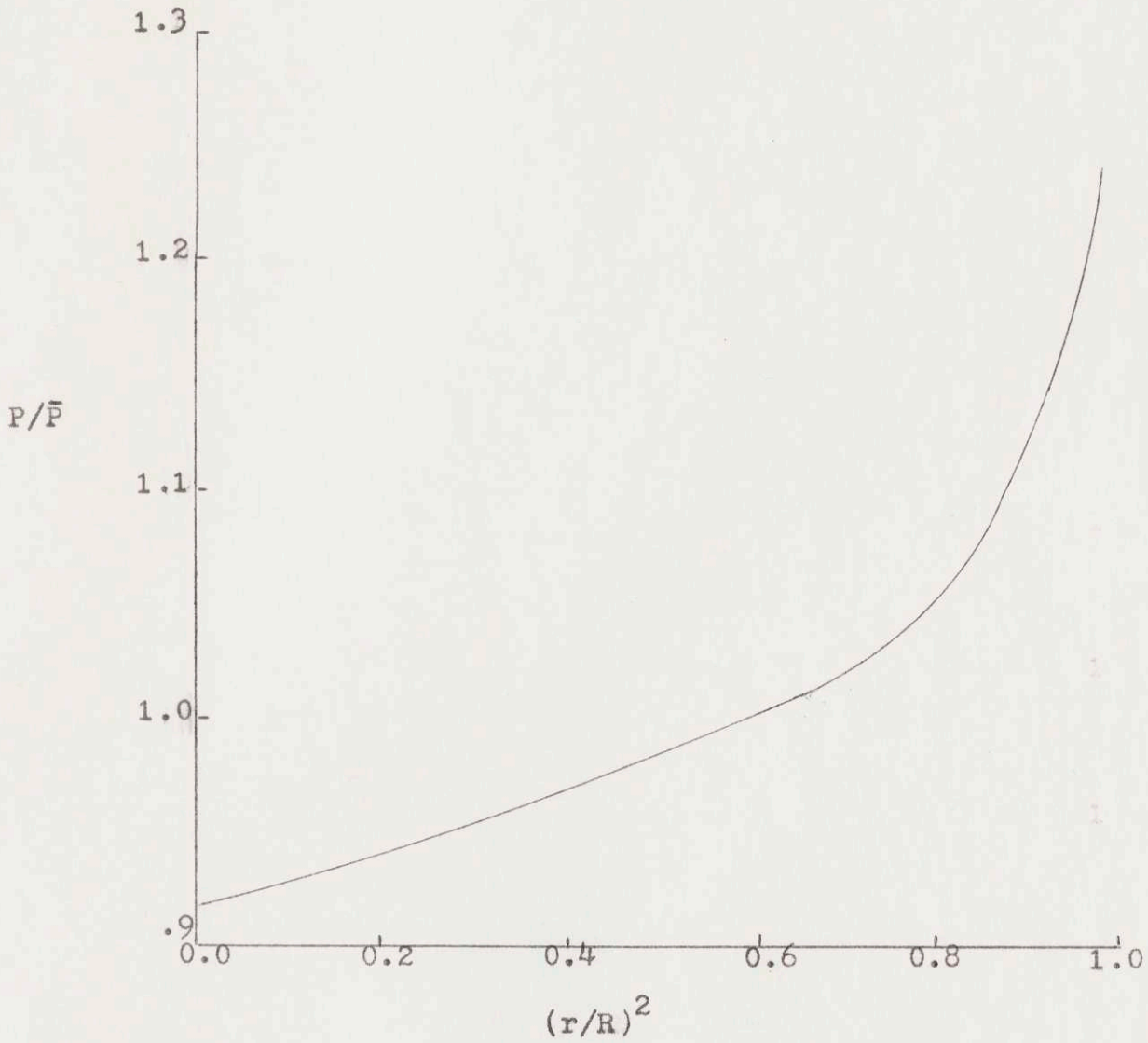

FIGURE A.5 (17)

RADIAL POWER PROFILE FOR C5B

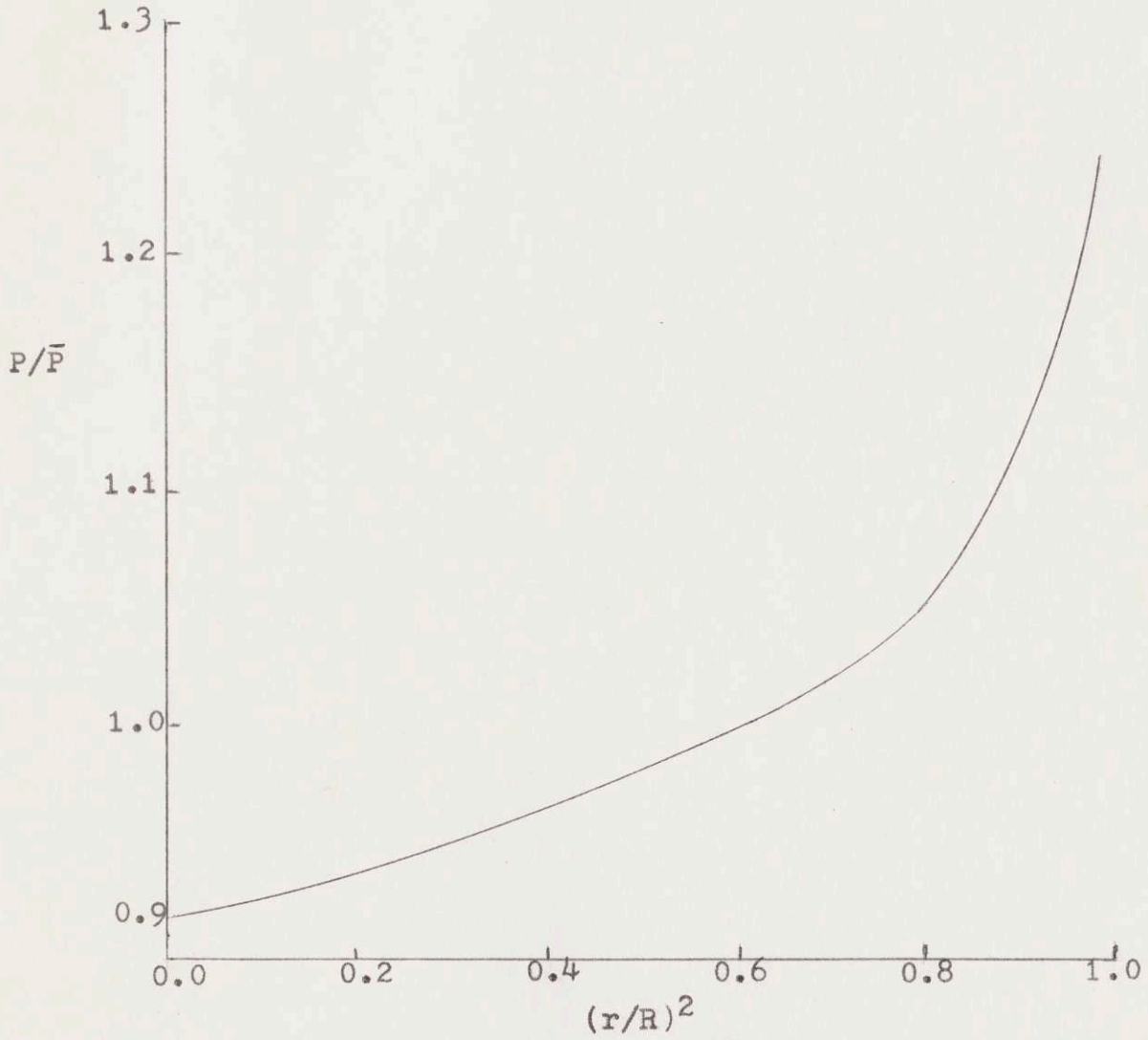

FIGURE A.3 (17)

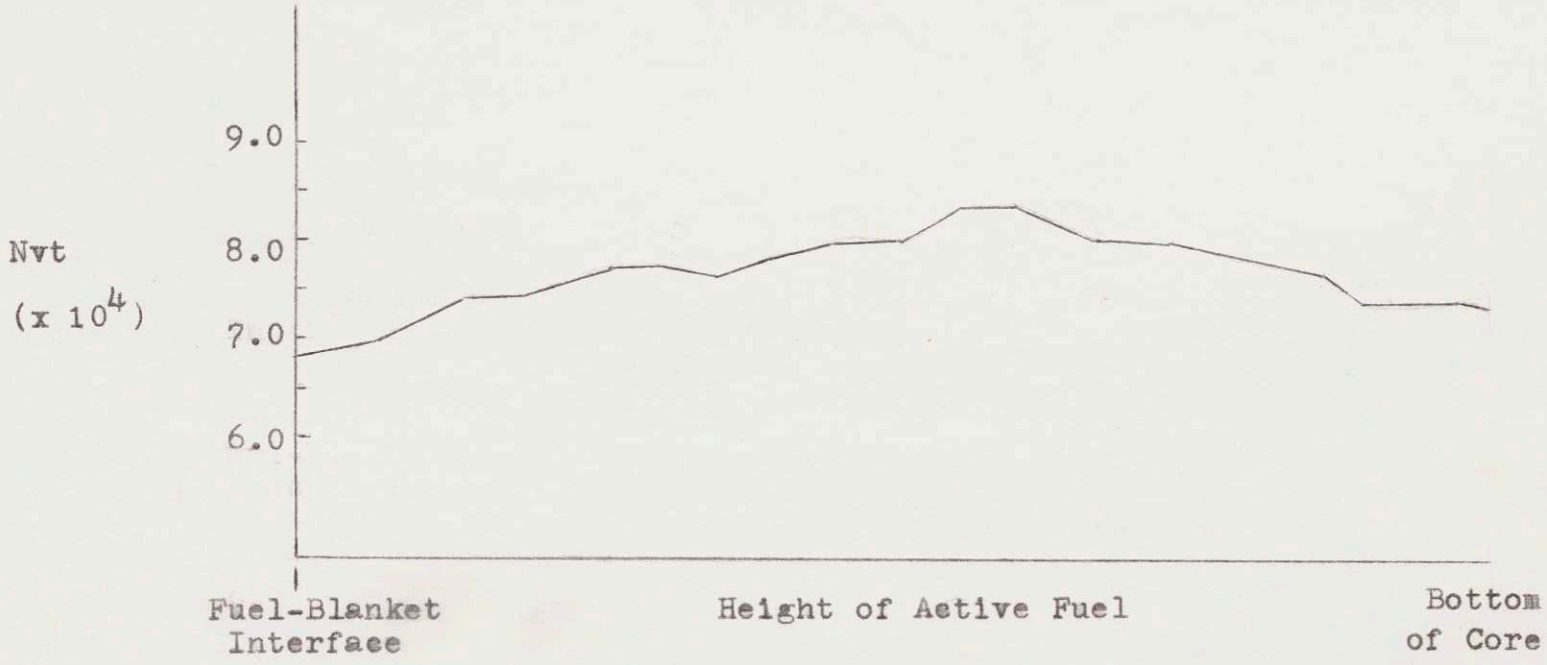

AXIAL FLUX PROFILE FOR C5A AND C5B

FIGURE A.6 (17)

TREAT CAPSULE GEOMETY FOR TESTS C5A AND C5B

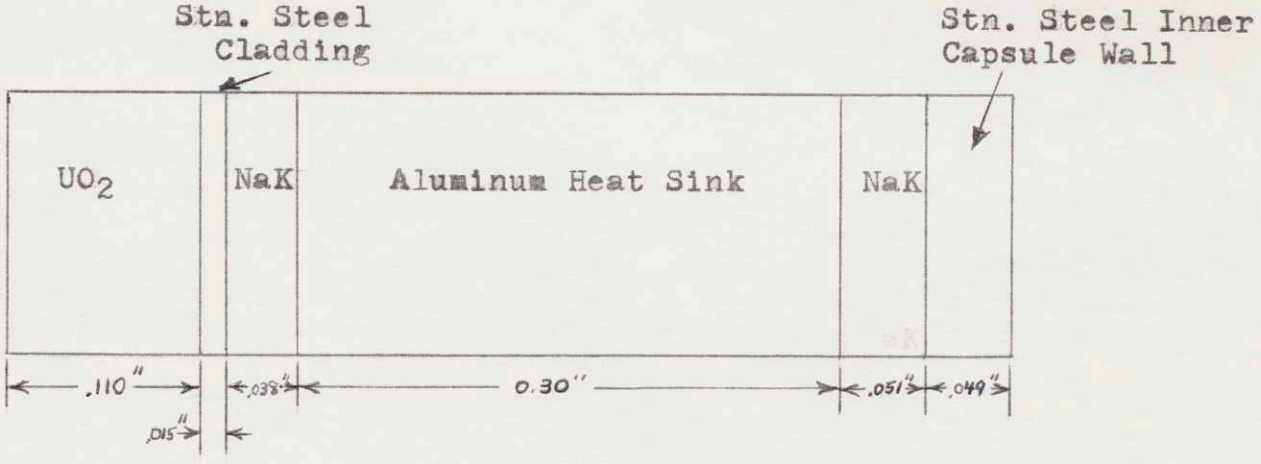

APPENDIX B

CALCULATIONS

The Heat Transfer Module of SAS1A was used for calculating the fuel temperature distribution for the second time step in the fuel movement calculations. As mentioned previously, SAS1A is not well suited for use with pins which have neutron flux depressions, since the code was designed for pins with almost flat radial power shapes. To overcome this problem, the SAS1A results for the original (not considering any fuel movement) C5B test was compared with the known accurate results from THTD. A correction factor was thus obtained and this factor was employed in the use of SAS1A in the second time step. (The THTD results were used in the first time step, since they were available for that case.)

Sample calculations for the C5A case will now be given. Only calculations not explicitly explained previously will be shown.

To determine the amount of fission gas produced:

$$A = \frac{17800\ \text{MWd/Te}\ (136\text{gm. U})\ (10^{-6}\text{Te/gm})\ (.30\ \text{atoms gas/fission})}{3.7 \times 10^{22}\ \text{MWd/fission}}$$

$$A = 2.105 \times 10^{21}\ \text{atoms}$$

The gas volume at S.T.P.:

$$\frac{2.105 \times 10^{21}\ (2.24 \times 10^{4}\ \text{cc/mole})}{6.023 \times 10^{23}\ \text{atoms/mole}} = 78.29\ \text{c.c.}$$

The amount of gas in the melted region, from figure A.1, with $(r/R)^2 = (.068/.110)^2 = .382$, 38 % of the gas in the pin is

in the melted region.

Using the Lewis model, and dividing the fuel into regions which have a 100°F temperature difference, it is found that 27.8% of the gas in the melted region was released in the steady-state irradiation. (For example, in the region of fuel that was between 2700°F and 2800°F in the steady state irradiation period, 5½% of the total fission gas was located. Of this, 44% was released in the steady-state. Thus .44(.055)= .0242 of the total fission gas in the pin was released in this particular region of fuel. By summing all the regions, a total is found.)

A sample internal pressure calculation:

In C5A, 21.53 cc of gas released in the transient, and 1.606 cc of gas already occupying the pores, must occupy a volume of .73 cc.

The pressure:

$$\frac{1 \text{ atm.}\ (23.14\text{cc})(5610^\circ\text{R})}{(.73\text{cc.})\quad(492^\circ\text{R})} = 361.4 \text{ atm, or}$$

5312.9 psia.

Now, considering fuel motion in an isothermal case, an equation for the final fission gas volume can be derived. Since the fuel is incompressible, one is only concerned with the gas volumes.

Subscripting the fission gas variables by f and the plenum gas variables by p, and superscripting the original values by o and the final values by f, one can write:

$P_f^f V_f^f = P_f^o V_f^o$ = RT, a constant in the isothermal case.

Now the final equilibrium position can be assumed to be reached when $(P_f^f - P_p^f)A = Mg$, by a force balance. (M here is the mass of the fuel, with the mass of the gases neglected in comparison.) Substituting:

$$(Amg + P_p^f)\, V_f^f = P_f^o\, V_f^o$$

Now $P_p^f = P_p^o\, V_p^0 / V_p^f = P_p^o\, V_p^o / (V_{tot} - V_f^f)$

Substituting this result, and calling $V_f^f = x$, the equation reduces to:

$$x^2 AMg - x(V_{tot} AMg + P_p^o\, V_p^o + P_f^o V_f^o) + P_f^o V_f^o V_{tot} = 0$$

or, writing $ax^2 + bx + c = 0$ with a, b, c defined by comparison,

$$x = \frac{-b \pm \sqrt{b^2 - 4ac}}{2a}$$

Thus, substituting,

$$V_f^f = (V_{tot} AMg + P_p^o V_p^o + P_f^o V_f^o) \pm ((V_{tot} AMg + P_p^o V_p^o + P_f^o V_f^o)^2 - 4AMg P_f^o V_f^o\, V_{tot})^{\frac{1}{2}} \Big/ 2AMg$$

APPENDIX C
PROPERTIES USED FOR TRANSIENT TEST ANALYSIS

Fuel

Density(solid) = 617 lbm/ft.^{3} Latent Heat = 120BTU/lbm.
9.6% Density Decrease On Melting Phase change Temp.= 5150° F

Temp. (°F)	300	500	750	1000
Thermal Cond. (BTU/hr.ft.^{2} °F)	3.84	3.30	2.88	2.46
Special Heat (BTU/lbm. °F)	0.060	0.0625	0.0650	0.0676
Temp. (°F)	1125	12500	1375	1500
Thermal Cond. (BTU/hr.ft.^{2} °F)	2.31	2.14	2.02	1.91
Special Heat (BTU/lbm. °F)	0.0690	0.0700	0.0714	0.0725
Temp. (°F)	1750	200	2400	2552
Thermal Cond. (BTU/hr.ft.^{2} °F)	1.76	1.65	1.53	1.50
Special Heat (BTU/lbm. °F)	0.0750	0.0775	0.0812	0.0828
Temp. (°F)	2750	3500	4500	5150
Thermal Cond. (BTU/hr.ft.^{2} °F)	1.50	1.50	1.50	1.50
Special Heat (BTU/lbm. °F)	0.0844	0.0910	0.0998	0.105

316 Stainless Steel (clad)

Density= 501 lbm/ft.^{3} Latent Heat = 122BTU/lbm. Phase Change
Temp. = 2500°F

Temp. (°F)	0	200	400	600
Thermal Cond. (BTU/hr.ft.^{2} °F)	7.30	8.20	9.10	9.95
Special Heat (BTU/lbm. °F)	0.114	0.118	0.123	0.128
Temp. (°F)	800	1000	1200	1400
Thermal Cond. (BTU/hr.ft.^{2} °F)	10.9	11.8	12.7	13.5
Special Heat (BTU/lbm. °F)	0.133	0.138	0.142	0.147
Temp. (°F)	1600	1800	2000	2200
Thermal Cond. (BTU/hr.ft.^{2} °F)	14.4	15.3	16.2	17.1
Special Heat (BTU/lbm. °F)	0.152	0.157	0.162	0.167
Temp. (°F)	2400	2500		
Thermal Cond. (BTU/hr.ft.^{2} °F)	18.0	18.4		
Special Heat (BTU/lbm. °F)	0.171	0.174		

Coolant (NaK)

Density = 54.2 lbm/ft.^{3} Latent Heat=1100BTU/lbm. Phase Change
Temp. = 1440 °F

Temp. (°F)	200	300	400	500
Thermal Cond. (BTU/hr.ft.^{2} °F)	13.5	14.0	14.4	14.8
Special Heat (BTU/lbm. °F)	0.223	0.219	0.216	0.214
Temp. (°F)	600	700	800	900
Thermal Cond. (BTU/hr.ft.^{2} °F)	15.0	15.2	15.2	15.1
Special Heat (BTU/lbm.°F)	0.212	0.210	.0209	0.204

Temp. (°F)	1000	1100	1200
Thermal Cond. (BTU/hr.ft.^{2}°F)	15.1	15.6	14.9
Special Heat (BTU/1bm. °F)	0.209	0.209	0.210
Temp. (°F)	1300	1440	
Thermal Cond. (BTU/hr.ft.^{2}°F)	14.7	14.5	
Special Heat (BTU/lbm. °F)	0.211	0.213	

Aluminum

Density=169lbm./ft.^{3} Latent Heat=170BTU/lbm. Phase Change Temp. = 1080 °F

Temp. (°F)	0	100	200
Thermal Cond. (BTU/hr.ft.^{2} °F)	8.45	9.00	9.33
Special Heat (BTU/1bm. °F)	0.221	0.226	0.230
Temp. (°F)	300	400	500
Thermal Cond. (BTU/hr.ft.^{2} °F)	9.57	9.75	9.90
Special Heat (BTU/lbm. °F)	0.234	0.239	0.243
Temp. (°F)	750	1080	
Thermal Cond. (BTU/hr.ft.^{2} °F)	10.2	10.5	
Special Heat (BTU/lbm. °F)	0.254	0.268	

ACKNOWLEDGEMENTS

The author wishes to express his gratitude to Professor Neil E. Todreas for his many hours of guidance. The personal attention afforded me by Professor Todreas has been deeply appreciated.

The author would also like to thank Mr. Mujid Kazimi for his time and patience in assisting me in several areas.

Helpful discussions were also held with Mr. Garry Thomas and Mr. Robin Stuart of the General Electric Company, and Mr. Jack Travis of Argonne National Laboratory.

My wife, Kathleen, helped with the typing and, as always, contributed her patient support and understanding during the thesis preparation.